INSTITUTO SUPERIOR TÉCNICO
Universidade Técnica de Lisboa

Energy efficient solutions in GSM/UMTS based on traffic profiling models

Diogo Martins dos Reis Santos Silva

Dissertation submitted for obtaining the degree of
Master in Electrical and Computer Engineering

Jury

Supervisor:	Prof. Luís M. Correia
Co-Supervisor:	Eng. Clara Lourenço
President:	Prof. José Bioucas Dias
Members:	Prof. António Rodrigues

April 2012

To my parents

Acknowledgements

After more than one year of constant work, the production of this thesis was only possible with the support of the people I love, and that were always by my side during all the hours that were spent developing this thesis. Specially at weekend nights, and during the summer months, their words kept me on the right path to conclude this thesis.

First of all, I would like to thank Professor Luís M. Correia, for giving me the wakeup call about the subject of mobile communications, for the possibility to have this thesis with the partnership of an external company, and for all the corrections, guidance and learning process concerning the thesis and even outside the telecommunications issues.

To Optimus, and specially to Clara Lourenço, for the support and for being always available to help with any obstacle that I came across during the development of this thesis.

To my RFII colleagues, and now good friends, João Pato, Pedro Carreira, Ricardo Batista and Tiago Gonçalves, for all the support, for being always available to clarify any minor doubt that emerged along the return trip from Monsarraz or Prainha. With their company, this journey become easier to go through.

To all my good friends, that always stood by me, giving me strength and motivation, to Margarida Louro, Carolina Silva, Marta Tavares, Henrique Pina, Ana Rita Caldeira and Hugo Sousa, for the company while writing our thesis, to the Monte Gordo group and the Titãs team, for the moments of leisure and laughs, their role was very important to keep my spirit high along the duration of this work.

Finally, my biggest gratitude goes to my mother and my father. Their efforts and daily sacrifices for giving me the possibility to have a great education and to complete my academical formation were always present in my mind, as the thesis was being produced, and my grandmother, for all the daily comprehension and patience. Their support was essential for the completion of this thesis.

Abstract

The main scope of this thesis is to evaluate the power consumption savings in GSM/UMTS with the use of energy efficient models, based on the switch off of RF equipment, in low traffic hours that vary within the urban regions. For each region, traffic models were developed for both voice and data traffic, to be used as input to the energy efficient models. The Traffic Model uses the collected traffic data to obtain voice and data traffic models. Four voice and three data traffic models were developed, which are associated with their respective regions, the most important being a double gaussian and tree stump behaviour for voice, and a pyramid and swing type for data. The Energy Efficiency Model uses the power consumption model and energy efficient algorithms to produce energy consumption daily profiles. In the Energy Efficient Algorithm the RF equipment is switched on and off according to the traffic load, producing energy savings that vary between 30% to 40% with the most favourable scenario, which considers the Dense Urban configuration at the weekend. It was also identified that the energy savings do not change with different demographic environment, leading to a monthly saving of 45€ to 55€ per sector.

Keywords

GSM, UMTS, Traffic, Power, Efficiency

Resumo

O âmbito geral desta tese é avaliar a poupança em consumo de potência com o uso de modelos de eficiência energética, que são baseados no desligar de equipamento RF. Os períodos de atuação destes modelos correspondem às horas de baixo volume de tráfego, que variam com a região urbana. Para cada região, são desenvolvidos modelos de tráfego tanto para a voz como para os dados, para serem usados como parâmetros de entrada nos modelos de consumo de potência. O modelo de tráfego usa os dados recolhidos para se obterem os modelos de tráfego para voz e dados. Foram desenvolvidos quatro modelos de tráfego de voz e três de dados, e foram associados com as respetivas regiões, sendo os mais importantes o comportamento de dupla gaussiana e cepo de árvore para a voz, e o tipo pirâmide e baloiço para os dados.O modelo de eficiência energética tem como parâmetros de entrada os modelos de tráfego que, em conjunto com a os modelos de consumo energético e os algoritmos de eficiência energética, produzem os perfis de variação diária de consumo de potência. No algoritmo de eficiência energética, o equipamento RF é ligado e desligado tendo em conta a intensidade de tráfego, produzindo tanto perfis de consumo eficiente de potência como de variação de portadoras. Deste trabalho, pode-se obter poupanças energéticas que variam desde 30% até 40% para o cenário mais favorável. Foi também identificado que a poupança energética não varia com diferentes ambientes demográficos, o que conduz a poupanças mensais entre 45€ e 55€ por sector.

Palavras-chave

GSM, UMTS, Tráfego, Potência, Eficiência

Table of Contents

List of Figures

List of Tables

List of Acronyms

16QAM	16 Quadrature Amplitude Modulation
2G	Second Generation
3G	Third Generation
3GPP	3rd Generation Partnership Project
4G	Fourth Generation
64QAM	64 Quadrature Amplitude Modulation
ArC	Air Conditioner
AC/DC	Alternating Current/ Direct Current
ARFCN	Absolute Radio Frequency Channel Numbers
BB	Baseband
BCH	Broadcast Channel
BCCH	Broadcast Control Channel
BS	Base Station
BSC	Base Station Controller
BSS	Base Station Subsystem
BTS	Base Transceiver Station
C	Carriers
CCCH	Common Control Channel
CN	Core Network
CoMP	Coordinated Multi-Point
CS	Circuit Switched
DCCH	Dedicated Control Channel
DC-HSDPA	Dual Carrier HSDPA
DDGM	Data Double Gaussian Model
DGM	Double Gaussian Model
DL	Downlink
DMIMO	Distributed MIMO
DPCCH	Dedicated Physical Control Channel
DS-CDMA	Direct-Sequence Code Division Multiple Access
DSP	Digital Signal Processing
DRX	Discontinuous Reception
DTrM	Data Trapezoidal Model
DTX	Discontinuous Transmission
DU	Dense Urban Scenario

EDGE	Enhanced Data rates for GSM Evolution
ETSI	European Telecommunications Standards Institute
FDD	Frequency Division Duplex
FDMA	Frequency Division Multiple Access
FFR	Fractional Frequency Reuse
FTP	File Transfer Protocol
GGSN	Gateway GPRS Support Node
GMSC	Gateway Mobile Switching Centre
GPRS	General Packet Radio Service
GSM	Global System for Mobile Communications
HLR	Home Location Register
HSDPA	High Speed Downlink Packet Access
HSUPA	High Speed Uplink Packet Access
HSPA	High Speed Packet Access
HS-DPCCH	High Speed Dedicated Physical Control Channel
HS-DSCH	High Speed Downlink Shared Channel
HS-SCCH	High Speed Shared Control Channel
HTTP	HyperText Transfer Protocol
ICT	Information and Communications Technology
IP	Internet Protocol
LAI	Location Area Identity
LTE	Long Term Evolution
ME	Mobile Equipment
MIMO	Multiple-Input Multiple-Output
MSC	Mobile Services Switching Centre
MS	Mobile Station
MT	Mobile Terminal
OFDMA	Orthogonal Frequency Division Multiple Access
OPEX	Operational Expenditure
OVSF	Orthogonal Variable Spreading Factor
PyM	Pyramid Model
PA	Power Amplifier
PDF	Probability Density Function
PS	Power Supply
QoS	Quality of Service
QPSK	Quadrature Phase-Shift Keying
Ru	Rural Scenario
R99	Release 99
RAT	Radio Access Technology
RF	Radio Frequency

RMSE	Root Mean Squared Error
RNC	Radio Network Controller
RRM	Radio Resource Management
S	Suburban Scenario
SwM	Swing Model
SDCCH	Standalone Dedicated Control Channel
SIR	Signal to Interference Ratio
SMS	Short Message Service
SNR	Signal to Noise Ratio
SGSN	Serving GPRS Support Node
TCH	Traffic Channel
TDMA	Time Division Multiple Access
TrM	Trapezoidal Model
TRX	Transceiver
TSM	Tree Stump Model
U	Urban Scenario
UE	User Equipment
UL	Uplink
UMTS	Universal Mobile Telecommunications System
USIM	UMTS Subscriber Identity Module
UTRAN	UMTS Terrestrial Radio Access Network
VLR	Visitor Location Register
WCDMA	Wideband Code Division Multiple Access

List of Symbols

α_j	Code Orthogonality of user j
Δ_p	Transmitted Power Coefficient
Δt_{Eff}	Carrier Traffic Load Evaluation Interval
η	Load Factor
η_{DL}	Downlink Load Factor
η_{UL}	Uplink Load Factor
μ_{PA}	PA Efficiency
ρ_r	Load of Resource r
σ_{avg}	Standard Deviation
τ_i	Gaussian Deviation
ν_j	Activity Factor of user j
a_{Dgn}	Gaussian Amplitude
a_{pd}	Average Power Decay
a_{trn}	Exponential Initial Value
a_{gauss}	Double Gaussian Function
a_{trap}	Trapezoidal Model Function
b_{trn}	Exponential Decay Factor
c	Gaussian Upper Limit
c_{tr}	Linear Constant Value
cf	DC to RF Conversion Factor
d	Cell Coverage Radius
d_{Dg2}	Second Gaussian Offset
E_b	Energy per bit
f_{avg}^{sec}	Average Daily Traffic Profile
f_{Dgauss}	Double Gaussian Traffic Model
$f_{Dgaussdata}$	Data Double Gaussian Traffic Model
f_{MOD}	Traffic Model Profile
f_{pyram}	Pyramid Traffic Model
f_{swing}	Swing Traffic Model
f_{trap}	Trapezoidal Traffic Model
$f_{trapdata}$	Data Trapezoidal Traffic Model

f_{tstump}	Tree Stump Traffic Model
$f_{wd/we}^{sec}$	Sector Daily Traffic Profile
$f_{wdn/wen}^{sec}$	Daily Traffic Profile
i	Normalised Inter-cell Interference
G_P	Process Gain
G_r	Receiving Antenna Gain
G_t	Transmitting Antenna Gain
L_C	Cooling Loss
$\overline{L_{pj}}$	Average Path Loss of user j
L_{PS}	Power Supply Loss
L_{PSBB}	Battery Backup and Power Supply Loss
L_{ref}	Reference Path Loss
$L_{TX_{NL}}$	Transmitted Power Loss Dynamic Component
L_{TXst}	Transmitted Power Loss Static Component
N_{carr}	Number of Active Carriers
N_{CH}	Number of available channels
$N_{codsf128}$	Number of Occupied Codes with SF 128
$N_{codsf16}$	Number of Occupied Codes with SF 16
N_{frcod}	Number of Available Codes with SF16
N_L	Number of Active Users
N_0	Noise Power Spectral Density Ratio
N_{pApSec}	Number of PAs per Sector
N_{PDCH}	Number of PDCH Channels
N_R	Number of Available Resources
N_{SDCCH}	Number of SDCCH Channels
n_{sec}	Pre-selected Sector Index
N_{sec}	Total Number of Pre-selected Sectors
N_{Sector}	Number of Sectors
N_{TCH}	Number of TCH Channels
N_U	Number of user per cell
N_{UGSM}	Number of full rate users in on GSM cell
N_{TCH}	Number of traffic channels
N_{TRX}	Number of placed TRXs
$N_{wd/we}$	Total Number of Daily Traffic Profiles
p	Gaussian Amplitude
p_1	First Gaussian Amplitude
p_2	Second Gaussian Amplitude
$P_{AC/DC}$	AC/DC Power Consumption

P_{ArC}	ArC Power Consumption
P_{ArC0}	0ºC ArC Power Consumption
P_{ArCMAX}	Maximum ArC Power Consumption
P_{ArCmed}	Medium ArC Power Consumption
P_{ArCtyp}	Typical ArC Power Consumption
$P_{backhaul}$	Backhaul Connection Power Consumption
P_{BB}	BB Power Consumption
P_{cst}	Fixed Power Consumption Value
P_{DSP}	DSP Power Consumption
$P_{inMacro}$	Macro BS Consumed Input Power
$P_{inMicro}$	Micro BS Consumed Input Power
P_{MAX}	Maximum RF Output Power Consumption
P_{max_M}	Macro BS Maximum Emitted Power
P_{PA}	PA Power Consumption
P_{PS}	PS Power Consumption
P_r	Received Power at the Antenna
P_{site}	Site Power Consumption
P_{SP}	Signal Processing Overhead
P_{SPst}	Static Signal Processing Power Consumption
$P_{SP_{NL}}$	Dynamic Signal Processing Power Consumption
$P_{staticM}$	Macro BS Traffic Independent Consumed Power Value
$P_{staticm}$	Micro BS Traffic Independent Consumed Power Value
P_{TRX}	TRX Fixed Power Consumption
P_{TU}	User Assigned Power
P_{TX}	Total Transmission Power
P_{TX_M}	Macro BS Output Power
P_{TX_m}	Micro BS Output Power
r	Resource Index
R_b	Bit Rate
R_{b16QAM}	16QAM Modulation Maximum Theoretical Throughput
R_{b64QAM}	64QAM Modulation Maximum Theoretical Throughput
R_{bcarr}	Carrier Capacity
R_{bMAX}	Maximum Data Rate Value
R_{bQPSK}	QPSK Modulation Maximum Theoretical Throughput
R_C	Chip Rate
t_1	Morning Shifted Peak Hour
t_2	Afternoon Shifted Peak Hour
t_{b1}	First Shifted Function Breakpoint

t_{b2}	Second Shifted Function Breakpoint
T_{in}	Air Temperature Inside the BS Container
t_h	Hour Value
t_l	Shifted Lunch Hour
$t_{lunchshitf}$	Shifted Lunch Hour
T_{MAX}	Maximum ArC Working Temperature
t_{nshift}	Number of Shifted Hours
T_{out}	Outside Air Temperature
Trh_{OFF}	Carrier Switch-off Threshold
T	Traffic Load
T_{NORM}	Normalised Traffic Load
T_{ON}	Power-On Limit
T_{OFF}	Power-Off Limit
t_{shift}	Shifted hour Time
t_t	Shifted Peak Hour
T_{thn}	Temperature Threshold
$t_{trnshift}$	Shifted Breakpoint Hour

List of Software

Mathworks Matlab 2010a	Numerical computing software
Microsoft Excel 2007	Calculation and graphical chart tool
Microsoft Word 2007	Text editor software
Microsoft PowerPoint 2007	Graphical presentation software
Adobe Photoshop CS5.1	Graphical editor tool

Chapter 1

Introduction

In this chapter, a brief overview of the work is presented. The context where this thesis work is framed is introduced, as well as energy savings procedures. The scope and the work structure of this thesis are also provided at the end of the chapter.

1.1 Overview

The first mobile communications systems were analogue and provided only voice, being commonly referred to as the first generation of mobile communications. Then came the Global System for Mobile Communications (GSM), also called second a generation system (2G), which development started in 1982 and was first published in 1990 by the European Telecommunications Standards Institute (ETSI). With this system, two goals were achieved, a better and more efficient technical solution for wireless communications, and a global standardisation within Europe that enabled roaming across borders. Though it was originally developed as a European system, the success of GSM exceeded all expectations, and it has spread all over the world in the meantime. Since then, GSM has become the most adopted worldwide mobile communications standard.

To extend the services provided by the mobile communications network, General Packet Radio Service (GPRS) was introduced, giving the ability of higher data rates and the transmission of small amounts of data, and the Short Message Service (SMS) was developed. GPRS brought the packet-switched bearer services to the existing GSM. In GPRS, the user can access public data networks directly using its standard protocol addresses. Furthermore, with the efficient use of modulation with EDGE (Enhanced Data rates for GSM Evolution), GSM became often referred to as the 2.5 generation system, as its functionalities are beyond those of a 2G one.

Third Generation (3G) systems were developed with the goal of enhanced person-to-person communication, along with high-quality multimedia files transmission, better spectral efficiency, higher data rates and new flexible communication capabilities. So, in 1999, the 3rd Generation Partnership Project (3GPP) launched the Universal Mobile Telecommunications System (UMTS), also called Release 99 (R99). This system uses Wideband Code Division Multiple Access (WCDMA) in its air interface, featuring data rates up to 384 kbps for the Downlink (DL) and Uplink (UL), despite having a theoretical maximum for DL of 2 Mbps [Moli05].

To respond to the need of higher data rates, 3GPP specified a DL solution in Release 5 called High Speed Downlink Packet Access (HDSPA), which was commercially deployed in 2005, and after it published Release 6, the High Speed Uplink Packet Access (HSUPA), in 2007. These evolutions are also called the High Speed Packet Access (HSPA). The key idea of HSDPA is to increase packet data throughput with like link adaptation and fast physical layer retransmission combining. The initial peak data rate of HSDPA was 1.4 Mbps, and at the end of 2007 7.2 Mbps were achieved. More recently, 14.4 Mbps peak data rates are available, with the migration to the mobile Internet Protocol (IP) [HoTo07].

Furthermore, HSPA Evolution, also called HSPA+, was specified in Release 7 with the introduction of the Multiple Input Multiple Output (MIMO) feature, which allows users to achieve data rates up to 42 Mbps [HoTo07]. The appearing Long-Term Evolution (LTE) technology, supported on a new access technique called Orthogonal Frequency Division Multiple Access (OFDMA), enables data rates of 160 Mbps, as specified in Release 8. This system is also called fourth generation (4G) of mobile communications.

All these systems are designed to coexist with the ones previously installed so, for one site, it is predictable that more than one technology equipment may be installed. Despite being the oldest system, GSM is still the most used solution to cover all the network area of an operator. Then, on top of that, UMTS network is deployed and, due to their coexisting nature, it is possible to perform handovers between systems as well as dual-mode operating modes. Those layers of 2G, 3G and 4G networks result in a considerable amount of equipment working simultaneously in every site, leading to a high energy consumption when considering the entire network, most of them not being used at low traffic hours.

Currently, 3% of the world-wide energy is consumed by Information and Communications Technology (ICT) infrastructures [GCJH10]. In mobile communications, 90% of energy consumption is done at the Core Network and Base Stations (BSs), so with the increase in the number of sites, due to larger capacity and bandwidth requirements, energy efficient solutions became a major concern for telecommunications operators. In addition to minimising the environmental impact of the industry, cellular network operators are as well interested in reducing the energy consumption of their networks to reduce their Operational Expenditure (OPEX), and therefore increase profits.

Furthermore, over 80% of power in mobile telecommunications is consumed in the radio access network, more specifically in the BSs, so by optimising energy consumption or creating adaptive operating mode solutions of the equipments at the sites, there are considerable savings in energy at the BS and in the expenditure for operators [RiFF09].

With the energy aware adaptive solutions comes the importance of traffic load modelling, where daily, weekly or even seasonally, telecoms users' migratory patterns can be studied and then modelled to improve the operators knowledge of its network. The reduction of traffic in some areas of the cellular network is due to the combination of the typical day-night behaviour of mobile phone users, like the daily swarming of users carrying their mobile terminals from residential areas to offices and back, resulting in the need for high capacity in both areas at peak usage times; on the opposite, the family weekends where the mobile phones are put aside, leading to a decrease on the volume of voice calls on the networks at those days and therefore the energy waste of the same unused resources deployed for the weekdays traffic load. Knowing the duration and the timing of low traffic hours, when virtually all BSs are operating at low load, or even not serving any user at all, is crucial in order to increase the energy efficiency of the network.

For the operators is also important to have some insight about the power consumption of each equipment inside a site, and their contribution for the overall site consumption, in order to have energy savings by investing in technological development of the most consuming equipment. This evaluation needs to be considered for all 2G, 3G and 4G technologies, as well as for all BSs sizes. Instead of the purchase of better equipment, power consumption variation factors must also be studied, and then used as parameters for intelligent energy aware models.

Apart from the evolution process of the Radio Access Technologies (RATs), like LTE and LTE-Advanced that are responsible for the decrease of cell radius, and therefore power consumption, the opposite approach is to extend and renew the existing mobile network architecture, with an energy

efficient point of view. The energy efficiency of the equipment is necessary to continuously improve the network but, nevertheless, the installation of additional equipment from new RATs will always result in the increase of power consumption for the network. Hence, the green network solutions have a major importance on the future mobile communications networks, where procedures like cooperative BSs communication, multi-hop, backhauling techniques, and network coding lead to a commonly called intelligent network, which adapts to the needs of the users at the current time. The combined use of these techniques has the ultimate goal of 50% energy reduction among all radio networks [EARTH10b].

1.2 Motivation and Contents

The main scope of this thesis is to evaluate the energy efficiency of intelligent techniques for carriers switch on/off for both 2G and 3G networks, with the analysis of power consumption profiles with and without energy efficient procedures, using previously developed traffic models as input. These profiles are obtained from an urban area traffic load analysis, and the development of traffic models characterise each region of the studied cities. Furthermore, GSM and UMTS BSs power consumption is analysed, regarding the dependencies of the most energy consuming equipment on external factors, as temperature or traffic load.

To allow a better development of the work, a partnership was established with Optimus, a mobile communications operator in Portugal. From Optimus, one obtained important data for the work, technical specifications for several equipments, and important guidelines to where the thesis work should be conducted.

This thesis is composed of 6 chapters, including the present one. In Chapter 2, an overview of the GSM and UMTS networks is presented, with the description of the networks architecture, radio interface configurations, capacity and coverage limitations, and improvement techniques for these two systems. Then, an extensive description of traffic models is made, concerning both data and voice services, and temporal traffic variations are studied, giving special attention to daily traffic variation profiles. Thereafter, a power consumption model is described, containing equipment from the entire site, where the total power consumed is distributed by all equipment, being described how that consumption varies in time. Finally, several energy efficient models are presented and their use and advantages are characterised, paying special attention to Switch Off Schemes.

In Chapter 3, a brief description of the collected traffic load data is done, as well as of its analysis, with the specifications and the assumptions used to this data treatment, in order to obtain the traffic profiles used in the traffic models. Besides, one explains how the 2G and 3G data collected from the network are separated into voice and data services. Then, the procedure for the voice and data traffic models is described, from which three voice and four data traffic models are obtained. Furthermore, the fitting results of these models are evaluated, and then, with a Root Mean Squared Error (RMSE)

comparative evaluation, the voice and data models are distributed along the sectors from the studied networks. Finally, the correlations between voice and data traffic profiles, and for weekdays and weekends, are analysed.

In Chapter 4, one presents a characterisation of the four Power Consumption Models that use the obtained traffic models and daily traffic consumption profiles are the outcome. These models are supported on 2G and 3G sites, with Macro, Micro and Pico sites being characterised from the power consumption distribution point of view. The distribution of power consumption is made among the major consuming equipment of the sites, from the Air Conditioner (ArC) to the RF equipment, and the most important variation dependencies are defined. Furthermore, for these two equipments, the power consumption variation is also modelled according to its own dependencies. Then, 2G and 3G Energy Efficient Algorithms are developed to be used together with the Power Consumption Model, in order to obtain the Energy Efficient Models, and therefore both absolute and relative power savings results.

In Chapter 5, distinct power consumption scenarios are developed based on pure voice and pure data traffic profiles, as well the mixture of voice and data traffic profiles for co-localised BSs. Then, power consumption profiles and carriers' daily variation average traces are obtained for the 2G or 3G Energy Efficient Models, with and without standard deviation. From these results, one obtains more realistic daily power consumption values, and absolute and relative energy savings. Finally, a co-localised scenario is analysed taking the joint GSM and UMTS base station power consumption into account.

Finally, in Chapter 6, this work is finalised, by drawing the main conclusions, and some general relations between traffic and power consumption results. Then, suggestions for future work are pointed out.

A group of annexes with auxiliary information and results are also included at the end of this document, being referenced in the thesis to serve as a complementary source for the comprehension of the current subject.

Chapter 2

Fundamental Concepts

This chapter provides an overview of the main ideas to understand this thesis. In Section 2.1, the GSM/UMTS architecture is presented, in Section 2.2 a brief description of each system air interface is done, and in Section 2.3 capacity and coverage characteristics are discussed for both systems. In Section 2.4, daily traffic variation traces are analysed, as well as daily traffic models for voice and data. Finally, in Section 2.5 power consumption models are described, and in Section 2.6 energy efficient solutions are presented and analysed.

2.1 Network Architecture

In this section, one describes the basic aspects of GSM and UMTS, i.e., architecture, radio interface, and capacity and coverage limitations, based on [HoTo04].

GSM/UMTS network architecture consists of several logical network elements and their interfaces. They can be grouped into three functional elements [HaRM03], Figure 2.1:

- MS/UE – Mobile Station (GSM) or User Equipment (UMTS), the interface between the user and the radio network (PDA, Laptop, Cell Phone).
- BSS/UTRAN – Base Station Subsystem/UMTS Terrestrial Radio Access Network, which handles all radio related functionality.
- CN – Core Network, deals with switching and routing calls and data connections to external networks.

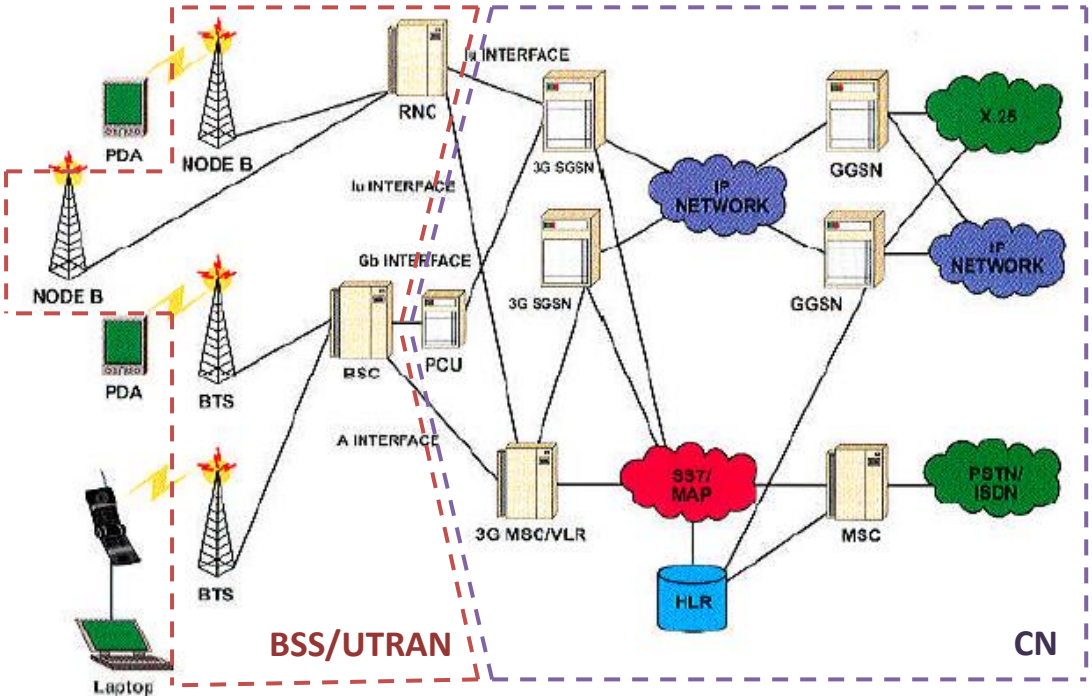

Figure 2.1 – GSM/UMTS network architecture (adapted from [Corr10]).

The MS/UE is composed of two elements:

- The Mobile Equipment (ME), used for radio communication over the interface between the ME and the BS, which will be referenced as Mobile Terminal (MT) from now on.
- The UMTS Subscriber Identity Module (USIM), which contains the subscriber information, authentication and encryption keys.

BSS/UTRAN also consists of two distinct elements:

- The Base Transceiver Station (BTS) or Node B, also known as BS, converts the data flow between the MT and the radio access network, and has a role in Radio resource Management (RRM).
- The Base Station Controller (BSC) or Radio Network Controller (RNC) manages and controls all BSs in its service area, performing the major RRM functions, e.g., power and handover control and broadcast signalling.

The CN is based on the GSM/GPRS CN, which is composed of Circuit Switched (CS) and Packet Switched elements. The CN contains CS elements, such as:

- Mobile Services Switching Centre (MSC), a switch that handles the CS services at the UE level.
- Gateway MSC (GMSC) is responsible for the connection between the CN and the external networks.

and Packed Switched elements:

- Serving GPRS Support Node (SGSN), responsible for all the data service in its service area.
- Gateway GPRS Support Node (GGSN), connected to the packet switched external networks, being responsible for the connection between both.

Finally, there are the PS and CS data based elements:

- Home Location Register (HLR), located in the user's home system and stores the master copy of the user's service profile, which is composed by allowed services and call forwarding, among others.
- Visitor Location Register (VLR), a temporary database with the information of the MTs using a specific service area. This information is a copy of the one in the HLR.

2.2 Radio interface

The radio interface is the most relevant part of the mobile communications network. It is located between the MT and the BSs, and for the scope of this thesis, both GSM and UMTS approaches must be described, according to [Moli05].

2.2.1 GSM

GSM uses two frequency ranges, between [890, 915] MHz for UL and [935, 960] MHz for DL at GSM-900, and also between [1710, 1785] MHz for UL and [1805, 1880] MHz for DL (GSM-1800). It employs both Frequency Division Multiple Access (FDMA) and Time Division Multiple Access (TDMA), so each frequency band is divided into carriers spaced by 200 kHz, which are numbered consecutively by the ARFCNs (Absolute Radio Frequency Channel Numbers.

Each 200 kHz carrier has 8 timeslots, allowing eight users to share it. The timeslots are numbered from 0 to 7, and have the duration of 576.92 μs, which is equivalent to 156.25 bits. A group of 8 timeslots is called frame, and it has the duration of 4.615 ms. Each subscriber accesses a specific timeslot in every frame of a frequency carrier, establishing a physical channel. The type of data that is transmitted over that physical channel depends on the mapping of the logical channels.

There are two major types of logical channels, for traffic and signalling purposes. The traffic channels (TCH) carry all the voice and data between the BS and the MTs. To increase the capacity of a cell, these can be converted between full-rate and half-rate traffic channels, where two users can share the

same timeslot, using it alternately.

As for the signalling, there are three types, broadcast, common control and dedicated control channels. The broadcast Channels (BCH) are only used in the DL, being used as beacon signals. They provide the MT with the information needed to establish the synchronisation on both time and frequency. The MTs have to track these channels not only before a connection but all the time, to provide enough information about possible handovers. Within this type of channels, one encounters the Broadcast Control Channel (BCCH), responsible for the transmission of the cell-specific information, which includes the Location Area Identity (LAI) or the actual available traffic channels. The Common Control Channels (CCCH) are used to send information to a certain MT to initiate the setup stage before a channel is allocated to that MT. Finally, the Dedicated Control Channels (DCCH) are bidirectional and transmit the signalling information that is necessary during a connection, such as the assurance that BS and MT stay connected during the authentication process, the information update of the signal quality received at the MT, or handover procedures. In particular, the Standalone Dedicated Control Channels (SDCCH) ensures that the MT and the BS stay connected after the authentication process, and only then one TCH is assigned for the MT.

Finally, the GPRS allows packet-switched based services to GSM. It can achieve a theoretical maximum data rate of 171.2 kbps, using the aggregation of all eight timeslots, dynamically allocated to the MT. It is supported by the Dedicated Physical Data Channel (DPDCH).

2.2.2 UMTS

UMTS FDD (Frequency Division Duplex) mode frequencies range in [1920, 1980] MHz in the UL and [2110, 2170] MHz in DL. It uses WCDMA, which is based on DS-CDMA (Direct-Sequence Code Division Multiple Access). This access method leads to higher bit rates, and also the possibility to grant variable data rates for different subscribers. UMTS has DL and UL carriers separated by 5 MHz, with a chip rate of 3.84 Mcps, allowing the use of 4.4 MHz channel bandwidth.

Spreading is used to separate the physical data from control channels at the same MT in UL, and to distinguish different users in DL. It has two types of code, channelisation and scrambling codes. The former is only used in the DL, to guarantee good separation of the signals for different users within one cell. The UL uses OVSF (Orthogonal Variable Spreading Factor) for spreading, which consists of the assignment of a spreading factor (SF) from 512 to 4 to a MT, therefore allowing variable data rates for different users in a cell. On top of spreading, scrambling codes are used to differentiate the sectors of a cell in DL, and to separate the MTs from each other without changing signal bandwidth, in UL. For R99, SF can vary from 256 to 4, and each MT is associated to a code picked from the code tree, therefore, varying the data rate of the MT associated to that SF, while in HSDPA the SF is fixed to 16, allowing a maximum theoretical data rate of 1.4 Mbps per code, but limiting the number of users to 15 for each carrier, as one of the codes is used for signalling and control purposes.

Power control, soft and softer handovers are the most important features in the UMTS air interface. As for the first one, without it, a single overpowered MT could block a whole cell. There are two types of

power control: inner loop is necessary to adapt to fast fading for speeds up to 500 km/h, for lower bit rates, and is important in keeping interference to a minimum and improving capacity, the outer loop power control adjusts the SIR (Signal to Interference Ratio) to a target level, in order to achieve a better Quality of Service (QoS) using as low power as possible. Finally, soft handover occurs when an MT is associated to two sectors from different BSs, while softer handover happens when those two sectors are from the same BS. The difference between these two operations is that the first is managed by de respective RNC, or the MSC if the sectors belong to different RNCs, and the last is done at the BS.

Similarly to GSM, UMTS has two types of logical channels, also called transport channels. The common channels are the ones shared by all the users in the sector, and dedicated channels are used to transmit both signalling and actual user data between the BS and an MT.

Considering the common channels, one has the BCH, which is also only found in the DL, like the GSM control channel. This channel is responsible for the transmission of both cell-specific and network specific information over the covered cell. It is used to inform all MTs about free access codes and available access channels. These common control channels have a constant SF of 256.

As for the dedicated channels, they are present in UL and DL, being used to transmit higher layer signalling and actual used data, allowing the adaptation of the data rate on a frame-by-frame basis. The Dedicated Transport Channel (DCH) is the only type of dedicated logical channel, allowing the addressing of each MT to a unique spreading code.

With HSDPA, two of the most fundamental features of UMTS, variable SF and fast power control are replaced by Adaptive Modulation and Coding (AMC), which is an extensive multi-code operation based on a fast and spectrally efficient retransmission strategy [Hoto07]. For this evolution, the High Speed Downlink Shared Channel (HS-DSCH) is introduced for data transmission, and the High Speed Shared Control Channel (HS-SCCH) and High Speed Dedicated Physical Control Channel (HS-DPCCH) for signalling in the DL and UL, respectively. HDSPA uses a fixed SF of 16, where 15 codes are used for data transmission, and the other one for signalling and control.

High order modulations are also used to achieve higher data rates, apart from the Quadrature Phase-Shift Keying (QPSK), which is used to ensure the coverage and robustness of the radio network, and allows a maximum theoretical throughput of 2 Mbps. Hence, 16 Quadrature Amplitude Modulation (16QAM) and 64 QAM are used in situations where the Signal-to-Noise Ratio (SNR) is favourable, giving the ability to achieve maximum theoretical throughputs of 7.2 and 14.4 Mbps, respectively.

2.3 Capacity and Coverage

Capacity and coverage are closely related in GSM and UMTS networks, and therefore, there are parameters that must be considered [HoTo04] and [Corr10], as shown in Table 2.1.

Table 2.1 – Key parameters that can create limitations on coverage and capacity of a BS (adapted from [HoTo04]).

Capacity	Coverage
• Number of available codes. • BS transmission power. • System load.	• Propagation conditions. • Area Type Information. • Coverage regions.

Due to spectrum shortage, there is the need for frequency reuse to guarantee coverage and support the traffic of a certain area. In GSM, each cluster has four cells, while in UMTS it is formed by only one.

On top of the cellular architecture of mobile networks, sectorisation is also used to increase the capacity at the cellular level. The cell is divided into three sectors, as well as the channels at that BS.

2.3.1 GSM

Each GSM user has its own time slot, meaning that capacity basically depends on the cluster and cell sizes, along with the number of RF Transceivers (TRX) installed in the BS. Since the number of frequency channels in GSM is constant, it is easy to obtain the theoretical maximum number of voice users at one cluster multiplying the number of available channels by 8 timeslots at each channel. However, not all the timeslots are used for traffic, and 10% of each BS capacity is reserved for signalling and control. Finally, it is possible for two users to share the same timeslot, but with half of the bit rate, being noticeable by the human ear.

Furthermore, to reduce interference, with the use of frequency planning just a few channels are assigned to a BS, according to the dimensioned number of TRX, [KrFr97]. With the increase or decrease in the number of TRXs within a BS, the GSM capacity of a cell can be higher or smaller. Therefore, with a variable number of TRXs, one has for the number of users at full rate in one GSM cell, N_{UGSM}:

$$N_{UGSM} = (N_{TRX} \times 8) \times 0.9 \times \frac{N_{TCH}}{N_{CH}} \quad (2.1)$$

where:

- N_{TRX} is the number of TRX placed in one GSM site.
- N_{TCH} is the number of traffic channels.
- N_{CH} is the number of available channels.

GSM BSs transmitters have power classes that limit the transmitted power, as well as MTs. Due to the use of FDMA/TDMA, the maximum power is the same for all users, so the only limitation in coverage is by path loss. For this reason, GSM cells are used to guarantee the coverage levels, enabling the user to make a call from everywhere.

Finally, in order to reduce signalling and control communication between BSs and MTs, when the MT is idle, its location is known only at the service area level. When it becomes active, the nearest BS locates the MT at cellular level.

2.3.2 UMTS

Since in UMTS users share the same frequency band, they are always interfering with each other, meaning that capacity and interference are user dependent.

The interference margin, M_I, is needed to include the effect of the traffic generated by users in a BS in the coverage of that cell. This margin is given by [Corr10]:

$$M_{I[\mathrm{dB}]} = -10\log_{10}(1-\eta) \tag{2.2}$$

where:

- η: load factor.

The load of a cell is characterised by η and this is used to estimate the amount of traffic a BS supports. The load factor depends on the type of service, and for UL if is defined for a given user *j* by [Corr10]:

$$\eta_{UL} = 1 + i\sum_{j=1}^{N_U}\frac{1}{1+\frac{G_{Pj}}{\left(E_b/N_0\right)_j}\upsilon_j} \tag{2.3}$$

where:

- i: normalised inter-cell interference ratio, typically between 40% and 60%;
- N_U: number of users per cell;
- $(E_b/N_0)_j$: SNR of user *j*, given by the ratio between the energy per bit (E_b) and the noise power spectral density ratio of the UE (N_0), in order to meet a predefined QoS;
- υ_j: activity factor of user *j*, typically 50% for voice and 100% for data;
- G_{Pj}: processing gain of user *j*, given by:

$$G_{Pj} = \frac{R_c}{R_{bj}} \tag{2.4}$$

- R_c: chip rate;
- R_{bj}: bit rate of user *j*;

The UL load factor depends strongly on the number of users in the cell, because the MT has its own transmitter power. On the other hand, in DL, the transmitted power of the BS is shared by all active users, which leads to a limited capacity due to restrictions in this transmitted power.

$$\eta_{DL} = \sum_{j=1}^{N_U}\upsilon_j\frac{\left(E_b/N_0\right)_j}{G_{Pj}}\left[\left(1-\alpha_j\right)+i_j\right] \tag{2.5}$$

where:

- α_j : code orthogonality of user *j*, typically between 0.5 and 0.9;
- i_j : inter-cell interference ratio of user *j*.

Therefore, the DL load factor is very important for the calculation of the total transmission power of the BS, P_{TX}, being expressed by:

$$P_{TX\,[\mathrm{W}]} = \frac{N_0 R_c}{1-\overline{\eta_{DL}}}\sum_{j=1}^{N_U}\upsilon_j\overline{L_{p_j}}\frac{(E_b/N_0)_j}{G_{Pj}} \tag{2.6}$$

where:

- $\overline{\eta_{DL}}$: average DL load factor value across the cell;
- $\overline{L_{p_j}}$: average path loss between the Node B and UE for user *j*;

The total transmission power of the BS is divided into two components, one for the traffic channels and the other for the common channels, which means that the power used for data is always lower than the one obtained by the previous expression. At the common channels, the transmission power is used for synchronisation, channel estimation accuracy and the reception quality of the broadcast channel.

Assuming data for the user activity factor (ν = 100%), and that every user is at the same distance from the BS, requesting the same bit rate, one gets:

$$P_{TX\,[\mathrm{W}]} = \frac{N_0 R_b N_U \overline{L_p} \left(\frac{E_b}{N_0}\right)}{1 - \eta_{DL}} \tag{2.7}$$

Considering that each user has the same power received by the BS, P_{TU} is defined as the power assigned for each user,

$$P_{TU\,[\mathrm{W}]} = \frac{P_{TX\,[\mathrm{W}]}}{N_U} = \frac{N_0 R_b \overline{L_p} \left(\frac{E_b}{N_0}\right)}{1 - \eta_{DL}} \tag{2.8}$$

The raise of the load factor causes the increase of the interference margin, which leads to the reduction of the coverage radius. In rural areas, coverage depends on η_{UL} and on MTs P_{TX}. On the other hand, in urban environment, η_{DL} has the biggest dependency of cell capacity.

The coverage radius of a given cell can be estimated using the definition of the path loss and the model of the average power decay with distance, being given by:

$$d_{[\mathrm{km}]} = 10^{\frac{P_{TX\,[\mathrm{dBm}]} + G_{t\,[\mathrm{dBi}]} - P_{r\,[\mathrm{dBm}]} + G_{r\,[\mathrm{dBi}]} - L_{ref\,[\mathrm{dB}]}}{10 a_{pd}}} \tag{2.9}$$

where:

- G_t: gain of the transmitting antenna;
- P_r: power available at the receiving antenna;
- G_r: gain of the receiving antenna;
- L_{ref}: propagation model losses;
- a_{pd}: average power decay.

Taking (2.8) and (2.9), one obtains an expression that gives the maximum number of users for a specific data rate:

$$N_U = \frac{1 - 10^{\frac{-P_{TU\,[\mathrm{dBW}]} - G_{t\,[\mathrm{dBi}]} - G_{r\,[\mathrm{dBi}]} + \left(E_b/N_0\right)_{[\mathrm{dBW}]} - G_{p\,[\mathrm{dB}]} + \overline{L_p}_{[\mathrm{dB}]} + N_{0[\mathrm{dBW}]} + 10 a_{pd} \log(d_{[\mathrm{km}]})}{10}}}{\frac{E_b/N_0}{G_p}[(1-\alpha)+i]} \tag{2.10}$$

Finally, with some manipulation of the previous equation to determine the cell radius for a specific user data rate, one gets:

$$d_{[\mathrm{km}]} = 10^{\frac{P_{TU\,[\mathrm{dBW}]} + G_{t\,[\mathrm{dBi}]} + G_{r\,[\mathrm{dBi}]} - \left(E_b/N_0\right)_{[\mathrm{dBW}]} + G_{p\,[\mathrm{dBi}]} - \overline{L_p}_{[\mathrm{dB}]} - N_{0[\mathrm{dBW}]} + 10\log_{10}\left(1 - N_U \frac{E_b/N_0}{G_p}[(1-\alpha)+i]\right)}{10 a_{pd}}} \tag{2.11}$$

UMTS does not have power classes, so BSs are divided in macro-, micro- and pico-cells, each cell having its transmitted power interval. The MT has one interval of transmitted power, but it is much larger, among 10 and 33 dBm, and using power control, it is possible to reduce interference between MTs. However, the cell coverage radius is strongly dependent on the data rate requested by the user, so the higher the data rates, the lower the cell range.

2.4 Traffic Models

Traffic is not uniform, neither in time nor in space. In this section, using [KhVT02] for voice and [EARTH10a] and [Mica10] for data, general characteristics for both kinds of traffic are described, and profiles are presented for weekdays and weekends, either in urban and suburban areas. Then, according to [AlQu98] and [SaMu10], temporal models that describe the evolution of traffic along the day are presented.

2.4.1 Voice Traffic

Voice traffic is always associated to a smooth transmission of information, whether inside a timeslot in GSM or using a scrambling code in UMTS, which leads to low requirements for the data rate. However, voice traffic is extremely sensitive to packet loss and has low tolerance to packet delay, because it degrades voice quality.

Traffic intensity at the cellular level is measured according to the traffic load that arrives to a certain BS, coming from two possible situations, in the arrival of a new user access performing a voice or data service, or by handover. In the latter, data traffic is considered a new arrival, but for an incoming handover voice call, this user must have priority among the new call arrivals.

The analysis of a certain urban region leads to the gathering of cells that have similar characteristics [KhVT02] (cell size, number of channels and daily traffic variation trace) and makes possible the creation of distinct activity areas, each one with a specific traffic trace. Hence, three major classes can be defined: an urban centre (downtown), a residential area, and a suburban area. Figure 2.2 illustrates the voice traffic volume along the day at work days and weekends, for two of those regions. The presence of main roads crossing those regions is also of major importance, and can create differences from the expected traffic trace of the respective area.

The urban centre is occupied mainly by offices, which justifies the morning and afternoon peaks at work days, and the low traffic intensity at lunch hour. On the other hand, the residential area is composed by residences and some commerce, being characterised by low and smooth traffic variations at work days, and high peaks at weekends. The suburban area has lower population density and is mainly composed by residential areas.

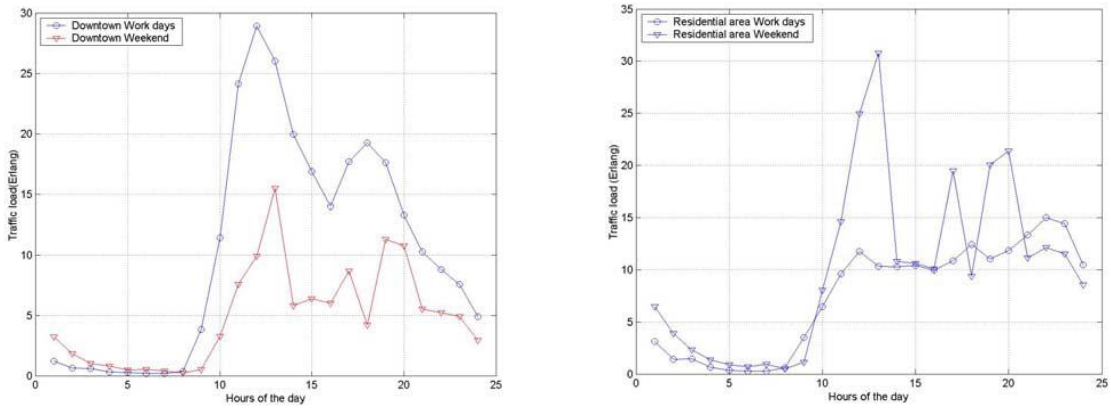

a) Downtown area. b) Residential area.

Figure 2.2 – Daily voice traffic trace (extracted from [KhVT02]).

In [AlQu98], the voice traffic generated at the urban area of Lisbon is analysed, and two types of temporal models, the double-gaussian and the trapezoidal function, were obtained. The first one consists of two gaussian functions with different deviations and centred at the peak of the rush hours (morning and afternoon), with a breakpoint at the lunch hour, and is expressed by:

$$a_{gauss}(t) = \begin{cases} p_1 e^{-\frac{(t-t_1)^2}{2{\tau_1}^2}}, & t < t_l \\ \min\left(p_1 e^{-\frac{(t-t_1)^2}{2{\tau_1}^2}};\ p_2 e^{-\frac{(t-t_2)^2}{2{\tau_2}^2}}\right), & t = t_l \\ p_2 e^{-\frac{(t_{desv}-t_{2desv})^2}{2{\tau_2}^2}}, & t > t_l \end{cases} \quad (2.12)$$

where:

- t: shifted hour time, 5 hours earlier, to obtain a simple analytical model.
- p_1: first gaussian amplitude.
- t_1: morning shifted peak hour.
- τ_1: first gaussian deviation.
- t_l: shifted lunch hour.
- p_2: second gaussian amplitude.
- t_2: afternoon shifted peak hour.
- τ_2: second gaussian deviation.

The traffic intensity is also normalised from its peak level in order to able a better comparison between the approximation parameters. Figure 2.3 represents the trace of the double gaussian function:

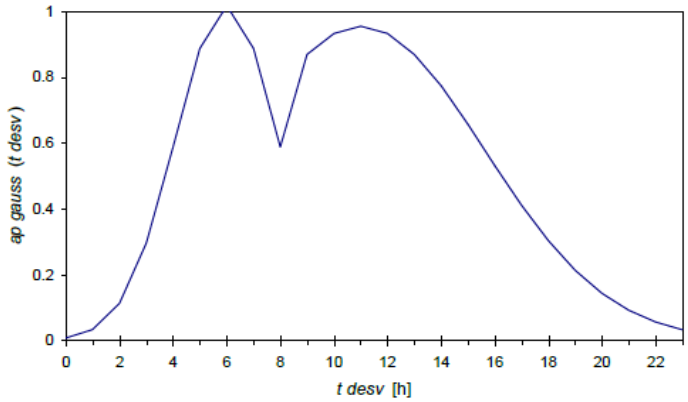

Figure 2.3 – Double gaussian function (extracted from [AlQu98]).

The trapezoidal function is an upper limited gaussian, and is applied when the traffic volume trace is approximately constant for several hours, or when there are more than just two high peaks along the day, Figure 2.4. This function is expressed by:

$$a_{trap}(t) = \begin{cases} pe^{-\frac{(t-t_t)^2}{2\tau_t^2}}, & t < t_{b1} \\ c, & t_{b1} \leq t \leq t_{b2} \\ pe^{-\frac{(t-t_t)^2}{2\tau_t^2}}, & t > t_{b2} \end{cases} \quad (2.13)$$

with: $c = pe^{-\frac{(t_1-t_t)^2}{2\tau_t^2}} = pe^{-\frac{(t_2-t_t)^2}{2\tau_t^2}}$

and where:

- p: gaussian amplitude.
- t_t: shifted peak hour.
- τ_t: gaussian deviation.
- t_{b1}: first shifted function breakpoint.
- c: gaussian upper limit.
- t_{b2}: second shifted function breakpoint.

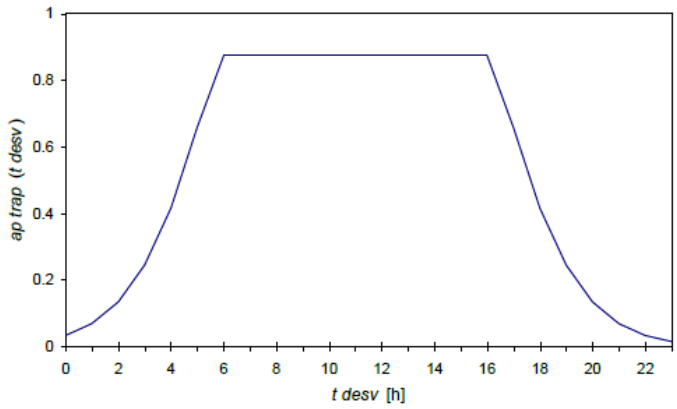

Figure 2.4 – Trapezoidal function (extracted from [AlQu98]).

2.4.2 Data Traffic

Data traffic uses data bursts, and therefore attempts to use as much bandwidth as the network or the user subscription allows. The amount of required bandwidth depends on the application, but for FTP (File Transfer Protocol), it uses the maximum bandwidth available for the subscriber. It is “insensitive” to packet loss and packet delay, and with the use of retransmission the information can be received correctly, just with a decrease on the data rate.

In [EARTH10a], a data traffic variation profile along the day is presented, Figure 2.5, obtained by gathering daily data traffic from several european cities, and doing the average of those profiles. Although each city carries its own cultural population day-to-day routines, the profile evolution can be analysed as the general tendency of daily data traffic generation at cellular level.

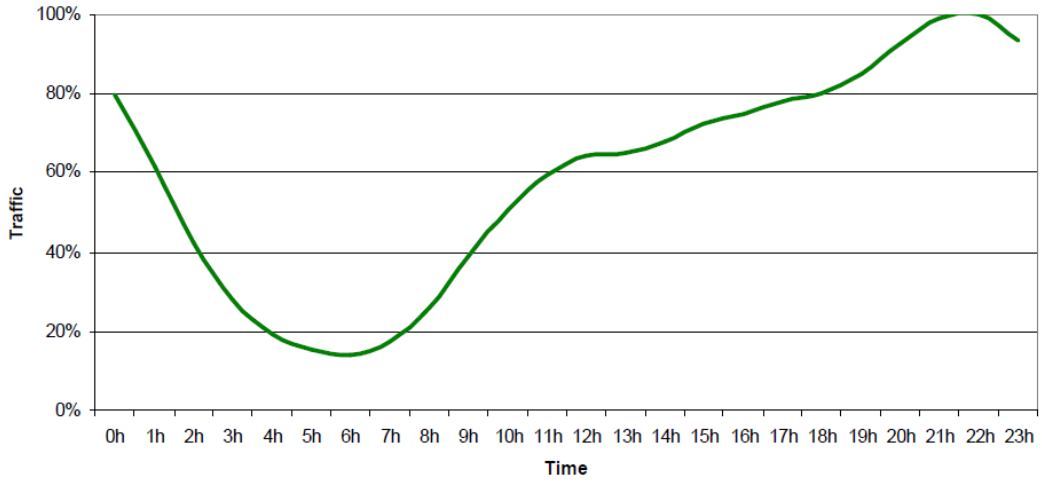

Figure 2.5 – Normalised data traffic daily profile, using the average of European cities profiles (adapted from [EARTH10a]).

For data traffic, there is only one peak that corresponds to the late night period when users are at home downloading all sorts of files, and at lunch hours there is no decrease in traffic as seen for voice. This can be explained by the fact that, at lunch although users do not make voice calls, they still generate FTP or HTTP (Hypertext Transfer Protocol) traffic.

In [Mica10], data traffic measurements from Copenhagen were taken, Figure 2.6. It is also concluded that the average volume of traffic is about 25% lower in weekends than in weekdays. Besides, the busy hour generally occurs at 9pm, which is earlier than the one observed at [EARTH10a].

Analysing the traffic profile of Figure 2.6, one can observe that during an 8 hours period (from 02h00 to 09h00) traffic intensity is about half of the peak value, and that the minimum volume of traffic is 75% lower than the busy hour. This situation leads to inefficient power consumption of the cells with low traffic, for at least 7 hours of the day.

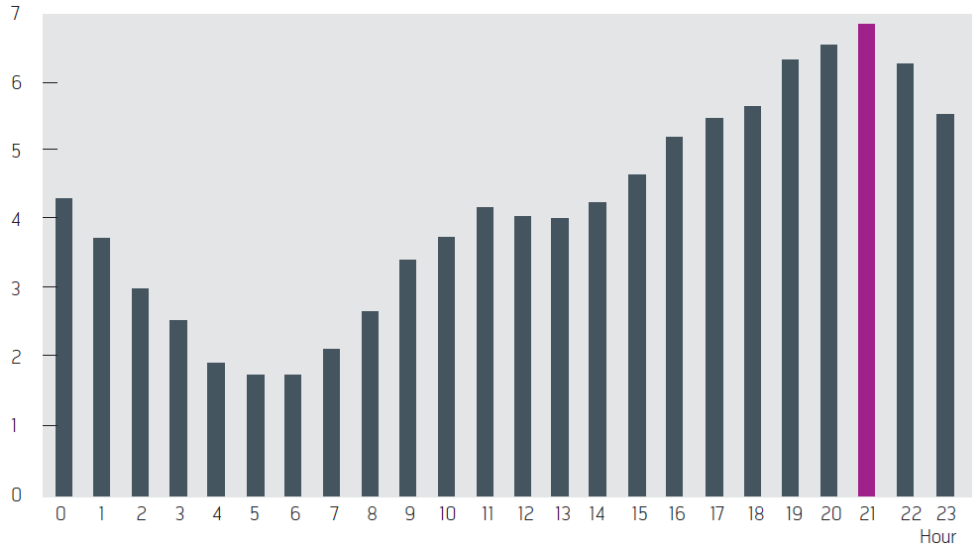

Figure 2.6 – Daily data traffic variation, based on the accumulated volume of HDSPA traffic, normalised over 24 hours (extracted from [Mica10]).

2.5 Base station power consumption

Base stations are the most energy demanding element of cellular networks, amongst the most energy consuming elements being the cooling equipment, power amplifiers (PA), radio frequency (RF) feeders, and AC/DC conversion units. According to [BoCo11], [HHAK11], [KoDe10] and [CZBF10], the energy consumed at one BS is distributed among its composing elements. Then, BS power models are presented at [CZBF10], [ARFB10] and [DVTJ10] in order to determine the dependency of BS power consumption with the users traffic load.

Besides, the cooling equipment has a fair share of the overall consumption, and it depends mainly on the weather conditions, as in a macro-cell the equipment inside the container may cause the increase of the air temperature inside the BS. The backhaul also has to be taken into account, when there is the presence of a microwave link, responsible for communication with the network, in opposition to the use of fibre to link the BS with the backhaul, Figure 2.7 – Site and BS power consuming equipment.. At the BS, the RF carrier and the PA have the biggest slice of the energy consumed, whether the required bandwidth, the SNR and the number of transmitting and receiving antennas are the most relevant aspects for the RF carrier energy consumption, while at the PA, despite the high dependence with the RF output power, it can be very inefficient at low traffic hours. The BB and the DSP consumption depend mainly on the technology platform that is used, as well as the AC/DC converters that connect every BS to the electrical power grid, and the PS, needed to provide a clean and regulated DC power supply to the BS.

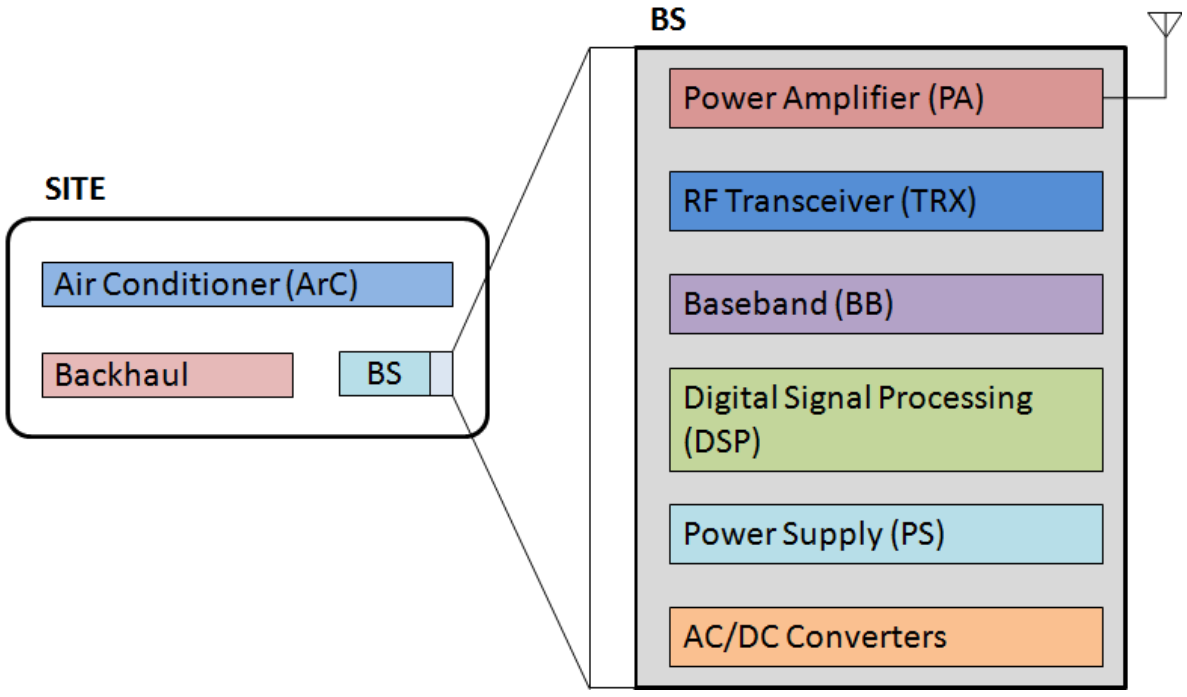

Figure 2.7 – Site and BS power consuming equipment.

As seen in Figure 2.8, the BS has 57% of the power supplied to the site, where the RF carrier and the PA are the major responsible equipments for those high consumption levels. However, with energy efficient solutions, these levels can be reduced, so it is important to distinguish between the elements

from which the power consumption have high dependency with traffic intensity, or other equipment that consumes the same energy despite daily traffic variation.

The power consumption model of a BS consists of two parts. The first one is static, which means that the consumption is independent of the traffic load, so it can only be reduced with equipment upgrades. The other part, dependent on the traffic intensity, is the main focus of energy efficient solutions.

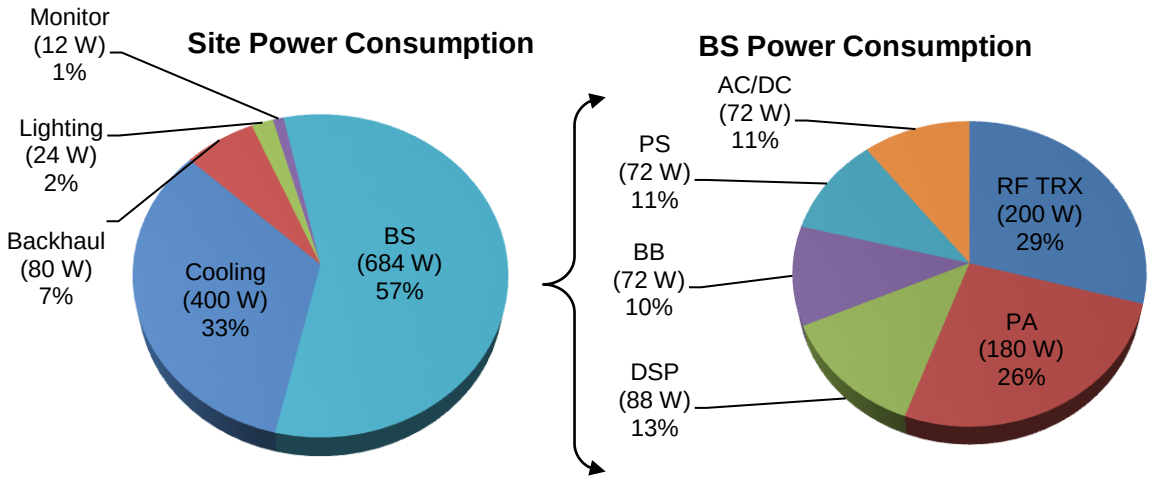

a) Site level. b) Base station level.

Figure 2.8 – Power consumption in different networks levels.

In [CZBF10], [DBMK10] and similarly in [EARTH10a], a very simple linear model is developed, where the output power at the antenna P_{TXM} is calculated as a function of the consumed input power $P_{inMacro}$ at macro-cell BSs:

$$P_{inMacro[\mathrm{W}]} = P_{staticM[\mathrm{W}]} + \Delta_P P_{TXM[\mathrm{W}]}, \quad 0 \le P_{TXM} \le P_{maxM} \tag{2.14}$$

where:

- $P_{staticM}$: traffic independent value of power consumed at macro-cell BS.
- Δ_P: transmitted power coefficient.
- P_{maxM}: maximum transmitted power at the antenna.

In [KoDe10] and [RiFF09], a distinction between macro-cell BSs (considered traffic load independent) and micro-cell ones is done, with the use of the normalised traffic load T_{NORM} as a parameter for this model, taking advantage of features to scale their power consumption with user traffic intensity:

$$P_{inMicro[\mathrm{W}]} = T_{NORM}\left(P_{staticm[\mathrm{W}]} + \Delta_P P_{TXm[\mathrm{W}]}\right) \tag{2.15}$$

where:

- $P_{inMicro}$: consumed power at micro-cell BS.
- $P_{staticm}$: traffic independent value of power consumed at micro-cell BS.
- P_{TXm}: micro-cell BS transmitted power.

Finally, at [ARFB10] power models for both macro- and micro-cell BSs are developed, with higher complexity. Macro-cell BSs have a negligible amount of dynamic power, with daily power consumption variations of about 2% for GSM and 3% for UMTS, so the model is expressed as:

$$P_{inMacro[\mathrm{W}]} = N_{Sector} N_{PApSec} \left(\frac{P_{TXM[\mathrm{W}]}}{\mu_{PA}} + P_{SP[\mathrm{W}]} \right) (1 + L_C)(1 + L_{PSBB}) \quad (2.16)$$

where:

- N_{Sector}: number of sectors at the macro cell.
- N_{PApSec}: number of PAs per sector.
- μ_{PA}: PA efficiency.
- P_{SP}: signal processing overhead.
- L_C: cooling loss.
- L_{PSBB}: battery backup and power supply loss.

As for micro-cells, the power consumption is of a more dynamic nature due to higher variations in the number of users at the cell, so, one has:

$$P_{inMicro[\mathrm{W}]} = \left(\frac{P_{TXM[\mathrm{W}]}}{\mu_{PA}} L_{TXst} + P_{SPst[\mathrm{W}]} \right) (1 + L_{PS}) + \left(\frac{P_{TXM[\mathrm{W}]}}{\mu_{PA}} (1 - L_{TXst}) L_{TXNL} + P_{SPNL[\mathrm{W}]} \right) N_L (1 + L_{PS}) \quad (2.17)$$

where:

- L_{TXst}: static component of the transmitted power loss.
- P_{SPst}: static signal processing consumption.
- L_{PS}: power supply loss.
- L_{TXNL}: dynamic component of the transmitted power loss.
- P_{SPNL}: dynamic signal processing consumption.
- N_L: number of active users.

In [SaEl10], a generic energy consumption model is presented. The most important feature of this model is its dependence on the number of active TRXs, on top of the traffic load variation factor. So, the total BS energy consumption is given by P:

$$P(\rho_1, \rho_2, \ldots, \rho_R)_{[\mathrm{W}]} = P_{cst[\mathrm{W}]} + \sum_{r=1}^{R} \left(P_{TRX[\mathrm{W}]} + \rho_r \frac{P_{MAX[\mathrm{W}]}}{c} \right) \quad (2.18)$$

where:

- P_{cst}: fixed power consumption value, due to transport and processing units.
- R: number of available resources (for example, number of TRXs).
- r: resource index.
- P_{TRX}: fixed power consumption of the TRX.
- ρ_r: load of the resource r.
- P_{MAX}: maximum RF output power consumption.
- c: DC to RF conversion factor.

In [Eric11], a comparative study of the total BS power consumption per area is developed, for different cell sizes. This study considers the same simple linear power consumption model, but as the cell size is reduced, the relative weight of the dynamic component increases.

2.6 Energy efficient Models

Energy efficiency can be achieved by several areas of intervention, as seen in [EARTH10b], [CCMM09] and [MCCM09]. At the network implementation level, energy efficient deployment strategies must be developed to guarantee the coverage/capacity trade-off at the minimum power consumption levels. Hence, the use of mixed cell sizes, like indoor femto-cells, low power BSs or the deployment of repeaters or relays, can decrease the energy consumed at macro-cell sites. At the RRM level, resource blocks and transmission power are allocated to the different users in order to optimise one or a set of metrics, like throughput, delay, outage probability and from now on power consumption as well. However, most of those areas of intervention are out of the scope of this thesis.

The network management has the objective to provide self-organising networks, using techniques that enable minimising energy consumption, while meeting performance and QoS requirements for the different services. BS cooperation allows the use of energy efficiently with the communication between neighbour BS. One cooperative method that can be used is the principle of fractional frequency reuse (FFR) [CTZK09], which consists of dividing one cell into two regions: inner and outer regions, Figure 2.9. In the inner region, all of the available bandwidth is assigned, which is reused in all cells, while in the outer one, a frequency reuse of 3 is adopted among neighbouring cells.

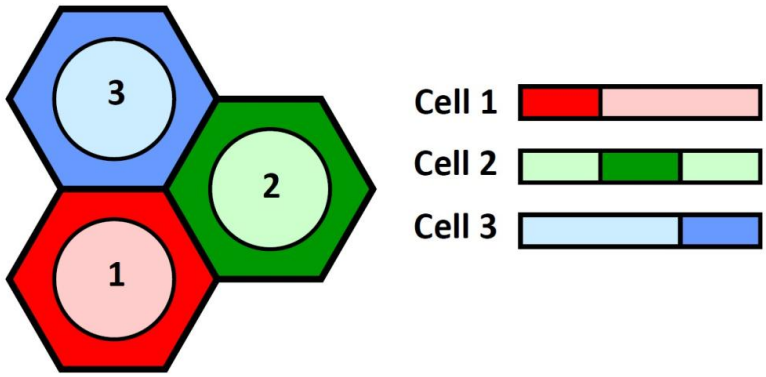

Figure 2.9 – FFR scheme, with frequency reuse of 3 (extracted from [CTZK09]).

Unfortunately, this static configuration for FFR results in inefficient spectral usage, because there may be cells with high traffic generation, while its neighbours can have low traffic intensity. In [CTZK09], a dynamic FFR scheme that can adapt to the cell load is proposed. Dynamic FFR schemes deliver higher cell throughput and spectral efficiency in asymmetric cell load scenarios with the capability of adjusting the spectral resources to each cell load condition.

Another possible approach for a cooperative method is BS cooperation, Figure 2.10, also known as coordinated multi-point (CoMP) communication. Considering perfect backhaul links, the CoMP system becomes equivalent to a distributed multiple-input multiple-output (DMIMO) system, where each antenna cooperates with the neighbours to transmit or receive data, in order to achieve higher SNR with lower transmission power.

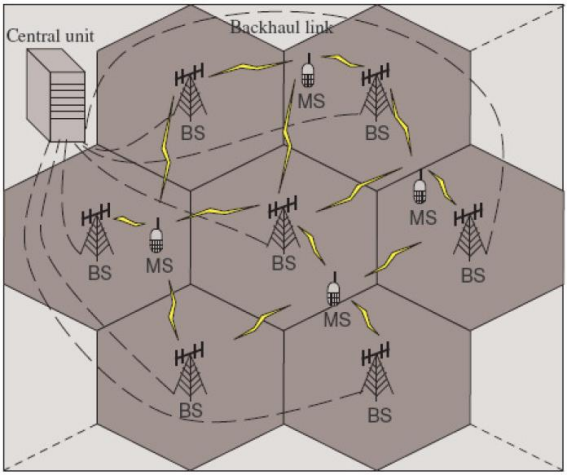

Figure 2.10 – Distributed MIMO system model (extracted from [EARTH10b]).

In [MaFe08], three cooperation schemes between BSs are presented. In the first case, both BSs receive the information from the network and transmit the same message to MTs, corresponding to additional load on backhaul links. The second case is most similar to a non-cooperative network, where just one BS receives the information to the MTs that are in its covered area, but then it forwards the signals via the backhaul in order to be transmitted by other BSs. Finally, it is considered the intermediate situation, where some messages arrive at one BS from the network and other come from the backhaul link between BSs.

Adaptive network solutions are responsible for decreasing the energy consumed at the BSs with the reduction of the number of active network elements, as seen in [Mica10], [FBZF10] and [MiMS10a], and the following solutions are presented: adaptive bandwidth utilization, cell DTX (Discontinuous Transmission), active base stations reduction (switch off schemes) and multi-RAT management. The first solution consists in adaptively adjusting the bandwidth utilization of the network with the daily variation of the traffic, which maximizes the energy efficiency of the PAs at the BSs. As for cells DTX, the main idea is to able energy efficient transmission of data with the interruption of the radio parts at the transceiver, meaning that either the transmitter or the receiver shutdown during one or several timeslots, when those are not being used.

The energy efficient method used in this thesis is to reduce the number of active carriers dynamically, taking into account the daily variation of traffic intensity. These procedures use switch off schemes, which are able to provide considerable energy savings, because the number of active carriers and the power needed from each one is managed and adjusted along the day, according to the network requirements. In [MiMS10a], the concept of cell breathing is used to switch off cells when traffic is low. In this situation, the cell radius for a specific data rate is larger than the radius of a fully loaded cell, and one can say that for low traffic hours the cells expand and overlap each other, making some cells redundant in areas with high density of sites. This procedure can be done either at site level, where all sectors within a particular site are switched off, or at cell level, where each cell is put into sleep mode individually, allowing a greater flexibility for the network to adapt to traffic variations. In addition, on top of putting the cells on sleep mode, electrical tilting of the antennas is performed to optimise coverage at cell boarders.

In [EARTH10b], static and dynamic models are implemented, using ½ and ¼ switch off schemes, which consist in configurations that just keep 1 of 2, or 1 of 4 BSs on, after the management action is performed. A static model applies only one switch off scheme along the day, while a dynamical model allows the transition between several schemes, depending on the load variation at a certain area. Using the ½ switch off scheme, with T_{NORM} being the normalised traffic load of the cell, when the normalised load is below 0.5, one of two cells can be switched off, as seen in Figure 2.11. However, while in the second time slot the energy savings are high using the ½ switch off scheme, for the first time slot it can be inefficient. Hence, there is the need for each cell to have more complex adaptive models to sudden changes of the traffic, like threshold intervals. In [CCMM09], two possibilities are considered. In the first, as soon as the switch off decision is taken, the BS blocks every new request, and waits until all services are processed to switch off the BS. The delay between the decision and the actual switch off depends on the duration of the longest service in progress at the time of the decision. The second possibility consists of forcing a handover from the Node B that is going to be switched off to the ones that remain active. Actually, this procedure is already used in case of special maintenance that needs to be performed to a specific BS. This way, the time between the switch off decision and the actual switch off of the BS is very low, so as to maximise the energy saving.

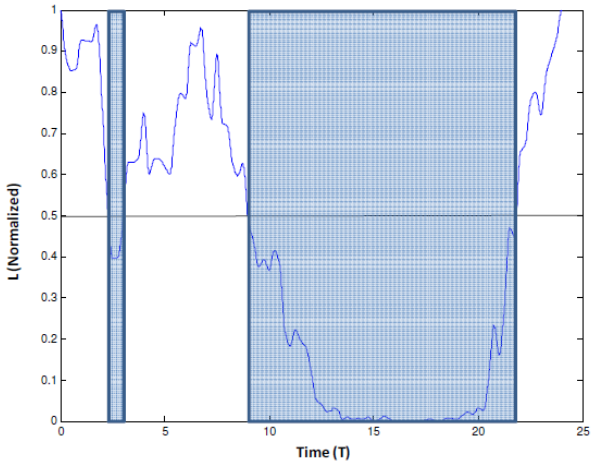

Figure 2.11 – Time slots for ½ switch off schemes (extracted from [EARTH10b]).

The third adopted solution consists of multi-RAT management, Figure 2.12, in which macro-cells, also called umbrella cells [CCMM09], with higher locations should provide basic coverage, and micro-cells deployed for capacity reasons, using other RATs are the potential candidates for energy savings. From this point of view, the GSM network guarantees coverage requirements, and is mostly used for conversational services, while the UMTS network is responsible for data.

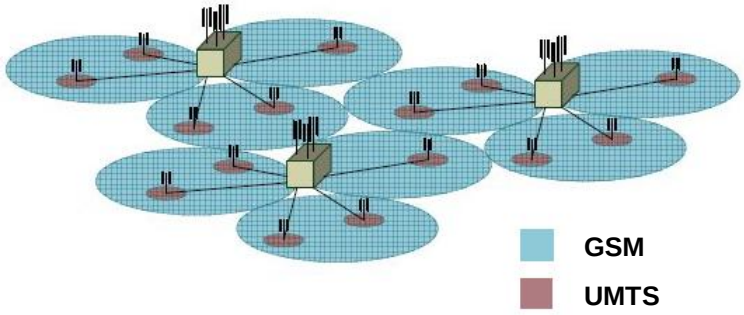

Figure 2.12 – Distinct RAT cells overlay for the increase of capacity (adapted from [3GPP10]).

In [MiMS10b], the objective of reducing energy consumption at the BS without resulting in QoS degradation is explored. When traffic load is low, one of the carriers is shutdown because the use of two parallel carriers leads to the need of two PAs, and these equipments power consumption has a large contribution to the total BS one. The developed feature analyses traffic variations to see whether it is possible to switch off one of the carriers. If the load in a particular sector is low enough so that all users can be guaranteed their minimum requested data rate over a single carrier, then and only then can the secondary carrier be switched off. This procedure gives energy savings from 14% to 36%, considering different traffic load scenarios.

In [SaEl10], sleep modes for the carriers are also presented, but in this case, concerning two major issues that may lead to problems in the network. At first, the carrier activation time is analysed due to the possibility of call and handover arrivals being blocked while the equipment is activating. so, a conservative frontier is defined, below the limit of load in which all available resources are used. The second approach concerns the so-called “ping-pong effect”, in which the equipment is activated/deactivated several times due to oscillations in the traffic load near the capacity frontier. To avoid this, a hysteresis time is defined before deactivating a resource when its deactivation frontier is crossed, to make sure that the traffic is really decreasing.

Chapter 3

Traffic Models

In this chapter, the traffic models developed in this thesis are presented. In Section 3.1, the process of data collection and analysis is described, in Section 3.2 voice and data traffic models are constructed, and then in Section 3.3 the approximation results are analysed. Finally, in Section 3.4 the use of the traffic models along with the collected data is analysed, and correlation scenarios are shown and discussed.

3.1 Data Analysis

Traffic load within one cell has strong variations over the day, caused by the daily user activity. To understand and characterise these daily variations, traffic data was collected from two Portuguese cities, one with 65 GSM and 72 UMTS sectors serving 56 000 inhabitants in an interior region of Portugal, and with a slightly irregular terrain, and the other with 93 2G and 127 3G sectors serving 127 000 inhabitants living near the coastline, and its area composed of regular and plane surfaces. Both these regions have dense urban to rural areas. Traffic values are divided between voice and data services, which are measured in Erl and Mbps, respectively, and data traffic from R99, HSDPA and HSUPA being gathered within a one hourly data traffic measure.

The collected data consists of hourly traffic values from 00:00 to 24:00, for 8 consecutive days, 6 of them being weekdays and the other two from weekend, taken in May, to minimize the effect of season migratory increase of population during holydays in those regions, which would lead to the increase of population and therefore the load of the network. Even though, the existence of a religious holiday in May 13th increased drastically the maximum value of traffic load generated at certain BSs, which was neglected to produce scenarios with a good approximation to reality. In this way, peak traffic load values up to 22.24 Erl are put apart from the absolute traffic load analysis. This leads to more accurate results from each region traffic load generation point of view, and as well as concerning a comparative perspective between regions.

For each sector, after the voice/data and weekday/weekend division, one obtained 6 voice and data traffic profiles for weekdays, and 2 for weekends, as seen in Annex A. Then, a daily profile is made for each case, with the average of the 6 and 2 days, respectively, both for voice and data, which is called from now on weekday or weekend sector daily traffic profile $f^{sec}_{wd/we}(t_h)$, given by:

$$f^{sec}_{wd/we}(t_h) = \frac{1}{N_{wd/we}} \sum_{n=1}^{N_{wd/we}} f^{sec}_{wdn/wen}(t_h) \tag{3.1}$$

where:

- t_h: hour value.
- $N_{wd/we}$: total number of weekday or weekend daily traffic profiles.
- n: daily traffic profile index.
- $f^{sec}_{wdn/wen}(t_h)$: hourly traffic load value, from the weekday or weekend traffic profile.

Then, each sector profile is normalised to its maximum daily traffic value and shifted five hours, in order to match the lowest value of the traffic profile with the origin of each graph, as suggested in [AlQu98]. If, for voice, this value of shifted hours is known to produce the best approximation values, for data, the best shift needs to be determined. The normalisation will preserve the daily traffic load variation shape despite the size of the BS, while the shift will minimise the error between profiles and models, as shown later.

Each sector profile is analysed in order to perceive certain tendencies on the daily evolution of the traffic load. Then, for each tendency, similar traffic profiles are grouped and finally an average is made

between the similar traffic profiles, for each group of similar profiles, using just the sectors that have maximum traffic load value larger than 0.5 Erl for 2G or 0.7 Erl for 3G, and 0.4 Mbps for data. Thus, one obtains several average traffic profiles, as shown in (3.2), one for each group of similar daily traffic variation profiles. The difference between the threshold of the 2G and 3G sectors is explained by the profiles daily behaviour, as the irregularity of the 3G profiles must be balanced with a higher decision limit. These criteria for the use of pre-selected sector profiles are based on the analysis of each daily traffic profile.

$$f_{avg}^{sec}(t_h) = \frac{1}{N_{sec}} \sum_{n_{sec}=1}^{N_{sec}} f_{wd/we}^{sec}(t_h) \tag{3.2}$$

where:

- f_{avg}^{sec}: average daily traffic profile.
- N_{sec}: total number of pre-selected sectors.
- n_{sec}: pre-selected sector index.

After the average traffic profile, one also obtained the standard deviation $\sigma_{avg}(t_h)$ between the first and all similar sector profiles, which is used further in the power consumption models, given by:

$$\sigma_{avg}(t_h) = \sqrt{\frac{1}{N_{sec}} \sum_{n_{sec}=1}^{N_{sec}} \left(f_{avg}^{sec}(t_h) - f_{wd/we}^{sec}(t_h) \right)^2} \tag{3.3}$$

from which one obtains the average standard deviation from each group of pre-selected sectors:

$$\overline{\sigma_{avg}} = \frac{1}{24} \sum_{h=1}^{24} \sigma_{avg}(t_h) \tag{3.4}$$

To better understand the network from which the traffic data was collected, one obtained the Probability Density Functions (PDFs) from which one can perceive the number of sectors with the approximate value of maximum traffic load, for voice and data. Voice sectors were separated into 2G and 3G, because, as it would be expected, the 3G network does not give priority to the voice service, so the maximum voice traffic load values registered are lower than the ones obtained for the 2G network. Hence, as seen in Figure 3.1, while for 2G the largest amount of sectors has 2 Erl of maximum traffic load, in the 3G network the mode is around 0.5 Erl. Furthermore, one can see that the highest value of traffic load of the 2G sectors is more than two times the one from the 3G sectors. This situation justifies the choice of the pre-selection thresholds for the voice traffic profiles, giving a lower value for the 2G sectors, and a higher limit for 3G, reducing the number of irregular 3G voice traffic profiles that integrate the model approximation procedure. Taking into account the weekday to weekend profiles' relation in traffic load, one concludes that there is a considerable reduction in the load values. For instance, the maximum values of traffic load at weekends obtained are 6.74 Erl for 2G and 1.90 Erl for 3G, and if the traffic load value to which most of the sectors are associated is kept at 2 Erl for GSM, it decreases to 0.25 Erl for UMTS.

As for data, and regarding 3G, one observed that most of the sectors have a maximum value of traffic load of 1.5 Mbps, and that the sector with the highest peak of traffic load has 4.26 Mbps, Figure 3.2. Unlike voice at weekends, the sectors PDF is similar between weekdays and weekends, with a slight decrease on the value of traffic to which the largest number of sectors is associated. On the other hand, the absolute maximum of data traffic load is observed at the weekend, with 4.63 Mbps of peak

value. The absolute values of the maximum traffic load are described in Chapter 5 along with the scenario description, to introduce the use of traffic load amplitude as input of the Energy Efficient Model.

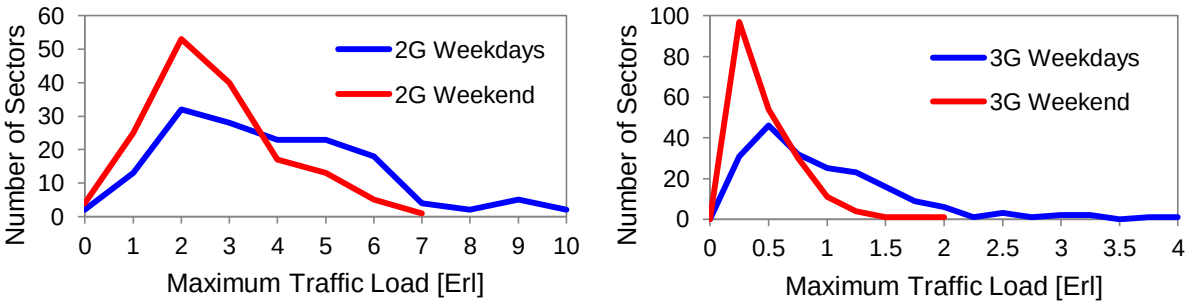

a) 2G. b) 3G.

Figure 3.1 – Sectors' PDF among the maximum value of traffic load, for voice.

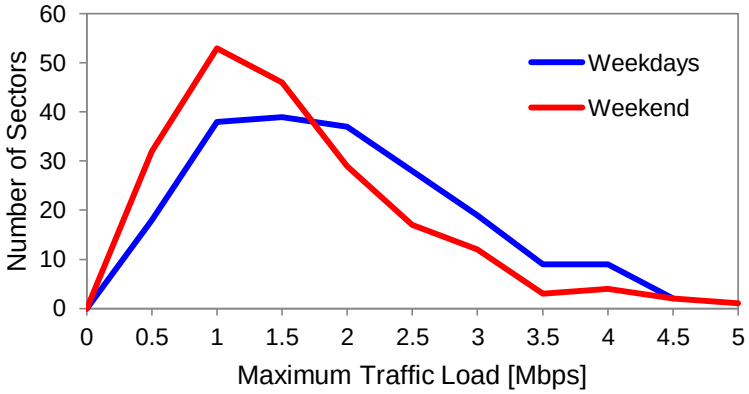

Figure 3.2 – Sectors' PDF among the maximum value of traffic load, for data.

To obtain the traffic models, one uses simple analytical functions and, to get a better approximation, the models are composed by piecewise sections of these functions, with the guarantee of continuity between the distinct sections, and between the last point (corresponding to 24h00) and the first (corresponding to 00h00) of each traffic model. For voice, and according to [AlQu98], two traffic models are already considered, while for data only one traffic model is regularly published, as seen in [EARTH10a].

3.2 Traffic Models

3.2.1 Fitting Process

Each average traffic profile was used to create a traffic model, using the function "fit" from Matlab, which is based on the Large Scale Trust-Region Reflective Least Squares algorithm, in order to obtain the best fit of the average profile, and then each model is evaluated using the Root Mean Squared Error (RMSE) and the Coefficient of Correlation R^2, given by:

$$RMSE = \sqrt{\frac{1}{24}\sum_{h=1}^{24}\left(f_{avg}^{sec}(t_h) - f_{MOD}(t_h)\right)^2} \tag{3.5}$$

where:

- $f_{MOD}(t_h)$: traffic model profile.

$$R^2 = 1 - \frac{\sum_{h=1}^{24}\left(f_{avg}^{sec}(t_h) - f_{MOD}(t_h)\right)^2}{\sum_{h=1}^{24}\left(f_{avg}^{sec}(t_h) - \overline{f_{avg}^{sec}}\right)^2} \tag{3.6}$$

where:

- $\overline{f_{avg}^{sec}}$: average value of the pre-selected traffic profile.

As explained before, the average traffic profiles are shifted in time, so, instead of having the standard temporal axis t, one has:

$$t_{shift[\mathrm{h}]} = \begin{cases} t_{[\mathrm{h}]} - t_{nshift}, & t_{hshift} \le t_{[\mathrm{h}]} < 24 \\ t_{[\mathrm{h}]} - t_{nshift} + 24, & 0 \le t_{[\mathrm{h}]} < t_{nshift} \end{cases} \tag{3.7}$$

where:

- t_{shift}: shifted hour time.
- t_{nshift}: number of shifted hours.

The reason to use the parameter t_{nshift} is to study the results of the approximations between average profiles and each model for different values of shift. For the voice profiles, the value of 5 hours is commonly known and should provide the best results but, for data traffic profiles, there is the need to compare between several shift hours (5, 6 and 7 hours), because there are no published results or studies around this subject.

3.2.2 Voice Traffic Models

One of the models developed in [AlQu98] is the Double Gaussian Model (DGM). It is defined by two sections, each one with a gaussian function adjusted to the morning and afternoon peaks. The junction point between the two functions represents the lunch hour, Figure 3.3.

$$f_{Dgauss}(t_{shift}) = \begin{cases} a_{Dg1}e^{\left(-\left(\frac{(t_{shift}-t_{Dg1})}{\tau_{Dg1}}\right)^2\right)}, & t_{shift} \le t_{lunchshitf} \\ d_{Dg2} + a_{Dg2}e^{\left(-\left(\frac{(t_{shift}-t_{Dg2})}{\tau_{Dg2}}\right)^2\right)}, & t_{shift} > t_{lunchshitf} \end{cases} \tag{3.8}$$

with $f_{Dgauss}(t_{lunchshitf}) = a_{Dg1}e^{\left(-\left(\frac{(t_{lunchshift}-t_{Dg1})}{\tau_{Dg1}}\right)^2\right)} = d_{Dg2} + a_{Dg2}e^{\left(-\left(\frac{(t_{lunchshift}-t_{Dg2})}{\tau_{Dg2}}\right)^2\right)}$.

where:

- a_{Dg1}: first gaussian amplitude.
- t_{Dg1}: morning shifted peak hour.
- τ_{Dg1}: first gaussian deviation.
- $t_{lunchshitf}$: shifted lunch hour.
- a_{Dg2}: second gaussian amplitude.
- t_{Dg2}: afternoon shifted peak hour.

- τ_{Dg2}: second gaussian deviation.
- d_{Dg2}: second gaussian offset.

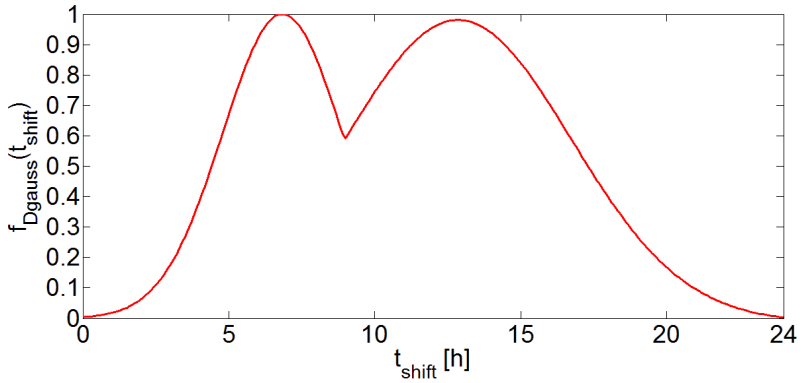

Figure 3.3 – Double Gaussian Traffic Model.

The second model in [AlQu98] is the Trapezoidal Model (TrM), Figure 3.4. This model consists of two exponential sections joined with a linear constant function.

$$f_{trap}(t_{shift}) = \begin{cases} a_{tr1}e^{b_{tr1}t_{shift}}, & t_{shift} < t_{tr1shift} \\ c_{tr}, & t_{tr1shift} \leq t_{shift} \leq t_{tr2shift} \\ a_{tr2}e^{b_{tr2}t_{shift}}, & t_{shift} > t_{tr2shift} \end{cases} \quad (3.9)$$

with $c_{tr} = a_{tr1}e^{b_{tr1}t_{shift}} = a_{tr2}e^{b_{tr2}t_{shift}}$

where:

- a_{tr1}: first exponential initial value.
- b_{tr1}: first exponential decay factor.
- $t_{tr1shift}$: first breakpoint shifted hour value.
- c_{tr}: linear constant value.
- $t_{tr2shift}$: second breakpoint shifted hour value.
- a_{tr2}: second exponential initial value.
- b_{tr2}: second exponential decay factor.

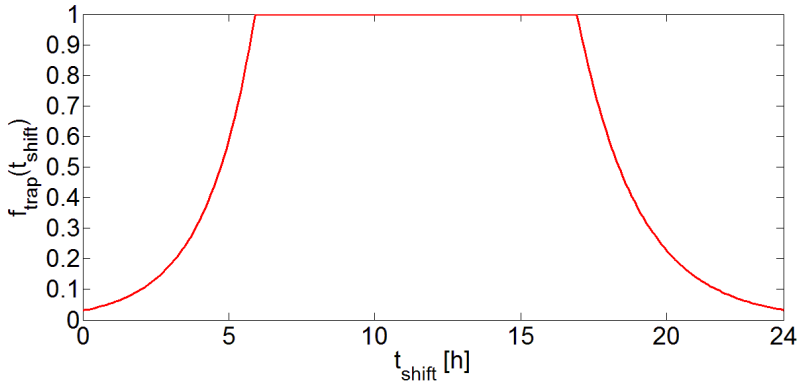

Figure 3.4 – Voice Trapezoidal Traffic Model.

A third voice traffic model is developed in this thesis, called the Tree Stump Model (TSM). Like the Trapezoidal Model, it is defined by two exponential sections and one linear function between them, but in this case the linear segment has a positive slope to adjust to the growing trend seen in several profiles, Figure 3.5.

$$f_{tstump}(t_{shift}) = \begin{cases} a_{ts1}e^{b_{ts1}t_{shift}}, & t_{shift} < t_{ts1shift} \\ m_{ts}t_{shift} + c_{ts}, & t_{ts1shift} \leq t_{shift} \leq t_{ts2shift} \\ c_{ts2} + a_{ts2}e^{b_{ts2}t_{shift}}, & t_{shift} > t_{ts2shift} \end{cases} \quad (3.10)$$

with $c_{ts} = a_{ts1}e^{b_{ts1}t_{ts1shift}}$ and: $c_{ts2} = a_{ts2}e^{b_{ts2}t_{ts2shift}}$

where:

- a_{ts1}: first exponential initial value.
- b_{ts1}: first exponential decay factor.
- $t_{ts1shift}$: first breakpoint shifted hour value.
- m_{ts}: linear function slope.
- c_{ts}: linear function constant value.
- $t_{ts2shift}$: second breakpoint shifted hour value.
- a_{ts2}: second exponential initial value.
- b_{ts2}: second exponential decay factor.
- c_{ts2}: second exponential offset.

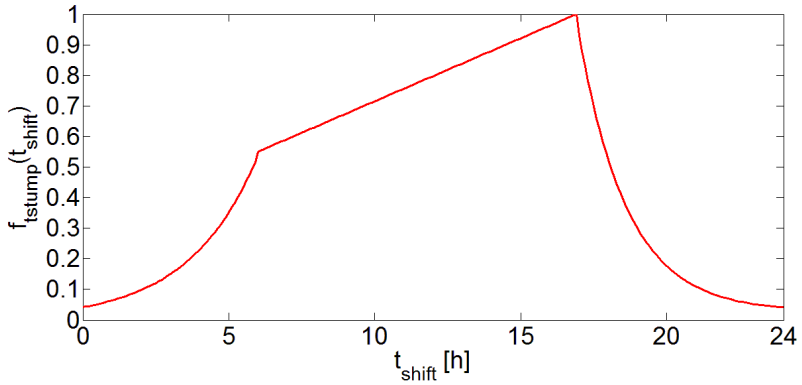

Figure 3.5 – Tree Stump Traffic Model.

3.2.3 Data Traffic Models

For the data traffic models, 4 daily traffic variation tendencies were selected, and therefore 4 traffic models were developed to characterise the use of data in urban areas.

The first model, associated to [EARTH10a], uses one exponential function for the first section, until the maximum value of data traffic load, and then a linear function with negative slope to represent the decrease of data traffic within the night hours, Figure 3.6. This model is called Pyramid Model (PyM) from now on.

$$f_{pyram}(t_{shift}) = \begin{cases} a_{py}e^{b_{py}t_{shift}}, & t_{shift} \leq t_{pymaxshift} \\ m_{py}t_{shift} + c_{py}, & t_{shift} > t_{pymaxshift} \end{cases} \quad (3.11)$$

with $f_{pyram}(t_{pymaxshitf}) = a_{py}e^{b_{py}t_{pymaxshift}} = m_{py}t_{pymaxshift} + c_{py}$

where:

- a_{py}: exponential initial value.
- b_{py}: exponential decay factor.

- $t_{pymaxshift}$: data traffic shifted peak hour value.
- m_{py}: linear function slope.
- c_{py}: linear function offset.

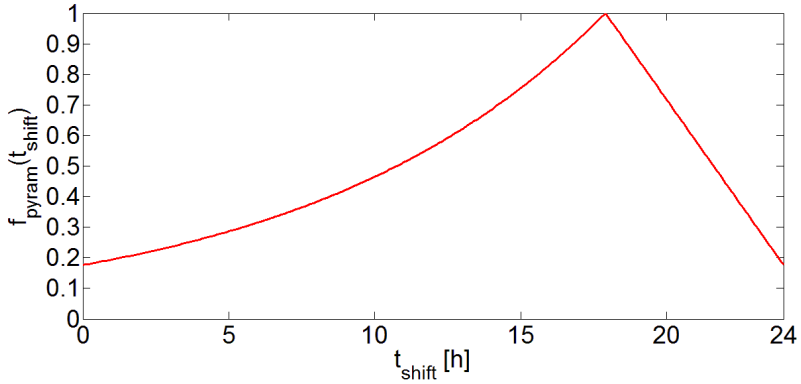

Figure 3.6 – Pyramid Traffic Model.

The second developed model is the Data Trapezoidal Model (DTrM), with two exponentials and one linear function between them, just like the voice traffic profiles, Figure 3.7. However, in this case, another parameter is needed for the offset of the second exponential.

$$f_{trapdata}(t_{shift}) = \begin{cases} a_{trd1}e^{b_{trd1}t_{shift}}, & t_{shift} < t_{trd1shift} \\ c_{trd}\,, & t_{trd1shift} \leq t_{shift} \leq t_{trd2shift} \\ c_{trd2} + a_{trd2}e^{b_{trd2}t_{shift}}, & t_{shift} > t_{trd2shift} \end{cases} \quad (3.12)$$

with: $c_{trd} = a_{trd1}e^{b_{trd1}t_{shift}} = a_{trd2}e^{b_{trd2}t_{shift}}$

where:

- a_{trd1}: first exponential initial value.
- b_{trd1}: first exponential decay factor.
- $t_{trd1shift}$: first breakpoint shifted hour value.
- c_{trd}: linear constant value.
- $t_{trd2shift}$: second breakpoint shifted hour value.
- a_{trd2}: second exponential initial value.
- b_{trd2}: second exponential decay factor.
- c_{trd2}: second exponential offset.

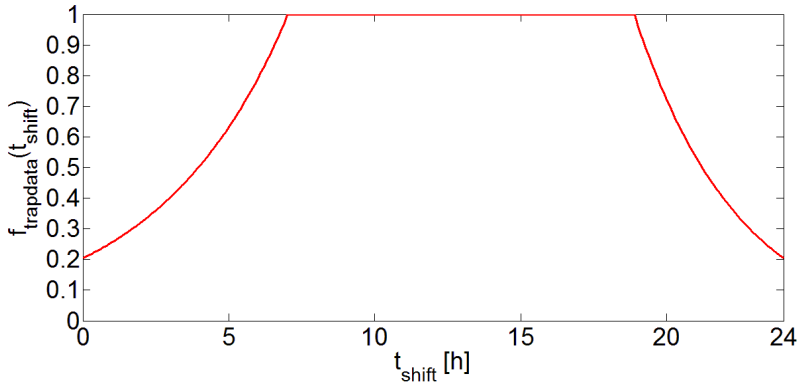

Figure 3.7 – Data Trapezoidal Traffic Model.

A third model, the Swing Model (SwM), was chosen to explain the tendency of several sector profiles to have medium to low data traffic load during the day, and high traffic load at night. It is defined by one exponential, one linear and one gaussian function, Figure 3.8. The use of three different functions

is explained by the distinct behaviours of the traffic variation. At first, the decrease is slow, hence, the use of the exponential function, followed by an interval of almost constant traffic load modelled by the linear function; finally, there is an abrupt increase of the traffic load, which best fit is made by the gaussian function.

$$f_{swing}(t_{shift}) = \begin{cases} a_{sw1}e^{b_{sw1}t_{shift}}, & t_{shift} < t_{sw1shift} \\ c_{sw}, & t_{sw1shift} \leq t_{shift} \leq t_{sw2shift} \\ a_{sw2}e^{\left(-\left(\frac{(t_{shift}-b_{sw2})}{c_{sw2}}\right)^2\right)}, & t_{shift} > t_{sw2shitf} \end{cases} \quad (3.13)$$

with $c_{sw} = a_{sw1}e^{b_{sw1}t_{sw1shift}} = a_{sw2}e^{\left(-\left(\frac{(t_{sw2shift}-b_{sw2})}{c_{sw2}}\right)^2\right)}$

where:

- a_{sw1}: first exponential initial value.
- b_{sw1}: first exponential decay factor.
- $t_{sw1shift}$: first breakpoint shifted hour value.
- c_{sw}: linear function constant value.
- $t_{sw2shift}$: second breakpoint shifted hour value.
- a_{sw2}: second gaussian amplitude.
- b_{sw2}: night shifted peak hour value.
- c_{sw2}: second gaussian deviation.

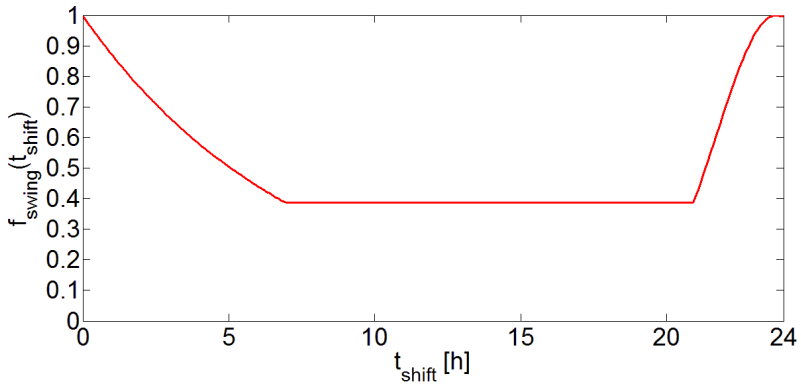

Figure 3.8 – Swing Traffic Model.

The fourth developed data traffic model is the Data Double Gaussian Model (DDGM), also very similar to the voice one, Figure 3.9.

$$f_{Dgaussdata}(t_{shift}) = \begin{cases} a_{Dgd1}e^{\left(-\left(\frac{(t_{shift}-t_{Dgd1})}{T_{Dgd1}}\right)^2\right)}, & t_{shift} \leq t_{lunchdshitf} \\ a_{Dgd2}e^{\left(-\left(\frac{(t_{shift}-t_{Dgd2})}{T_{Dgd2}}\right)^2\right)}, & t_{shift} > t_{lunchdshitf} \end{cases} \quad (3.14)$$

with: $f_{Dgaussdata}(t_{lunchdshitf}) = a_{Dgd1}e^{\left(-\left(\frac{(t_{lunchdshift}-t_{Dgd1})}{T_{Dgd1}}\right)^2\right)} = a_{Dgd2}e^{\left(-\left(\frac{(t_{lunchdshift}-t_{Dgd2})}{T_{Dgd2}}\right)^2\right)}$.

where:

- a_{Dgd1}: first gaussian amplitude.
- t_{Dgd1}: morning shifted peak hour value.
- T_{Dgd1}: first gaussian deviation.

- $t_{lunchdshitf}$: shifted lunch hour.
- a_{Dgd2}: second gaussian amplitude.
- t_{Dgd2}: afternoon shifted peak hour value.
- T_{Dgd2}: second gaussian deviation.

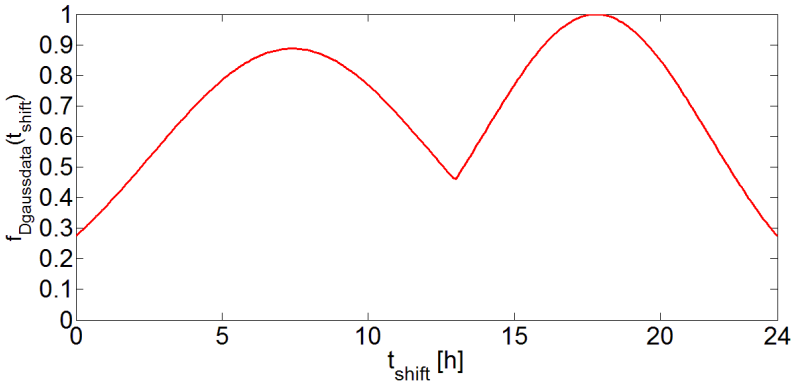

Figure 3.9 – Data Double Gaussian Traffic Model.

3.3 Models Approximation Results

Using the theoretical models previously described, one fitted them to the respective average traffic profiles to obtain the values of the parameters for each model. After each approximation, both traffic model and average profile are normalised to 1, using the maximum value of the traffic model (T_{MAX}) as a reference. Then, RMSE and R^2 are calculated for each model, as well as the average standard deviation σ_{avg}.

For the DG Traffic Model, the parameters are in Table 3.1, providing a good approximation, Figure 3.10, between the traffic profile and its model is visible, as there is a good proximity between them, especially in the morning and afternoon peaks, and at the lunch time minimum.

Table 3.1 – Double Gaussian Traffic Model parameters.

Section	Function	Interval [h]	Parameters			
1	Gaussian	[0;9]	a_{Dg1}= 0.895	t_{Dg1}= 6.937	τ_{Dg1}= 2.911	$t_{lunchshitf}$= 9
2	Gaussian	[9;24]	a_{Dg2}=0.889	t_{Dg2}=4.955	τ_{Dg2}=5.471	d_{Dg2}= -0.0115

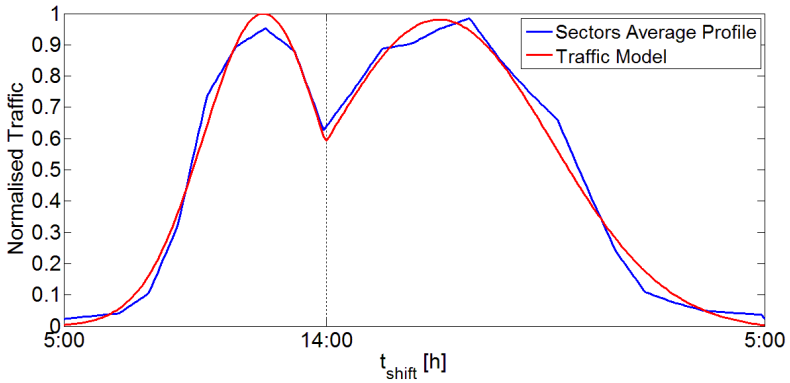

Figure 3.10 – Double Gaussian Traffic Model approximation to the average profile.

For the Trapezoidal Traffic Model, the same parameterisation was made, and the values obtained for the traffic model are shown in Table 3.2.

Table 3.2 – Trapezoidal Traffic Model parameters.

Section	Function	Interval [h]	Parameters		
1	Exponential	[0;6]	$a_{tr1}= 0.023$	$b_{tr1}= 0.590$	$t_{tr1shift}= 6$
2	Linear Constant	[6;17]	$c_{tr}= 0.776$		$t_{tr2shift}= 17$
3	Exponential	[17;24]	$a_{tr2}= 1.273$	$b_{tr2}= -0.482$	

The proximity between model and average profile is visible for both exponential sections, Figure 3.11, and, for the linear section one had to choose the situation with the lower RMSE.

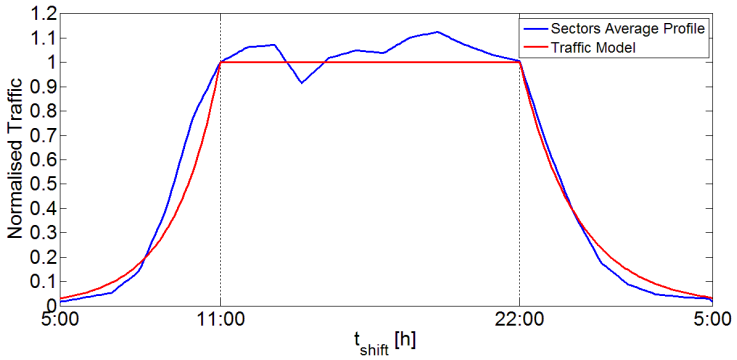

Figure 3.11 – Trapezoidal Model approximation to the average profile.

For the third Voice model, the Tree Stump Traffic Model, parameters were also calculated, Table 3.3, to get the best approximation to the variation of the average sectors profile.

Table 3.3 – Tree Stump Traffic Model parameters.

Section	Function	Interval [h]	Parameters		
1	Exponential	[0;6]	$a_{ts1}= 0.0342$	$b_{ts1}= 0.426$	$t_{ts1shift}= 6$
2	Linear	[6;17]	$m_{ts}= 0.0353$	$c_{ts}= 0.468$	$t_{ts2shift}= 17$
3	Exponential	[17;24]	$a_{ts2}= 1.687$	$b_{ts2}= -0.600$	$c_{ts2}= 0.0233$

In Figure 3.12, one can easily conclude that in the third section, the decreasing behaviour of the average profile is nicely modelled. On the other hand, a compromise had to be made so that the increasing behaviour of the linear section would be represented without sacrificing the values of RMSE, hence, the noticeable deviation of the first exponential section.

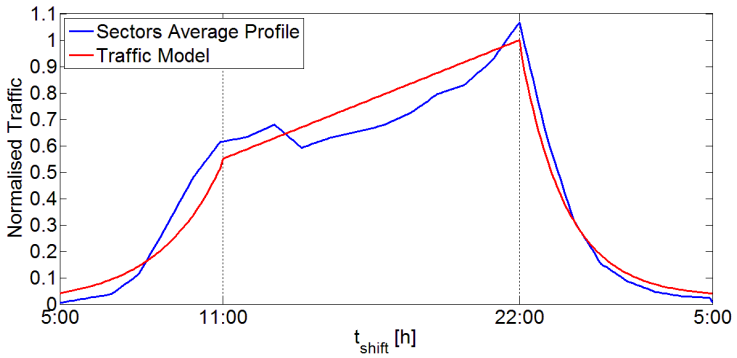

Figure 3.12 – Tree Stump Model approximation to the average profile.

The comparative results among the traffic models are shown in Table 3.4, regarding the fitting assessment parameters. One can conclude that the DG Model is the best approximated one due to its low value of RMSE and R^2. Furthermore, all three RMSE values are low enough to validate the developed models, as it would be expected from the graphical representation of these models, and their respective average sector profiles.

As for σ_{avg}, the obtained values are very similar, and although one needs to consider them on the Energy Efficient Model, their contribution will not incur in a great variation of the average power consumption profile. Finally, concerning T_{MAX}, one can observe that for the DG and the TS models, the original maximum value of the traffic model is already considerably high, so there is no big difference in the representation after the normalisation. On the other hand, for the Tr Model, Tr_{MAX} is lower than the other two, leading to conclude that the normalisation could incur in a situation where this model could lose its importance among the sector profiles collected from the live network.

Table 3.4 – Voice Traffic Models' approximation results.

Voice Traffic Model	RMSE [%]	R^2	σ_{avg} [%]	T_{MAX}
Double Gaussian	4.28	0.9867	29.68	0.8942
Trapezoidal	7.16	0.9737	29.61	0.7761
Tree Stump	7.20	0.9500	34.20	0.8554

Similarly, one proceeded the same way for the Data Traffic Models. For the Pyramid Traffic Model, one obtained the parameters shown in Table 3.5.

Table 3.5 – Pyramid Traffic Model parameters.

Section	Function	Interval [h]	Parameters		
1	Exponential	[0;18]	a_{py}= 0.144	b_{py}= 0.0969	$t_{pymaxshift}$= 18
2	Linear	[18;24]	m_{py}= -0.111	c_{py}= 0.822	

Figure 3.13 shows that, with the use of exponential and the linear sections, one can obtain the best fit for the average profiles. However, due to the irregular behaviour of the data profiles, the σ_{avg} values become higher than for the voice models.

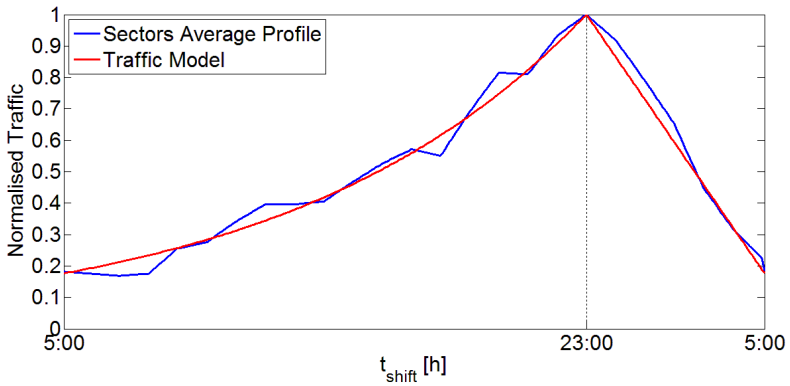

Figure 3.13 – Pyramid Traffic Model approximation to the average profile.

The Data Trapezoidal Traffic Model is characterised by the parameters shown on Table 3.6, which have great similarity with the ones obtained for the Voice Trapezoidal Traffic Model. Once again, data traffic variations create a lot of difficulties in the modelling process, Figure 3.14, even with the sectors pre-selection, the average profile having slight differences from the model.

Table 3.6 – Data Trapezoidal Traffic Model parameters.

Section	Function	Interval [h]	Parameters		
1	Exponential	[0;7]	$a_{trd1}= 0.139$	$b_{trd1}= 0.226$	$t_{trd1shift}= 7$
2	Linear Constant	[7;19]	$c_{trd}= 0.696$		$t_{trd2shift}= 19$
3	Exponential	[19;24]	$a_{trd2}= 1.266$	$b_{trd2}= -0.278$	$c_{trd2}= -0.0336$

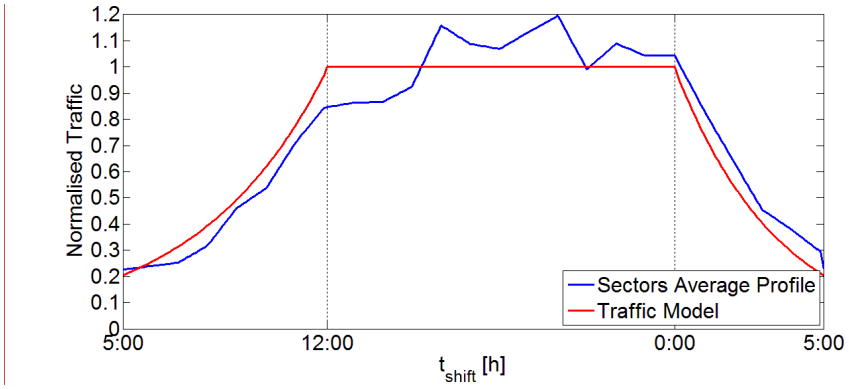

Figure 3.14 – Data Trapezoidal Traffic Model approximation to the average profile.

For the Swing Traffic Model, one obtained the parameters shown in Table 3.7.

Table 3.7 – Swing Traffic Model parameters.

Section	Function	Interval [h]	Parameters		
1	Exponential	[0;7]	$a_{sw1}= 0.858$	$b_{sw1}= -0.136$	$t_{sw1shift}= 7$
2	Linear Constant	[7;21]	$c_{sw}= 0.329$		$t_{sw2shift}= 21$
3	Gaussian	[21;24]	$a_{sw2}= 0.849$	$t_{sw2}= 2.856$	$\tau_{sw2}= 2.913$

Despite the highs and lows, even in the average profile, the model can approximate the slow decrease at early hours and the abrupt rise of the traffic load at late night, Figure 3.15.

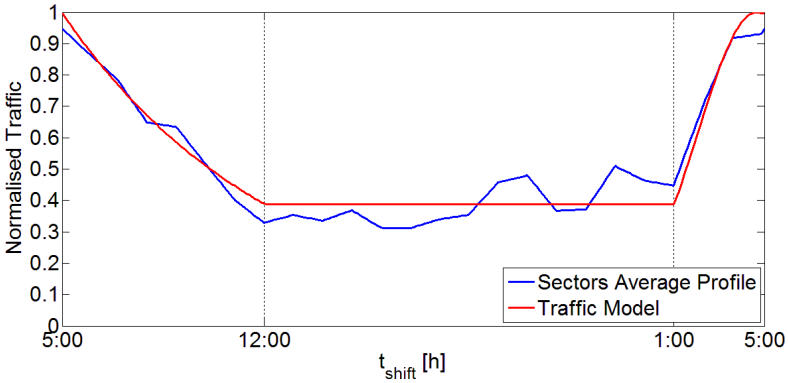

Figure 3.15 – Swing Traffic Model approximation to the average profile.

Finally, for the Data Double Gaussian Traffic Model, one has the parameters, shown in Table 3.8.

Table 3.8 – Data Double Gaussian Traffic Model parameters.

Section	Function	Interval [h]	Parameters			
1	Gaussian	[0;13]	$a_{Dgd1}= 0.8946$	$t_{Dgd1}= 6.937$	$\tau_{Dgd1}= 2.911$	$t_{lunchdshitf}= 9$
2	Gaussian	[13;24]	$a_{Dgd2}=0.8889$	$t_{Dgd2}=4.955$	$\tau_{Dgd2}=5.471$	

This last model was the hardest to approximate, due to its unpredictable variation. With the similar methodology done in the voice traffic models, in particular for the Double Gaussian Traffic Model, one assumed that the traffic load peaks match the maximum values of both gaussian functions. So, although the first section has difficulties to keep up with the traffic load variation, the second gaussian is a good representation of the traffic intensity. As seen in Figure 3.16, and only for this traffic model, the shift that results in lower RMSE between the Data Double Gaussian Traffic Model and the average sectors profile is 6 hours instead of the 5 hours used on the other three data traffic models.

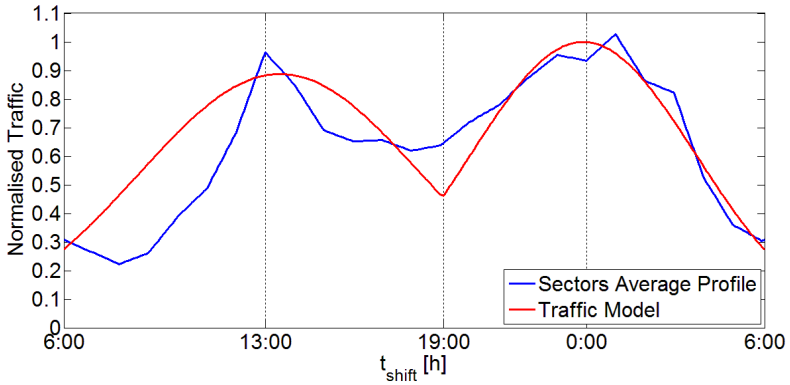

Figure 3.16 – Data Double Gaussian Traffic Model approximation to the average profile.

Finally, a comparative analysis of the results obtained from the models approximations, is presented in Table 3.9, for the Data Traffic Models. Considering the RMSE values, the Pyramid Model has the lowest result, as it would be expected due to the previous knowledge and publications regarding this data traffic model. On the other hand, the Double Gaussian Model has the highest result of RMSE, due to the compromise that had to be done to include the two gaussians. Nevertheless, the values obtained are low enough to validate all traffic models.

The values of σ_{avg} are considerable, taking into account that the profiles are normalised. This situation leads to high variations of the traffic load when this parameter is included in the traffic profiles. Finally, regarding T_{MAX}, the same situation that occurred for the voice traffic models is verified for the Data Trapezoidal Traffic Model, where a low value of this parameter may lead to loss of its weight among the data traffic models in the association process with the sector profiles.

Table 3.9 – Data Traffic Models' approximation results.

Data Traffic Model	RMSE [%]	R^2	σ_{avg} [%]	T_{MAX}
Pyramid	3.61	0.9798	49.56	0.8215
Trapezoidal	9.55	0.9092	47.57	0.6956
Swing	5.47	0.9220	43.14	0.8485
Double Gaussian	14.13	0.6569	41.52	0.7646

3.4 Results Assessment

Based on the traffic models obtained in Section 3.3, one can see to which voice or data traffic models each sector profile belongs to. Furthermore, an analysis of possible relations between weekday and weekend profiles, and voice and data profiles, can be developed with the obtained models.

3.4.1 Sector profiles distribution

The daily traffic variation profiles, with 0h00 as origin, are shown in Figure 3.17 and Figure 3.19, these models were used to verify the pre-selection of the sector profiles for each tendency, by comparing which had the minimum RMSE among the three voice models and four data ones, for each of the sector profiles. This procedure is called from now on Automatic Classification of Sector Profiles, and the results are shown in Table 3.10 and Table 3.11.

From the 150 voice pre-selected sector profiles distributed among the three traffic tendencies, 73 of them kept the same association, which means that 49% of the sector profiles maintained the association that was initially chosen, despite the approximations of the models to the average sector profiles, and the performed normalisation. One explanation for this result is that the maximum traffic load limit of the sector profiles taken into account for the pre-selection is too low, meaning that a considerable number of pre-selected voice traffic profiles are not ideal for the model to which it was selected. However, if this limit would be raised, the number of pre-selected sector profiles to be averaged would decrease, and the model would be a worse representation of the collected voice traffic data. On the other hand, one concludes that below those limits, all profiles fail to belong to a certain tendency, being just composed by peaks of activity at certain hours. For example, if the boundary of the 3G voice sectors was lowered, two problems appeared: first, the traffic models were not so distinct from each other due to the profiles irregularities, and second, the number of sector profiles that would remain associated to the pre-selected tendency decreases after the traffic models approximation, which invalidates the validation of the Automatic Classification procedure.

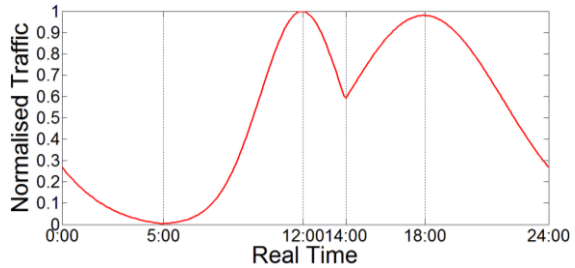

a) Double Gaussian.

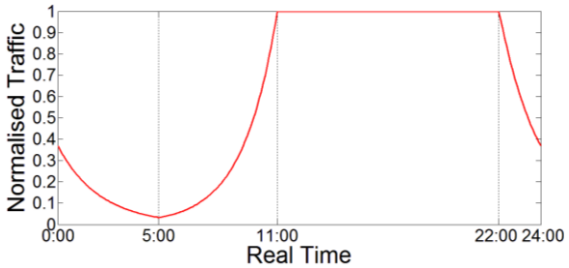

b) Trapezoidal.

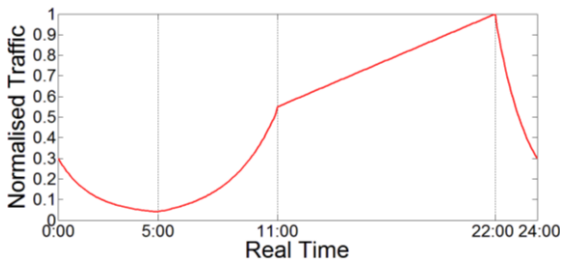

c) Tree Stump.

Figure 3.17 – Real Time Voice Traffic Models.

In Annex B, a list of the sectors, and consequently the BSs that they belong to, is presented containing the maximum value of traffic load in Erl for voice and Mbps for data, and the automatic classification of each sector. From this list, one obtains the Sector Distribution described in this chapter for the regular distribution of sectors.

For the data sector profiles, from the previously selected 112 sector profiles, and distributed by four data traffic models, 79 still remain belonging to the same tendency, representing 71% of profiles that kept their initial association to the traffic model developed.

Based on the Automatic Classification procedure, one obtained the sectors distribution according to their maximum traffic load, Figure 3.18. The PDF for the Trapezoidal model is in Annex C, as well as for the Data Trapezoidal, Swing and Data Double Gaussian ones. For all of these four profiles, the number of associated sectors is too low, hence, the reason for their results being disregarded.

Concerning the Double Gaussian and the Tree Stump models, one can see in Annex B

that for the first case the maximum value of traffic load obtained is 10.02 Erl and that the largest number of sectors has a maximum traffic load around 1 Erl. Similarly, for the Tree Stump model, 92 sectors have a maximum load near 1 Erl, but the maximum value observed is 9.47 Erl. As for the weekend profiles, for both models, there is an increase on the association of sectors with traffic load values around 1 Erl, as well as the reduction on the maximum traffic load obtained, as it would be expected. This situation leads to conclude that, at weekends, the differences between these two regions in the traffic load volume are low and there might be a slight balance with the daily traffic profiles of both urban areas, as it is seen in Section 3.4.4.

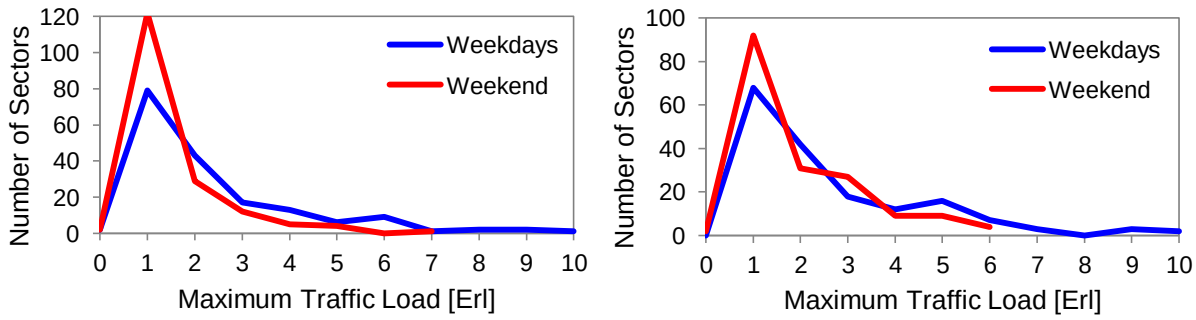

a) Double Gaussian. b) Tree Stump.

Figure 3.18 – Urban region PDF for the voice service.

Table 3.10 shows the distribution of sector profiles within all three voice traffic models. The traffic model “Other” is a group of sector profiles that do not belong to any of the previously developed models, this decision taking into account two conditions: either the RMSE of the sector profile is larger than 0.35, or the maximum traffic load of that traffic profile is lower than 0.1 Erl.

Voice sector profiles were divided in 2G and 3G sectors because some conclusions can be drawn from this decision. For the 2G profiles, it can be seen that the Tree Stump Traffic Model is applicable for most of the sectors, and there are just 7 profiles rejected by all three models do not meet both association conditions (belonging to BSs built to increase the 2G capacity in a certain area). On the other hand, for 3G voice profiles, the Double Gaussian is the model with the highest percentage of

associations, and there is a considerable number of "Other" profiles, mainly due to the priority use of the 3G network for data, which leads to a low voice traffic load or highly irregular daily voice traffic load variation, generating high values of RMSE.

Table 3.10 – Voice Sector Profiles Distribution.

	2G (158 Sectors)		3G (199 Sectors)		TOTAL (357 Sectors)	
Voice Model	**Number of Sectors**	**% of Sectors**	**Number of Sectors**	**% of Sectors**	**Number of Sectors**	**% of Sectors**
Double Gaussian	51	32.3%	101	50.8%	**152**	**42.6%**
Trapezoidal	6	3.8%	2	1.0%	**8**	**2.2%**
Tree Stump	94	59.5%	47	23.6%	**141**	**39.5%**
Other	7	4.4%	49	24.6%	**56**	**15.7%**

In general terms, among the total population of voice sectors, the DG and the TS models are equally used, there is a reasonable slice of the profiles that do not fit any of the developed traffic models, and the Trapezoidal Traffic Model is completely underused. An alternative distribution is developed, where instead of the normalised Trapezoidal Traffic Model, one decided to lower the maximum value of the constant linear function by multiplying the model by its corresponding T_{MAX} value.

The number of associations to the "Other" model, as described previously, can be controlled by varying the limit values of RMSE or maximum traffic load. However, for the 3G sector profiles, a significant number of associations with this model is always verified, leading to conclude that the main reason to this result is the behaviour of the data traffic along the day, which is clearly reflected on the available 3G capacity to be used for voice. So, apart from the non-prioritised use of voice in the 3G network, even that redirected slice of traffic is dependent on the data traffic load of the cell at a certain instant, leading to these highly irregular and very difficult to associate profiles.

All four data traffic models were also shifted to the real time hours, as shown in Figure 3.19, and were associated to the 3G data profiles, in order to perceive which ones were used with most regularity, or even if there were any negligible models.

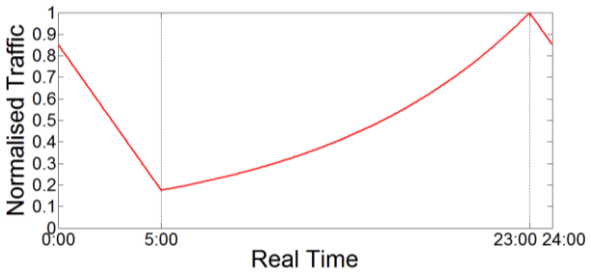

a) Pyramid.

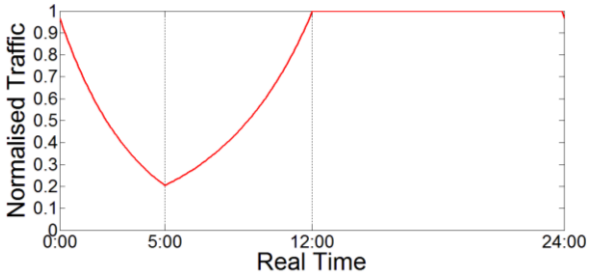

b) Trapezoidal.

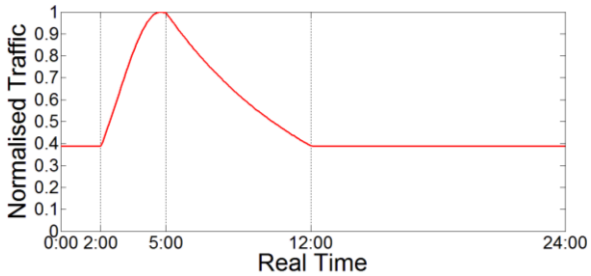

c) Swing.

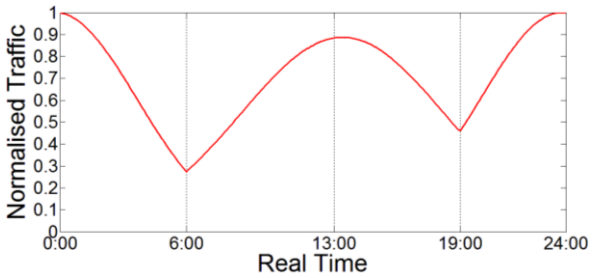

d) Double Gaussian.

Figure 3.19 – Real Time Data Traffic Models.

Similarly, to the voice traffic models, one obtained the sectors distribution according to their maximum traffic load value. In this case, the maximum value of traffic load is 4.26 Mbps, Figure 3.20 showing the PDF for the sectors associated to the Pyramid Traffic Model for weekdays and the weekend. Even though the largest number of sectors has a maximum traffic load of around 1 Mbps, one can conclude that, comparing with the PDFs obtained for voice, as seen in Figure 3.18, the density function is narrower from its peak for voice and for data the maximum values are spread more evenly among the traffic load values. In the PDF for the weekend traffic profiles, the maximum traffic load value obtained is 4.63 Mbps and the PDF shape becomes sharper than the weekdays one, with the decrease of sectors having traffic load values higher than 1.5 Mbps.

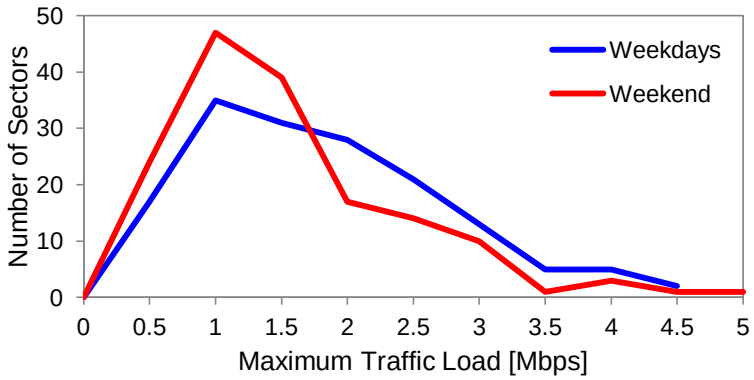

Figure 3.20 – Pyramid region PDF for the data service.

For data profiles, Table 3.11, it is clear that the Pyramid Traffic Model is the most associated tendency within all data traffic models, and the “Other” group has a small group of sector profiles. Similarly to the voice, the “Other” data traffic model was constituted with two conditions, RMSE values larger than 0.35 and maximum traffic load value smaller than 0.1 Mbps. So, one can conclude that the Pyramid Traffic Model has the highest weight among data traffic models, with 68.8% of the associated sectors. Finally, the use of both Swing and Double Gaussian Traffic Model is very low, so these two models can be neglected for use in a live network.

Table 3.11 – Data Sector Profiles Distribution.

Data Model	Number of Sectors	% of Sectors
Pyramid	137	68.8%
Trapezoidal	10	5.0%
Swing	15	7.5%
Double Gaussian	14	7.0%

Other	23	11.6%

3.4.2 Alternative Sector profiles distribution

As an attempt to even the use of the traffic models by the sector profiles, and in order to give a higher importance to the Trapezoidal Model for both voice and data sectors, given that it is one of the commonly known and studied models, an Alternative Distribution was developed. One used the T_{MAX}value of Voice and Data Trapezoidal Models, multiplied by the normalised functions of both, and finally obtaining the Sector Profiles Alternative Distribution results with a higher association to these two models, Table 3.12 and Table 3.13.

This alternative distribution gives a heavy contribution of the Trapezoidal Traffic Model to the association of sector profiles and, from the general view point, it is the most used model within all three developed ones. As for the Double Gaussian and Tree Stump models, the 2G and 3G asymmetry is also verifiable, and the "Other" group has the same amount of sectors than the ones of the original distribution. So, one can conclude that if it can be made an exception in which not all traffic models are normalised to 1, and the Voice Trapezoidal Traffic Model would be used as presented in this alternative distribution, the use of all three models is more balanced than in the regular distribution, leading to conclude that this process is favourable for voice communications.

The data Alternative Distribution is very similar to the original one, with the increase of sector profiles association to the Trapezoidal Traffic Model. The newly associated profiles come exclusively from the Pyramid Traffic model and the "Other" group, which grants a better knowledge of the analysed network, due to the decrease of sector profiles not belonging to any data traffic model. The percentage of sector association to the Pyramid Traffic Model is kept above 50% of all sector profiles. Besides, the use of the alternative distribution only increase the number of associated sector profiles to the Trapezoidal Traffic Model, but all of them were previously associated to the Pyramid Traffic Model, which leads to conclude that the use of the regular distribution is perfectly adjustable to a live network.

Table 3.12 – Voice Sector Profiles Alternative Distribution.

	2G (158 Sectors)		**3G (199 Sectors)**		**TOTAL (357 Sectors)**	
Voice Model	**Number of Sectors**	**% of Sectors**	**Number of Sectors**	**% of Sectors**	**Number of Sectors**	**% of Sectors**
Double Gaussian	32	20.3%	57	28.6%	**89**	**24.9%**
Trapezoidal	65	41.1%	82	41.2%	**147**	**41.2%**
Tree Stump	54	34.2%	15	7.5%	**69**	**19.3%**
Other	7	4.4%	45	22.6%	**52**	**14.6%**

Table 3.13 – Data Sector Profiles Alternative Distribution.

Data Model	**Number of Sectors**	**% of Sectors**

Pyramid	107	53.8%
Trapezoidal	43	21.6%
Swing	15	7.5%
Double Gaussian	14	7.0%
Other	20	10.1%

Regarding urban areas classification for voice, according to [AlQu98], it was established that the Double Gaussian Traffic Models belongs to the urban centre region, which is composed mainly of offices and commercial areas, hence, the two peaks of traffic at morning and afternoon, and the big drop at lunch hour, generated by the decrease of voice calls from workers that exit their offices at lunch time. This conclusion can be verified by the amount of sectors that best fit the Double Gaussian model, as they belong to cells in the urban centre of the two cities used for this thesis.

On the other hand, in the Trapezoidal Model, the traffic load is constant during the day and decreases from dinner time until it reaches a minimum at 05:00, beginning then to increase until the middle of the morning and, despite the suggestion in [AlQu98] that this should belong to a suburban area, one concludes that the profiles best approximated by this model should belong to a mixed area of offices and residential buildings, where there is no explainable daily migration pattern.

The suburban areas, primarily occupied by residencies and with some commerce, have the Tree Stump Model, which has the same behaviour at night as the previous model, but during day time, the voice traffic intensity is increasing, achieving its peak after dinner time, meaning that, as users are arriving home, they call their friends or families, mainly during and after dinner time.

Crossing this information with the Sector Profiles Distribution, and according to Table 3.10, one concludes that 2G sector profiles are mostly associated with the Tree Stump model due to its suburban locations, which verifies the usual choice of operator's network management to distribute 2G BSs by suburban and rural areas, where the most important priority is to guarantee the coverage levels. On the other hand, 3G is mostly used in urban centres, where the capacity of the network is of major importance, hence. the high percentage of association with the Double Gaussian Model.

3.4.3 Voice/data traffic profiles correlation

After the characterization of the voice traffic models within the studied urban areas, the same analysis for the data traffic models is required. 3G sector's traffic data can now be used to evaluate whether there is a relation between each sector's voice and data profiles, according to the previous established associations between voice profiles and the respective voice models. Although some 2G sectors are co-located with 3G ones, there is not enough geographical data to include that system in this correlation, in order to make this analysis more complete, so the voice service in 3G is used.

The results assessment is developed in two distinct perspectives. On the one hand, the three average voice profiles are used along with the Automatic Classification of traffic models, to gather all data sector profiles with the corresponding traffic model; this connection is made using each sector's traffic

profile classification. Then, the average profile of each group of data traffic profiles is calculated and, for each voice traffic model, both voice and data average profiles are normalised to the maximum value of the voice average traffic profile, this procedure being called from now on Voice to Data Profiles Correlation, Figure 3.21.

No conclusions can be withdrawn from the obtained figures, because in all of them the same Pyramid behaviour is observed for the data average profile, leading to conclude that there is no urban area associated with a Data Traffic Model that can be related to a Voice Traffic Model.

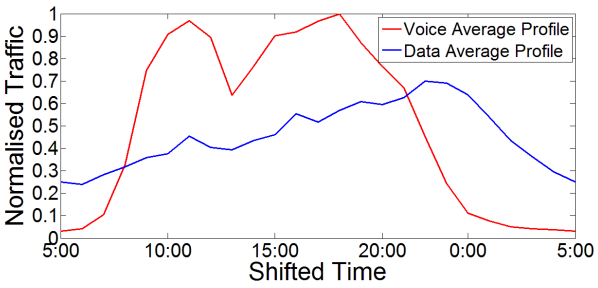

Figure 3.21 – Double Gaussian Voice to Data profiles correlation results.

On the other hand, for the opposite perspective, the procedure of sector profiles gathering is similar but, in this case, it uses the four average data profiles and their respective traffic models as the base for the aggregation of all voice sector profiles. Likewise, this is done using each sector's data traffic profile Automatic Classification, which allows the grouping of every voice sector profile with its data traffic model. Once again, these profiles are averaged and normalised to the maximum value of the data average profile, being referred from now on as Data to Voice Profiles Correlation, Figure 3.22.

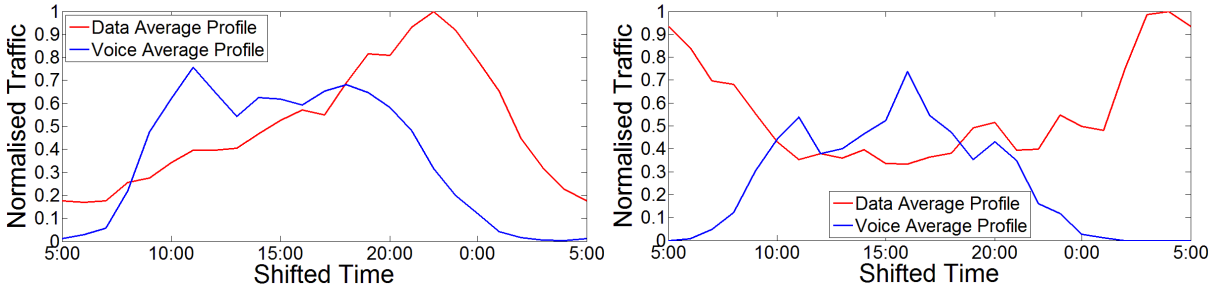

a) Pyramid. b) Swing.

Figure 3.22 – Data to Voice profiles correlation results.

From the figures' observation, one can notice that, for Pyramid, Trapezoidal and Double Gaussian data Traffic Models, the outcome of the associated average voice profile is very similar to the Trapezoidal Traffic Model. On the other hand, for the data average profile associated to the Swing Traffic Model, the voice one has no relation to either of the developed Voice Traffic Models.

In conclusion, once again no conclusive results can be taken from the obtained correlations because, as seen previously, the Voice Trapezoidal Traffic Model is assumed to belong to a mixed area between the urban centre and the suburban region. So, instead of the first rapid conclusion that the obtained voice average profiles would belong to the urban area modelled by the Voice Trapezoidal Traffic Model, these obtained voice profiles can also be the result of an average from all three modelled regions, hence, the trapezoidal outcome seen at the figures.

Using also the alternative sector distribution by traffic models, one also tried to observe any relation

between Voice and Data Traffic Models and their respective average profiles, and the other way around, to perceive any pattern between the data average profiles for the four traffic models and the respective voice average sector profiles.

Similarly to the regular distribution, the results obtained for the Voice to Data Correlation, seen in Figure 3.23, represent the general tendency for the data average profile to be associated to the Pyramid Traffic Model, therefore, leading to no conclusions for the relation between voice and data.

Regarding the Data to Voice Correlation, Figure 3.24, the obtained voice average profiles for the Pyramid and Data Trapezoidal Traffic Models once again is represented by an average profile that is best approximated by the Voice Trapezoidal Traffic Model. Likewise, the outcome of the data average profile associated with the Swing Traffic Model results in an unidentifiable profile, which at first sight does not belong to any of the developed voice traffic models. Finally, for the Double Gaussian Traffic Model, the resulting voice average profile can be represented by the Voice Double Gaussian Traffic Model, leading to conclude that for this situation, both voice and data services may share the same traffic model, each with its own parameters, obviously.

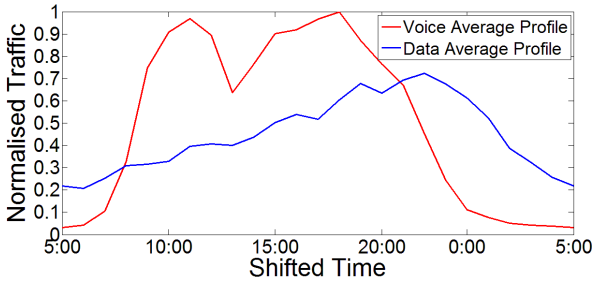

Figure 3.23 – Double Gaussian Voice to Data profiles' correlation results, with alternative distribution.

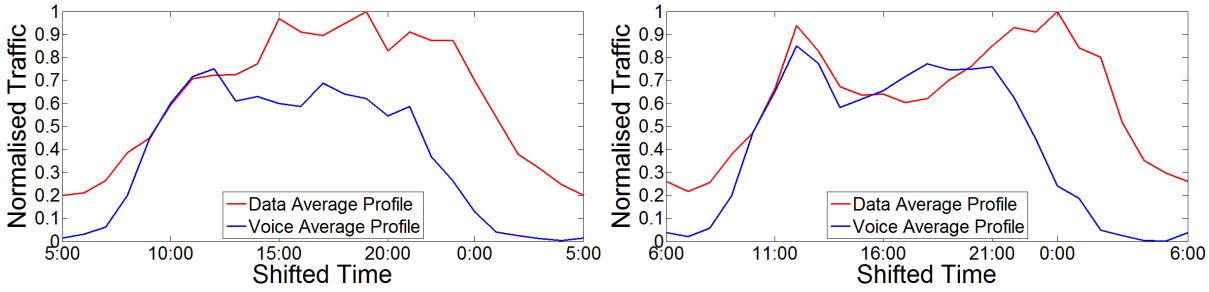

a) Data Trapezoidal. b) Data Double Gaussian.

Figure 3.24 – Data to Voice profiles' correlation results, with alternative distribution.

3.4.4 Weekday/Weekend profiles correlation

After the analysis of weekdays voice and data traffic profiles, there is the need to evaluate, if possible, the existence of a relation between weekday and weekend average profiles, for each of the traffic models and the respective urban region. Therefore, using the previously constructed average weekday sector profiles, the Automatic Sector Classification procedure in order to distribute all weekend sector profiles by their respective traffic model association, and then producing the mean of them all, one obtained three average weekend voice sector profiles and four data ones.

These profiles were compared with the respective weekday profile, in order to draw some relation to the respective traffic model associated to weekdays, or even if at weekends there is an association

with another traffic model. For the voice average profiles weekday to weekend relation, one can conclude that, for the Trapezoidal and the Tree Stump traffic model, the weekend average profiles keep the same daily variation as the respective weekday profiles. However, as seen in Figure 3.25-a), the weekend average profile associated with the Double Gaussian traffic model assumes a Trapezoidal Traffic Model shape, with the decrease of both morning and afternoon traffic peaks, and the rise of the lunch hour minimum. So, at weekends, in urban centre areas, instead of a Double Gaussian traffic model daily evolution, the model that best fits is the Trapezoidal Traffic Model.

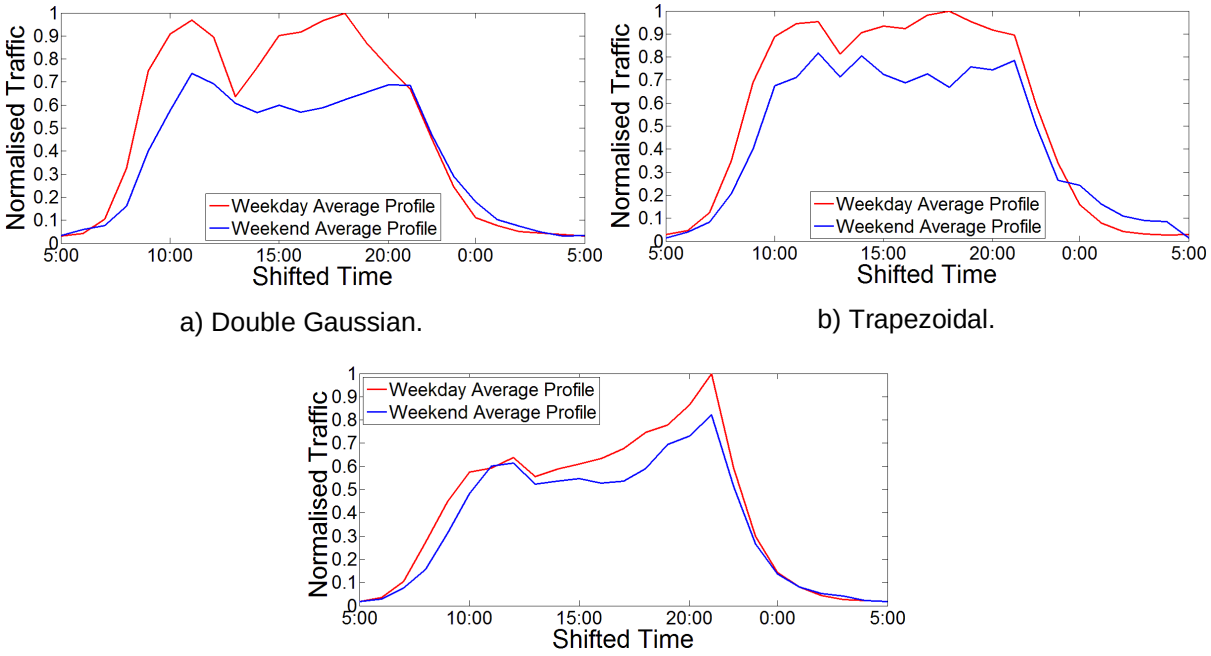

a) Double Gaussian.

b) Trapezoidal.

c) Tree Stump.

Figure 3.25 – Weekday to Weekend Voice Average Profiles Correlation.

As for the data traffic profiles, no conclusions can be drawn because, for all four data traffic models weekday profiles, the corresponding weekend average profiles do not fit any modelled traffic model, Figure 3.26.

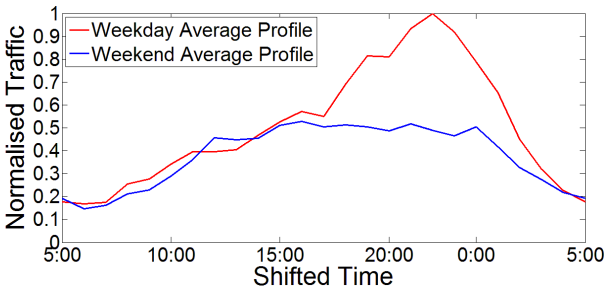

Figure 3.26 – Pyramid Weekday to Weekend Data Average Profiles Correlation.

For the alternative distribution, the same correlation analysis was performed and, for the voice average profiles, the general tendency is for all three profiles to be associated to the Trapezoidal Traffic Model at weekends. For the mixed urban area associated at weekdays with the Trapezoidal model, one only sees a intensity decrease of the traffic load but, for the Double Gaussian and the Tree Stump associated weekday profiles, the migratory patterns within the week cease to exist, as well as

the traffic load peaks originated at work hours, justifying the flattening of the weekend profiles, Figure 3.27.

Finally, for the data traffic, once again the weekend average profiles lead to no conclusions due to the inexistence of a noticeable daily traffic variation. The explanation of this occurrence should be that if at weekdays, data have certain unpredictability, but even this variation might be constrained within work hours or happy hours. On the other hand, during weekends, the disappearing of the work time leads to an even higher irregular data traffic variation.

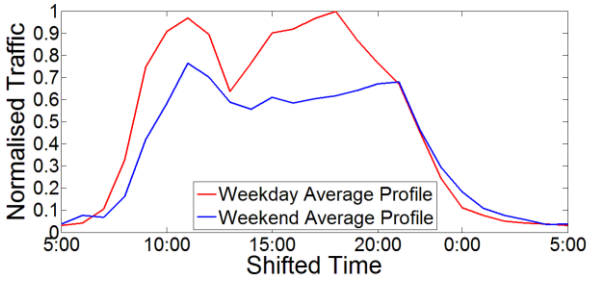

Figure 3.27 – Double Gaussian Weekday to Weekend Voice Average Profiles Correlation, with alternative distribution.

Similarly, even with the alternative distribution, none of the data models led to an identifiable average weekend profile. Despite the already known difficulty to perceive any data daily traffic evolution that can be modelled, this situation leads to conclude that, in the case that there are weekend traffic daily tendencies, there is the need of an extensive study for the 3G network and data use at weekends.

A general conclusion that can be drawn has to do with the relation between the traffic load at weekdays and weekends, where both profiles were normalised to the same maximum value, and nevertheless, the traffic intensity at weekends is considerably lower than the one at weekdays, as it would be expected in a live network, this situation being more recurrent for data profiles.

Chapter 4

Power Consumption Models

In this chapter, four Power Consumption Model configurations are described, for 2G and 3G systems, considering both indoor and outdoor BS equipments, and variation parameters, in Section 4.1. Then, in Section 4.2, 2G and 3G Energy Efficient Algorithms are described, and their features are analysed. Finally, in Section 4.3, their use in the Power Consumption Model is analysed and evaluated.

4.1 Power Consumption Model Description

Each mobile communications site needs to be characterised to better represent the energy consumption within the studied urban centres. In this case, for each site, 2G and 3G BSs are modelled according to their most power consuming elements, instead of the traffic models, which are separated between voice and data traffic. Hence, voice traffic models, which were originated from 2G and 3G traffic information, are used as input for the 2G Power Consumption Model, while data traffic models are used at the 3G Power Consumption Model. On top of these models, standard deviation values are also considered as an input of the Power Consumption models, to create a better approximation to the real communications environment, with high variations of the traffic load, instead of the average behaviour of the traffic models obtained in the previous chapter.

Apart from traffic load, the outside temperature and its daily variation is also taken into account, because it implies a consequent variation of the temperature inside the site container [METE11]. Hence, daily temperature variation profiles were obtained for the two studied urban centres, taking the time of the year that data was collected into account. Two distinct profiles were collected, but only one was used, because one of the cities does not present a considerable daily temperature variation at that specific time of the year, due to its geographical location and, as seen in Annex E, City 1 was chosen to be used as the temperature input.

An extensive list of the elements responsible for the higher values of power consumption within a site was established, containing elements outside the BS, as the ArC and backhaul connection, while inside the BS one has the RF carriers, the PA, DSP, BB, PS and AC/DC.

According to [EARTH10a], [BoCo11], [HHAK11], [KoDe10] and [DVTJ10], a list of power consuming elements was made for 2G macro-cell BSs, and three were made for 3G macro-, micro- and pico-cell BSs, Table 4.1. It is assumed that a 2G BS has four carriers and a 3G BS have 2 carriers for the Power Consumption Model Assessment. In Table 4.1, 2G site elements power maximum consumption is presented, being distinguished between the external equipment at the container and the one inside it, due to their different dependence factors. The ArC power consumption varies with the air temperature inside the container and the other external elements have no considerable impact on the power consumed. On the other hand, inside the BS all elements depends on the number of switched on carriers, and the RF equipment power consumption is also strongly dependent on the users traffic load within the covered cell.

One assumed a technological leap from the 2G Power Consuming Elements to the 3G ones. This evolution in power consumption was assumed to be only inside the BS, by 50%, but also considering the relation between all BS elements power consumption, according to [EARTH10a]. Outside the BS, it is assumed that for macro-cells, the container may be shared with the 2G equipment, and for micro- and pico- cells, there is no need for cooling, and the backhaul link power consumption becomes negligible.

One has two 3G carriers consuming 400 W, the PA consuming 66%% of the power considered for 2G

site, and then finally all the remaining BS elements consuming half the value assumed for 2G. Besides, from the macro- to the pico-cell the BS equipment consumption is scaled to represent the increase of relative power consumption by the BB as well as the weight of the PA on the overall BS power consumption [EARTH10a]. Finally, the dependencies on the equipment from all surrounding elements are kept the same, assumed equal, since the equipment functions are considered to be the same; only the 3G Carriers differ, but this also depends simultaneously of the cell traffic load and the number of active Carriers.

Table 4.1 – Selected Elements for the 2G Power Consumption Model.

Element	**Power Consumption [W]**			
	2G Site	**3G Site**		
		Macro BS	**Micro BS**	**Pico BS**
ArC	400 (33%)	400 (33%)	——	——
Backhaul	80 (6%)	80 (7%)	10.5 (7%)	——
BS				
• RF	200 (17%)	400 (33%)	40 (27%)	2.8 (14%)
• PA	180 (15%)	120 (10%)	27 (18%)	4.4 (22%)
• DSP	94 (8%)	57 (5%)	10.5 (7%)	1.6 (8%)
• BB	82 (7%)	53 (4%)	39 (26%)	7.4 (37%)
• PS	82 (7%)	45 (4%)	12 (8%)	2.2 (11%)
• AC/DC	82 (7%)	45 (4%)	11 (7%)	1.6 (8%)
Total	**1200 W**	**1200 W**	**1200 W**	**1200 W**

There is also the need to model how the factors' daily variation is represented by the elements that depend on it. At first, for the ArC, a simple heating/cooling linear model was developed for the outside temperature, as seen in [ToDI98], being used in both 2G and 3G macro-cell sites. For the indoor temperature variation, a 10ºC increment was used to the collected temperature profile, to approximate the environment inside the BS containers,

$$T_{in[^\circ C]} = T_{out[^\circ C]} + 10^\circ \tag{4.1}$$

where:

- T_{in}: Air temperature inside the BS container.
- T_{out}: Outside air temperature.

The ArC consumed power, P_{ArC}, as function of the air temperature inside the container, T_{in}, can be obtained by [OPTI11]:

$$P_{ArC[W]}\left(T_{in[^\circ C]}\right) = \begin{cases} P_{ArC0[W]} - \dfrac{\left(P_{ArC0[W]} - P_{ArCtyp[W]}\right)}{T_{th1[^\circ C]}} T_{in[^\circ C]}, & T_{in[^\circ C]} < T_{th1} \\ P_{ArCtyp[W]}, & T_{th1} \le T_{in[^\circ C]} \le T_{th2} \\ P_{ArCtyp[W]} + \dfrac{\left(P_{ArCMAX[W]} - P_{ArCtyp[W]}\right)}{T_{MAX[^\circ C]} - T_{th2[^\circ C]}} \left(T_{in[^\circ C]} - T_{th2[^\circ C]}\right), & T_{in[^\circ C]} > T_{th2} \end{cases} \tag{4.2}$$

where:

- P_{ArC0}: 0ºC ArC power consumption.
- P_{ArCtyp}: typical ArC power consumption, when the container temperature is just below the desired output temperature.
- T_{th1}: first threshold temperature between heating and low consumption operating mode.
- P_{ArCMAX}: maximum ArC power consumption
- T_{MAX}: maximum ArC working temperature.
- T_{th2}: second threshold temperature between low consumption and cooling operating mode.

To get the best approximation for the studied equipment, with an output temperature of 24ºC, maximum power consumption of 400 W and typical consumption of 300 W, one obtained the parameters for the ArC Power Consumption Variation Model, Table 4.2. The variation of the ArC power consumption as function of the container air temperature can be seen in Figure 4.1.

Table 4.2 – ArC Power Consumption Model parameters.

P_{ArCMAX} [W]	P_{ArCtyp} [W]	P_{ArCmed} [W]	T_{th1} [ºC]	T_{th2} [ºC]	T_{MAX} [ºC]
400	300	350	7	23	50

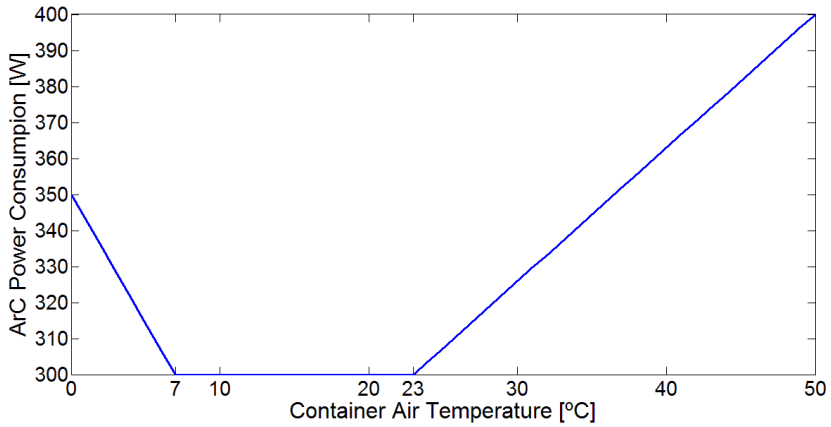

Figure 4.1 – ArC power consumption.

Finally, one can obtain a general expression for the power consumption in Watts at the 2G or 3G sites with the already known variables.

$$P_{site}(T) = P_{Arc}(T) + P_{backhaul} + N_{carr}(P_{RF} + P_{PA} + P_{DSP} + P_{BB} + P_{PS} + P_{AC/DC}) \quad (4.3)$$

where:

- P_{site}: site power consumption.
- $P_{backhaul}$: backhaul connection power consumption.
- N_{carr}: Number of active carriers.
- P_{PA}: PA power consumption.
- P_{DSP}: DSP power consumption.
- P_{BB}: BB power consumption.
- P_{PS}: PS power consumption.
- $P_{AC/DC}$: AC/DC power consumption.

4.2 Energy Efficient Model

When the traffic volume is very low, the consumption of all network resources becomes inefficient, leading to energy waste at the BSs. By automatically closing idle or little used carriers, one can save energy, reducing the expenses in electricity. 2G and 3G Energy Efficient Models receive as input, either 2G or 3G traffic load profiles based on the developed traffic models, their respective standard deviations, and the daily temperature profile. As output, one obtains both 2G and 3G Energy Efficient Power Consumption Profile, as well as the carriers' daily variation profiles.

4.2.1 2G Algorithm

A simple way to improve power consumption at the BSs is to adjust the use of carriers to the cell traffic load at that moment. For that, there is the need to construct an algorithm that varies the number of active carriers according to the traffic load along the day, Figure 4.2.

At first, all carriers are considered to be switched on, despite the initial values of the traffic load, and for this initial situation, a power consumption value is registered. From this point on, for every traffic load value one evaluates if is higher than a percentage of the available traffic capacity, which is called the Power-On Limit (T_{ON}), or if is lower than a percentage of the available traffic capacity, this threshold being named Power-Off Limit (T_{OFF}). These limits are considered at every Carrier Traffic Load Evaluation Interval ($\Delta t_{Eff[min]}$), to prevent constant switch on/off at the carrier due to the irregularities of active users traffic generation. Furthermore, adjacent traffic values that belong to the beginning of a replica of the original traffic load model are used to produce a power consumption interval that replaces the initial period of the power consumption profile, in order to represent any day typical power consumption profile, instead of the moment when the feature is activated.

The available traffic capacity is defined by the number of switched on carriers at the BS. This traffic capacity is evaluated as the percentage of available TCHs for the voice traffic. hence, 1 Erl of traffic load is equivalent to 1 TCH. It is important to refer that less than 0.5 Erl is also equivalent to 1 TCH, as 1 traffic channel is always needed to be available for traffic, Figure 4.2.

The channels' time-slots configuration for each GSM carrier was based initially on the typical carrier configuration [Moli05], and then based on the configuration applied to the live network [OPTI11]. For the first carrier, one assumes the BCCH for the BS broadcast information, 1 SDCCH to serve the carrier signalling and synchronisation requirements and 2 fixed PDCHs for the GPRS service of that cell; the dynamic PDCHs are not considered, because 2G data traffic is assumed to be negligible. Besides, for each additional carrier, typically one SDCCH is withdrawn from the available TCHs. So, one has the deployed carriers configuration in Table 4.3, which is used to evaluate the traffic load thresholds for the 2G Energy Efficient Algorithm,

$$N_{BCCH} + N_{PDCH} + N_{SDCCH} + N_{TCH} = N_{TRX} \times 8 \quad (4.4)$$

where:

- N_{BCCH}: Number of Broadcast Channels, occupying one channel in the first carrier.

- N_{SDCCH}: number of SDCCH channels.
- N_{PDCH}: number of PDCH channels.
- N_{TCH}: number of TCH channels.

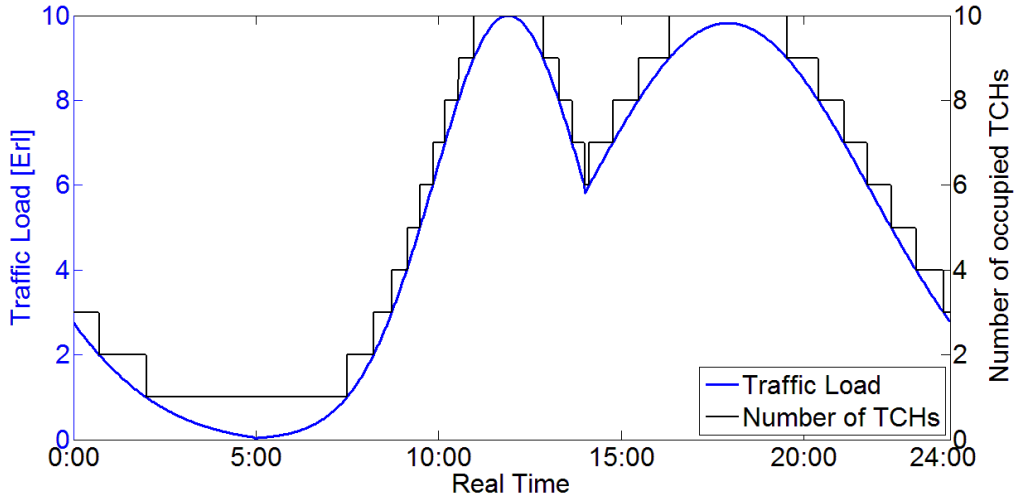

Figure 4.2 – TCHs daily profile, based on the traffic load amplitude variation.

Table 4.3 – 2G Energy Efficient Model TCHs configuration.

N_{carr}	N_{BCCH}	N_{PDCH}	N_{SDCCH}	N_{TCH}
1	1	2	1	4
2			2	11
3			3	18
4			4	25

The Power-On Limit is the threshold that enables the decision to switch on a TRX, so if the traffic channels occupation percentage is higher than this limit in a pre-determined instant, and there is at least one TRX switched off, a TRX is switched on and the power consumption value is calculated for that instant. As for the Power-Off Limit, this threshold determines the TRX switch off decision, but only if there are at least two active TRXs, because one TRX must stay on to guarantee cell coverage, and other signalling channels also need to be kept transmitting, like the broadcast channel.

Finally, there is the Emergency Switch-On Limit, defined as 90% being used as a protection for capacity overload, hence, in case of high user's traffic load, all TRXs are switched on to increase cell capacity to its maximum. Unlike the previous limits, this evaluation is done for every traffic load value, regardless of the granularity of the traffic load profile being smaller than the value determined for the Δt_{Eff}, which is only "seen" from the TRXs' Switch On/Off thresholds point of view. This procedure is done so that there are no users being blocked for a long period of time, or with no service from the BS at any moment. In Figure 4.3, one has the 2G Energy Efficient Algorithm scheme with the procedures described in this Section, and the outputs that result from this algorithm. From the 2G Energy Efficient Model one obtains the daily power consumption, the number of active carriers' variation and the daily TCHs variation profiles as outputs.

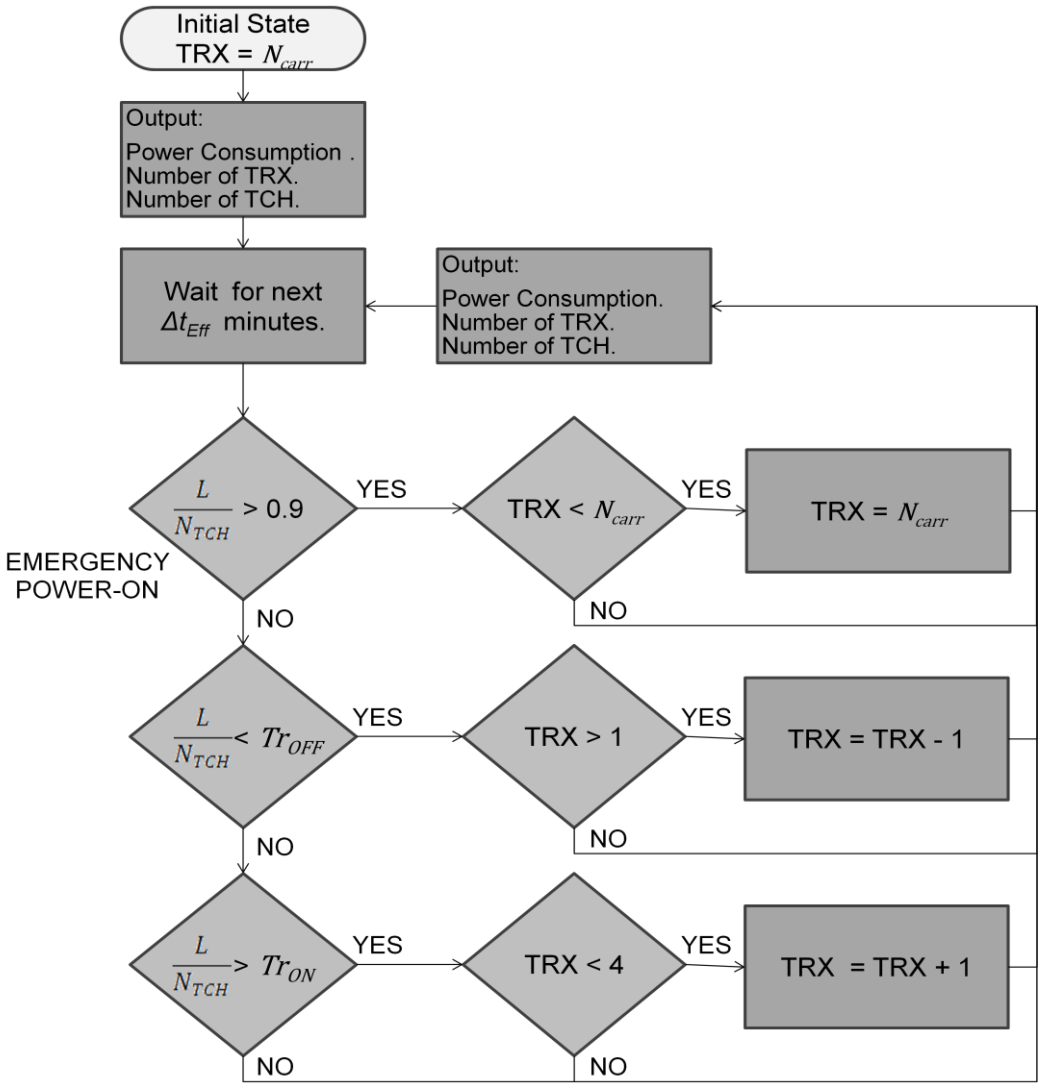

Figure 4.3 – 2G TRX Switch-off algorithm.

4.2.2 3G Algorithm

The 3G algorithm is very similar to the 2G one, as seen in Figure 4.4, due to the common main goal of switching on and off carriers to decrease the power consumed at the BS. The intelligent carrier power off is done by gradually decreasing the maximum transmitting power of the RF carrier until the low traffic in that carrier is smoothly handed over to the primary carrier. This power reduction is reflected on the RF equipment consumed power, and consecutively, on all BS equipment consumed powers, which have the same dependence on the number of active carriers, as the 2G one. The RF carrier power reduction algorithm decreases the number of carriers using a temporal step, instead of using an instant decrease. Furthermore, the switch off carrier decision is done according to the users' data rate within the cell, and therefore, one had to assume that the switch off threshold depends on the traffic load as in 2G

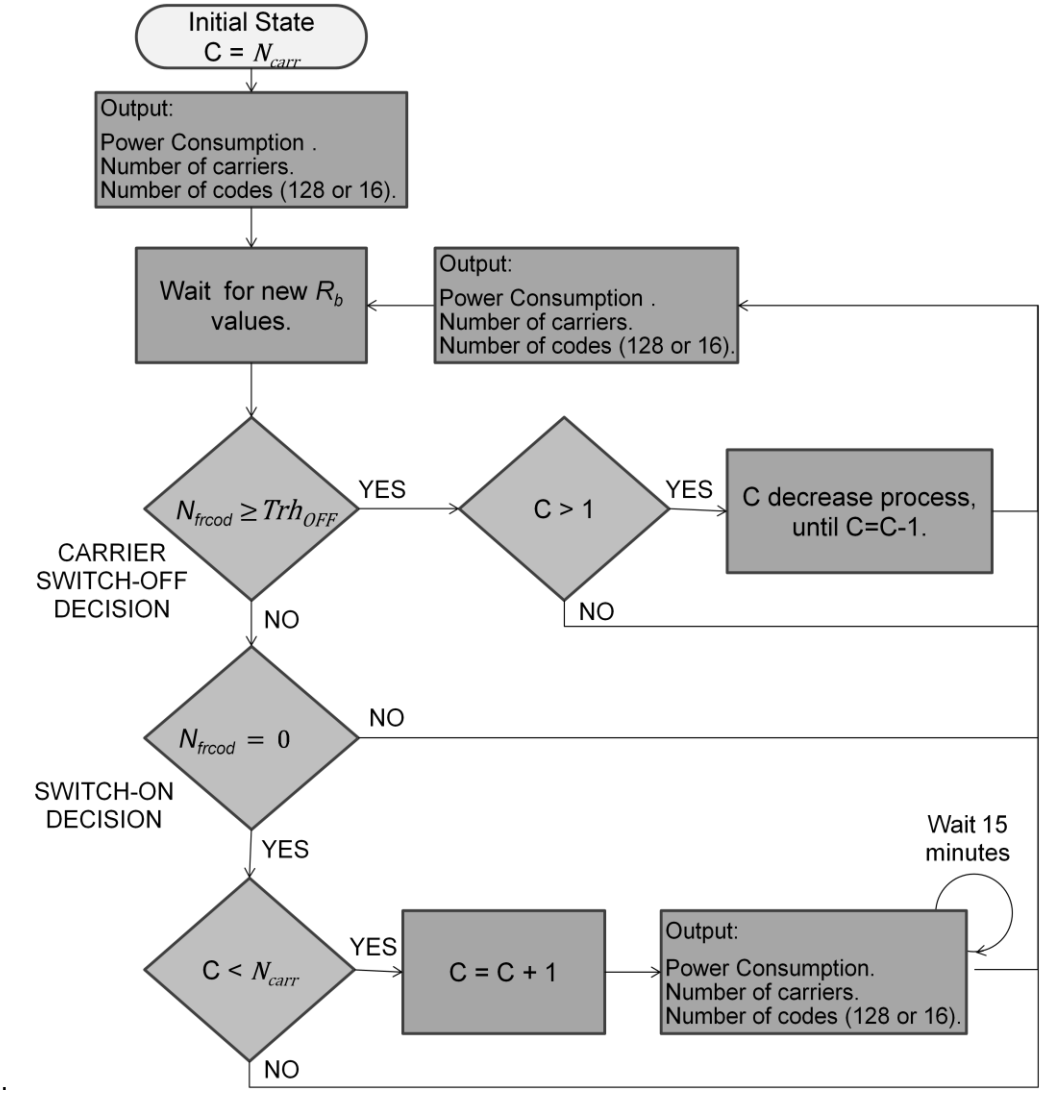

Figure 4.4 – 3G Cs Switch-off Algorithm.

According to [OPTI11], the first carrier is always occupied with a dynamic balance between R99 and HSDPA, the former being used for the voice traffic while the latter enables better data rates for the users. Voice uses codes of SF 128, while HSDPA data traffic uses a fixed SF of 16, meaning that calculations are made to evaluate the available codes of SF 16 for each instant, since it is always given priority to the voice. As for additional 3G carriers, they are only HSDPA, as they are intended to increase the data traffic capacity within the cell.

According to [Carv09], an average value of SNR was obtained from measures collected at a urban area, 9.52 dB, then a standard deviation being 3.75 dB. These values are used to model the 3G carriers' capacity according to a variable quality of the radio link.

A weighted average is done to produce a maximum throughput for the capacity of each carrier $\overline{R_{bcarr}}$ [Bati11], based on the average throughputs achieved among the three used modulations, QPSK, 16QAM and 64QAM, as seen in Annex F:

$$\overline{R_{bcarr}}_{[\text{Mbps}]} = 0.4 \times R_{bQPSK[\text{Mbps}]} + 0.35 \times R_{b16QAM[\text{Mbps}]} + 0.25 \times R_{b64QAM[\text{Mbps}]} \quad (4.5)$$

where:

- R_{bQPSK}: maximum theoretical throughputs with QPSK modulation.
- R_{b16QAM}: maximum theoretical throughputs with 16QAM modulation.
- R_{b64QAM}: maximum theoretical throughputs with 64QAM modulation.

The codes occupation is done according to the maximum throughput capacity assumed for each carrier, taking into account as well the number of codes with SF 128 already occupied by the voice traffic, where each code with SF 128 is equivalent to 1 Erl. So, one has for the calculation of the number of codes with SF 16 (4.6) and for codes with SF 128 (4.7)

$$N_{codsf16} = \left\lceil 15 \times \frac{R_{b[\text{Mbps}]}}{\overline{R_{bcarr}}_{[\text{Mbps}]}} \right\rceil \tag{4.6}$$

and

$$N_{codsf128} = \lceil T_{[\text{Erl}]} \rceil \tag{4.7}$$

where:

- $N_{codsf16}$: number of occupied codes with SF 16.
- R_b: data traffic load.
- $N_{codsf128}$: number of occupied codes with SF 128.

The voice traffic in 3G only uses one carrier, so its daily variation is negligible from the energy efficiency switch-off carriers' procedure view point. Therefore, the Carrier Switch-off Threshold Trh_{OFF} evaluates if any additional carrier is empty, based on the number of available codes of SF 16. If there are 15 available codes, there is necessarily one empty carrier that can be switched off (4.8).

$$N_{frcod} = N_{carr} \times 15 - N_{codsf16} - \left\lceil \frac{N_{codsf128}}{8} \right\rceil \tag{4.8}$$

where:

- N_{frcod}: number of available codes with SF16.

For the first data traffic load value, all carriers are also considered to be switched on, and then, for the following values, it is evaluated if those are above or below Trh_{OFF}. Then, every other value from the traffic profile is evaluated with the number of codes that are occupied. As in the 2G Energy Efficient Algorithm, the initial values of the traffic profile are revaluated and placed in the beginning of the 3G power consumption profile. Therefore, for the 3G Energy Efficient Algorithm, if more than one carrier is active, the Carrier Switch-off process is initiated, corresponding to a similar process of the decrease of the transmitted power, within the time interval between two traffic values, i.e., 1.5 minutes for the power decrease. With a higher granularity of the traffic load, the power decrease duration is shorter, as it should occur in the real equipment.

After the Carrier Switch-off, to enable again one additional carrier there is the need to have the active ones full, meaning that for the Carrier Switch-on Decision there is the need for 1 inactive carrier, and the data rate must lead to a situation where the available codes SF 16 are all occupied. The additional carrier is immediately switched on, with the condition that it will not be switched off for 15 minutes.

With the daily variation of active Carriers, one obtains the daily 3G Energy Efficient Power Consumption profiles, and also a daily variation of the number of switched on carriers and used codes of SF 128 or 16, whether one has voice or data traffic as input.

4.3 Models Assessment

In order to evaluate the 2G and 3G Energy Efficient Models, the daily power consumed by the BSs was validated according to three distinct situations, constant outside air temperature, no traffic load, and using a step function for the outside air temperature.

Considering the inputs, 4 GSM TRXs and 2 UMTS carriers are assumed, and voice traffic amplitude of 25 Erl and data maximum throughput of 10 Mbps are chosen, in order to explore both minimum and maximum capabilities of the Energy Efficient Algorithms, with the total use of TCHs or SF 16 codes.

As for the 2G and 3G Energy Efficient Algorithms thresholds, one chose the values that give the best results among a given range, but those do not represent the optimal energy saving values for the Power-on and Power-off Traffic Load Thresholds. One has, in Table 4.4, the chosen value for the time interval in which the carriers verify the voice and data traffic load Δt_{Eff}, the used values for the 2G Energy Efficient Algorithm, while for the 3G Energy Efficient Algorithm the decision value for the switch off is 15 codes of SF 16, meaning that there is one carrier with all its codes of SF 16 available.

Table 4.4 – Energy Efficient Algorithms Traffic Load Thresholds.

Threshold	$\Delta t_{Eff[min]}$	T_{OFF}	T_{ON}	Trh_{OFF}
Value	15	0.35	0.75	15

The validation process without temperature variation was processed using one of the temperature values that lead to minimum power consumption by the ArC. In this case, the outside air temperature used was 0º C, which leads to a container temperature of 10º C, and the last one is situated in an interval that consists of values between 7º C and 23º C that produce the lower power consumption assumed at the ArC. This procedure has the objective to isolate the traffic variation as an input, to observe that, as expected, for the maximum value of traffic load, the power consumption output is 1100 W with 4 active carriers, while for the minimum value, one has only 1 active carrier, leading to a minimum consumption of 560 W, Figure 4.5-a. Likewise, for 3G, the maximum power consumption obtained with 2 carriers is also 1100 W, while the minimum is 740 W.

Then, 2G and 3G carriers' variation profiles are obtained for this situation, Figure 4.6, and the carrier switch on/off procedure is verified, corresponding to the power consumption profiles' variation.

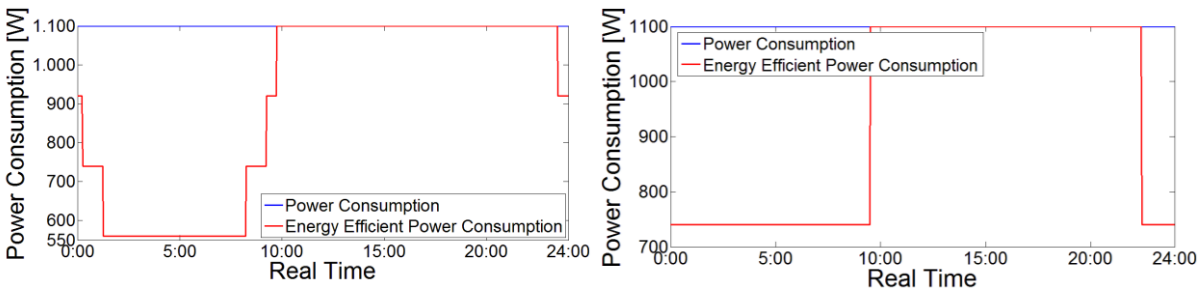

a) 2G.

b) 3G.

Figure 4.5 – Power Consumption Profiles with minimum AC power consumption.

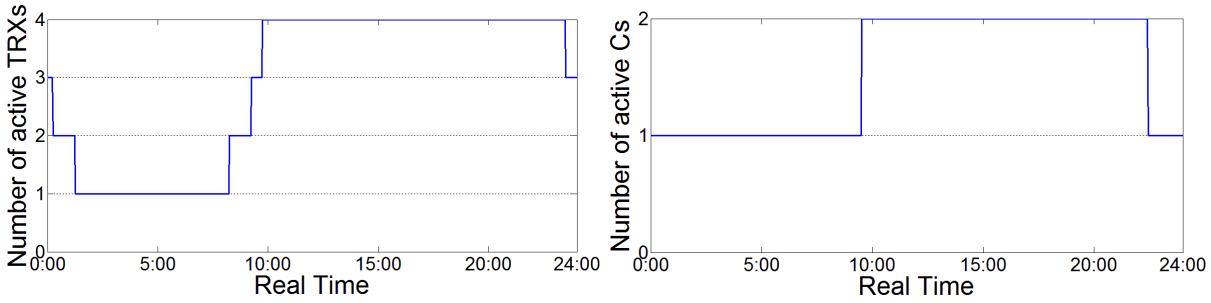

a) 2G. b) 3G.

Figure 4.6 – Carriers variation profiles with minimum AC power consumption.

The second process considers no traffic load as input of the power consumption model. Therefore, the traffic load is 0 Erl or Mbps for 2G or 3G, respectively, and the only considered input is the temperature variation, Figure 4.7. This process allow one to verify the minimum values of power consumption, but considering the outside air temperature, hence, enabling the visualisation of the power consumption variation with the daily temperature values. So, one can conclude that for both models, the power consumption without the energy saving procedures varies between 1050 W and 1150 W, without traffic load, this situation being the main reason that leads to the lack of efficiency in mobile networks at low traffic hours.

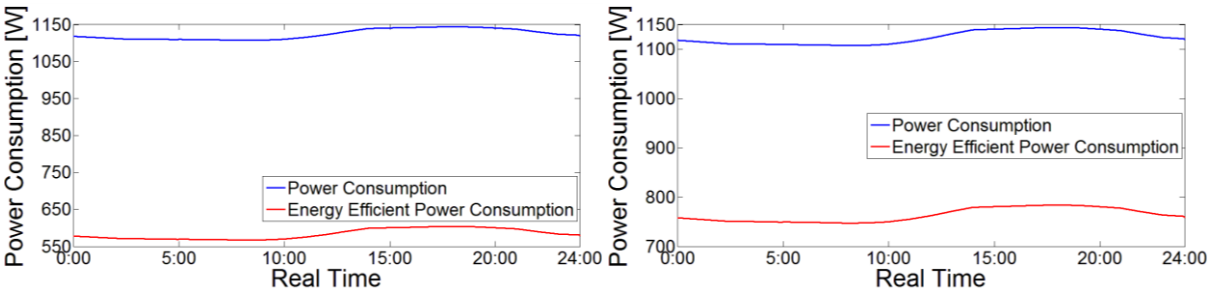

a) 2G. b) 3G.

Figure 4.7 – Power Consumption Profile without traffic load.

As for the third validation process, one assumed more complex inputs for both traffic load and temperature profiles. One used two step functions, with different step instants to enable a better perception of the power consumption output, Figure 4.8. One has a step function for the power consumption profile that has no traffic load for less than half of the day, and maximum traffic load for the second part of the day; for the temperature profile, one has another step function, with the lower floor corresponding to 0º C outside air temperature, and the upper floor being 40º C, to represent the maximum power consumption of the ArC. The timings of the step functions are separated, to allow the distinct evaluation of the power consumption variation due to traffic load peaks or sudden temperature variations. Furthermore, with the peak of the traffic load, the Emergency Switch-on procedure is also verified, with the instantaneous automatic switch-on off all 4 carriers.

One obtains Table 4.5 with the power consumption outcome for each of the assessment situations represented with the joint input functions. Three situations are defined: the first without traffic load and air temperature corresponding to minimum power consumption by the AC; then, the traffic load is maximum and the power consumed by the AC is minimum; finally, with the step of the temperature

profile, traffic load and temperature lead to maximum power consumption.

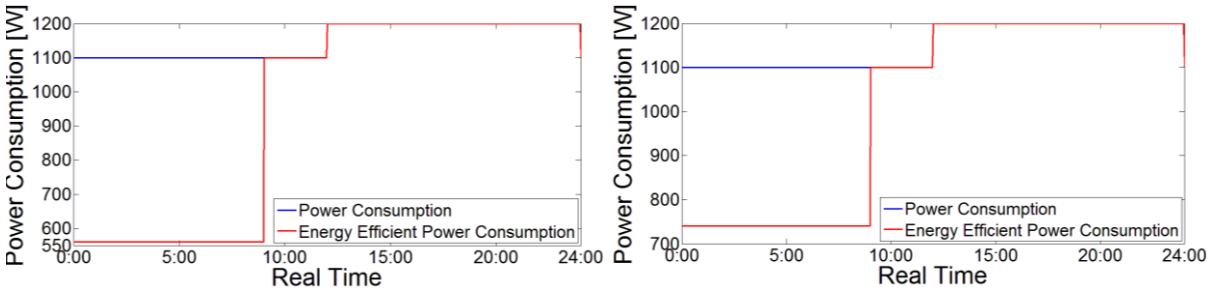

a) 2G. b) 3G.

Figure 4.8 – Power Consumption Profiles with the use of step functions as inputs.

Table 4.5 – Energy Efficient Model Power Consumption Assessment (with/without energy savings).

Model / Assessment	2G [W]	3G [W]
No load; Minimum AC consumption	560 / 1100	740 / 1100
Maximum load; Minimum AC consumption	1100	1100
Maximum load; Maximum AC consumption	1200	1200

Concerning the resulting power consumption values, all of them correspond to the values expected to be obtained from the Power Consumption Distribution described in Table 4.1. Using simple calculations, these values were verified taking into account the dependencies of each equipment to inputs as traffic load, temperature or active carriers' number.

Finally, the validation of the daily energy savings was made with the verification of the computed calculations, which consisted of simple integrations between two power consumption values, considering the used time interval, 90 seconds. This validation was performed using Excel, to verify whether there were irregularities in the models' results.

Chapter 5

Scenarios Analysis

In this chapter, power consumption scenarios are developed based on simple and mixed traffic profiles, being analysed from the power consumption and energy savings view point. In Section 5.1, a description of the inputs and output of the Energy Efficient Model is done, as well as of the main parameters used to approximate the Energy Efficient Model to the studied live network. Then, in Section 5.2 and Section 5.3, scenarios containing just voice or data traffic are analysed, respectively. Finally, in Section 5.4, mixed traffic scenarios are developed and analysed, with co-localised 2G and 3G BSs.

5.1 Scenarios Description

As both 2G and 3G networks have to guarantee voice and data services, one needs to create specific power consumption scenarios based on the respective traffic load variation profiles to adapt to the real daily power consumption profile obtained at the live network. The 2G network is mainly used for voice, while the 3G network is responsible to provide the capacity for both voice and data. So, different loads of voice and data traffic must be considered between the two systems to characterise users' behaviour, and the urban area considered for the specific scenario.

The considered scenarios are divided into three separate groups. Isolated voice traffic load is analysed in 2G, as well as isolated data traffic load in 3G, just considering one reference scenario, and then, mixed traffic profiles are used along with joint 2G and 3G, based on the live network most usual case of co-localised GSM and UMTS BSs. For each scenario, distinct traffic models, traffic load intensity values for weekdays and weekends, carrier capacity, cell sizes and the use of standard deviation are used according to the urban area to which they are associated to.

Regarding the Traffic Models, only the Double Gaussian and the Tree Stump models are used for urban, and suburban or rural areas, respectively. For the data traffic models, from the four models analysed, only the Pyramid and the Swing models are used, the first being the most common data traffic model, and the second as a particular case to be analysed on the suburban areas described in Chapter 3, and is mostly associated with the happy hours tariffs. In Table 5.1, traffic profiles' amplitude values for each voice and data traffic model are presented, which consist of the sum of the average traffic load with the standard deviation, in order to predict high load variations along the day. On top of the traffic models, maximum traffic load values were analysed for each of the developed traffic models, and a decrease on the traffic profiles' amplitude from the dense urban to the rural area is assumed for the developed scenarios. Therefore, in Table 5.1 one presents the maximum traffic load values, for weekdays and weekends, of the sectors associated with the voice traffic models. Likewise, the maximum traffic load values obtained from the sectors associated to the data traffic models are presented, for both weekdays and weekends. These values are related to the Urban Scenario, which is used as a reference scenario for the results analysis, as it contains traffic load amplitude values that are consistent with the data collected from the live network.

Table 5.1 –Traffic load maximum values, obtained at the live network.

Traffic Model	**Weekdays**			**Weekend**		
Voice T_{MAX}[Erl]	μ	$\mu + \sigma_{avg}$	$\mu + 2\sigma_{avg}$	μ	$\mu + \sigma_{avg}$	$\mu + 2\sigma_{avg}$
Double Gaussian	10.02	13.00	15.98	6.74	9.78	12.68
Tree Stump	9.47	12.90	16.33	5.82	9.25	12.68
Data R_{bMAX}[Mbps]						
Pyramid	4.26	6.56	8.86	4.63	6.93	9.23
Swing	3.72	5.71	7.70	2.66	4.65	6.64

Finally, one assume for the voice traffic, two perspectives of power consumption analysis: one at weekdays, and the other at weekends, with a decrease of 50% on the load amplitude. This approach is not implemented for the data traffic, due to the similarity in the load amplitudes at weekdays and weekends, as seen in Section 3.4.1.

Regarding the RF equipment in the BSs, for the 2G network one assumes the use of 4 TRXs for the dense urban scenarios, and then decreasing the number of carriers for each scenario, until 2 TRXs for the suburban and rural scenarios, Table 5.2.

Table 5.2 – Scenarios Description.

Scenario ID	**VOICE**				**DATA**	
	Traffic Model	Tr_{MAX}**[Erl]**	**TRX**	**TCH**	**Traffic Model**	R_{bMAX}**[Mbps]**
Dense Urban (DU)	DGM	15	4	25	PyM	7.5
Urban (U)	DGM	10	3	18	PyM	5.0
Suburban (S)	TSM	5	2	12	SwM	5.0
Rural (Ru)	TSM	3	2	12	PyM	2.5

As for 3G, two carriers are always assumed for every scenario, as it is the solution implemented within the studied urban areas. For voice traffic, R99 is considered, in which codes of SF 128 are used for voice. As for data, HSDPA uses codes with SF 16, meaning that, for the mixed traffic scenarios, a compromise between codes of SF 128 and 16 available must be managed, giving always priority to the first ones, to guarantee that voices calls are not blocked. To better adapt to the studied equipment, the first carrier is composed of a dynamic adjustment between R99 and HSDPA, while the second carrier only uses HSDPA. In the 3G network, three cell sizes are considered; macro-, micro- and pico-cells. These configurations allows one to perceive whether there are differences in the energy savings as the BSs considered are smaller, and therefore the power consumption distribution among the BS equipments is different as well.

One has in Table 5.2, a description of the several inputs for each scenario. Voice and data configurations are described separately, with the input parameters described in this section and, for the co-localised scenarios, one assumes both the voice and data inputs together, for each scenario. Beginning with the Urban Scenario (U), one uses both voice and data values of traffic load amplitude near the maximum ones observed in the studied urban areas. This scenario is also used as a reference, as it corresponds to a situation where voice and data generated by users is better approximated by the values obtained from real data of the live network.

From this reference scenario, one has the Suburban (S) and Rural (Ru) Scenarios with the decrease from 3 to 2 TRXs, and also the decrease in the traffic load amplitude. Furthermore, the amplitude of 3 Erl in the Rural Scenario is chosen to simulate the low traffic load in these areas, and therefore to explore this situation of energy consumption inefficiency in those BSs. The Dense Urban Scenario (DU) is developed from a long term forecast point of view, considering an increase of both voice and

data traffic loads, as well as with the increment to 4 carriers for the 2G network. This scenario leads to a situation where, with the introduction of twice the value of the standard deviation, the capacity of the 2G network is filled at its maximum.

To complete the scenarios analysis, traffic load amplitude and carrier capacity variations are evaluated for each scenario, in the co-localised BSs configuration. Three traffic profiles are produced as inputs, the first with just the average value of traffic load, the second with the average standard deviation added to the traffic load profile, and the third with twice the standard deviation values. As it is assumed that fast traffic load variations are generated according to a Normal Distribution, this procedure allows one to cope with traffic load peaks for 84% and 98% of the cases, with the addiction of the standard deviation and twice that value, respectively. In Figure 5.1, traffic load profiles are presented; the hourly values of the standard deviation also referred as standard deviation profiles, for each of the developed traffic models are shown at Annex H. With the use of these standard deviation values, one can produce the analysis of the energy savings with the predicted variation of the traffic load amplitude. Therefore, one has in Table 5.3, the input values of the maximum value of traffic load profiles for each voice and data scenario, considering the traffic load amplitude variation with the sum of the standard deviation.

Concerning the carrier capacity, one assumed a variation of SNR between the MT and the BS, as SNR level changes may be caused by variation in the channel conditions or distinct user's distribution within the covered cell, therefore, the maximum data rate available per carrier, with the use of the same procedure already described for the traffic load amplitude. As referred in Section 4.2.2, and according to [Carv09], an average SNR at the BS is defined for 3G as well as the value of standard deviation for this measurement. Therefore, assuming once again a Normal Distribution, one can cope with 84% and 98% of carriers' capacity variations with the reduction of once and twice the value of standard deviation for the SNR. One could consider the opposite where the SNR values would be added from the average value, but since there is an over dimensioning of the 3G networks for the studied urban areas, this approach would not reveal any changes in the power consumption profiles obtained for the Urban Scenario. So, one assume the decreasing quality of the radio link, which leads to an higher occupation of the 3G carriers by the dimensioned data rates for the Urban Scenario. The decrease of the carriers' capacity is not proportional to the standard deviation values; in Annex F, data rate expressions as a function of the SNR are shown, which allows one to obtain the variation of SNR values.

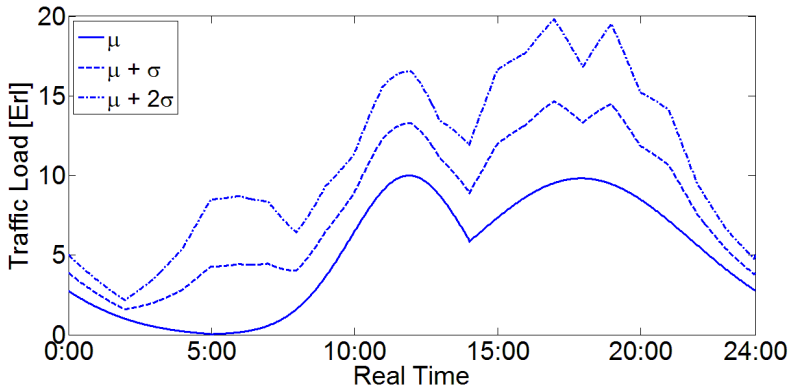

Figure 5.1 – Voice traffic load profile, with added standard deviation.

Table 5.3 – Voice scenarios traffic load amplitude variation.

Scenario	Voice T_{MAX}[Erl]						Data R_{bMAX}[Mbps]		
	Weekdays			Weekend			Weekdays		
	μ	$\mu+\sigma_{avg}$	$\mu+2\sigma_{avg}$	μ	$\mu+\sigma_{avg}$	$\mu+2\sigma_{avg}$	μ	$\mu+\sigma_{avg}$	$\mu+2\sigma_{avg}$
DU	15.0	18.0	21.0	7.5	10.5	13.4	7.5	9.8	12.1
U	10.0	13.0	16.0	5.0	8.0	10.9	5.0	7.3	9.6
S	5.0	8.4	11.9	2.5	6.0	9.4	5.0	7.0	9.0
Ru	3.0	6.4	9.9	1.5	5.0	8.4	2.5	4.5	6.5

In Table 5.4, the input values for the carrier capacity variation analysis are presented, which are obtained according to (4.5), the weighted average data rate based on the relative use of the QPSK, 16QAM and 64QAM modulations. As expected, a linear fall on the SNR value does not lead to a proportional decrease of the carrier capacity. So, for 7.5 dB of SNR degradation one has a shortage of almost 5.5 Mbps in each 3G carrier. This situation leads to an increase in the energy consumption, as the secondary carrier will be turned on earlier than for the regular carrier capacity situation.

Table 5.4 – Carrier capacity variation.

SNR variation	μ	$\mu-\sigma_{avg}$	$\mu-2\sigma_{avg}$
SNR [dB]	9.52	5.77	2.02
Average Carrier Capacity [Mbps]	10.00	7.04	4.59

5.2 Results analysis for the reference scenario

In this section, relative and absolute energy savings are calculated for the Urban Scenario configuration, which is also referred to as the Reference Scenario, as its traffic load amplitudes are based on real live network measures. The absolute energy savings results are obtained as the aggregate of the daily power consumption profiles.

For the reference scenario, voice is taken for the 2G network while data is used for the 3G one. From these input scenarios, a comparative analysis is made between daily power consumption profiles with and without energy efficient algorithms for both networks. Both power consumption and energy efficient model were executed simultaneously to give the clear perception of the difference of power consumption at every instant, whether one is at low traffic load hours or at the peak of traffic intensity at the network.

As seen in Figure 5.2, the Double Gaussian Traffic Model is used in the 2G Energy Efficient Model to produce the Urban Scenario. From this profile, it is visible that the energy efficient algorithm gives a considerable amount of power saving at low traffic hours, reducing the power consumption to almost half of the one obtained at the reference Power Consumption Profile, at this time of the day, with the

carrier' switch off procedure. Furthermore, as the traffic load increases after the low traffic hours, the power consumption increases proportionally too, but with the energy efficiency procedure, one can conclude that the smaller the slope of the load as it is rising, the longer is the gap between the TRXs switch on decisions, which leads to higher energy savings.

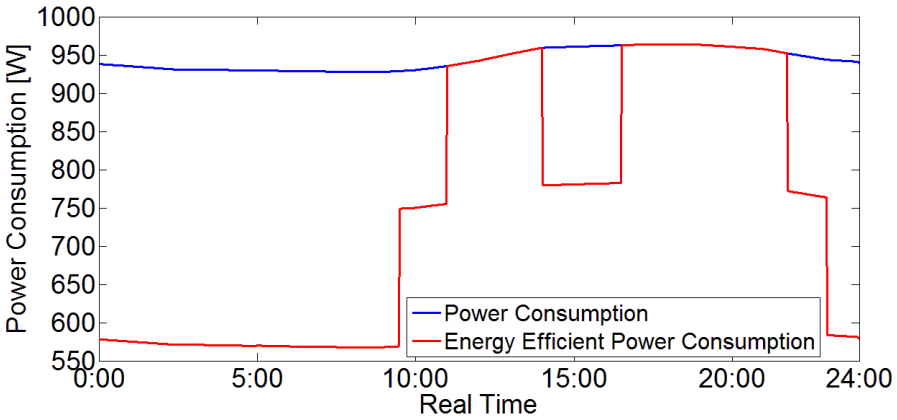

Figure 5.2 – Urban voice scenario daily power consumption profile.

With both power consumption profiles obtained, with and without energy efficient procedures, one can then calculate the daily power consumption for both profiles, and then the absolute and relative energy saving values, as shown in Table 5.5. For each of the traffic load profiles, one shown in the "Savings" column the percentage and the absolute value of energy saved with the use of the Energy Efficient Algorithm along the day, and for the "Total" column, the total of power consumed in one day, without any energy efficiency procedures, to be used as a reference value. For the reference 2G scenario one considers the average value of traffic load amplitude, achieving a relative energy saving of more than 20% for the complete 2G site, which leads to a considerable amount of 4.71 kWh of energy saved within the period of one day.

Table 5.5 –Reference scenario daily energy savings.

	Energy Savings		Total Energy Consumption [kWh]
Scenario	**[%]**	**[kWh]**	
Urban 2G	20.80	4.71	22.66
Urban 3G	32.03	8.64	26.98
Urban Co-localised	33.43	13.35	39.94

Considering the 3G Energy Efficient Model, one obtained as well the daily power consumption profiles with and without energy efficient procedures. For this scenario, the Pyramid Traffic Model is used, as is it the most commonly observed at the daily traffic profiles collected from the live network. As shown in Figure 5.3, one can see that the assumed data rate amplitude for the reference scenario, which is approximately the maximum value of data rate observed at one of the studied urban areas, leads to a situation where just one of the carriers is active along every hour of the day. This outcome is justified with the over dimensioning of active resources that was done for these two urban areas, which causes an excessive energy consumption of the 3G sites, and results in a inefficient deployment of 3G carriers.

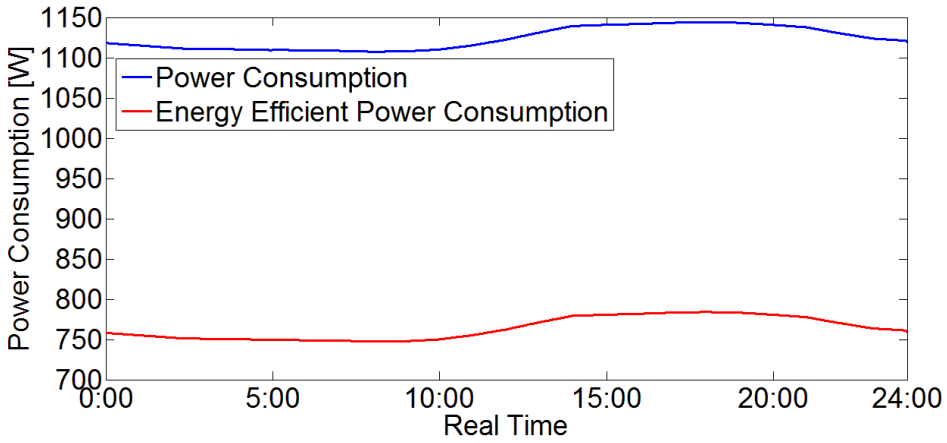

Figure 5.3 – Urban data scenario daily power consumption profile.

This waste of power consumption is also visible with the obtained results of energy savings and daily power consumption values, as shown in Table 5.5. For the average traffic load amplitude, the energy saving relative value is always larger than 30%, which means that in each day more than 8 kWh are saved because the secondary carrier is always switched off.

Finally, with the joint contribution of both 2G and 3G scenarios, one performed a co-localised power consumption analysis, using the Urban Voice and Data scenarios as the reference scenario once again, obtaining the daily power consumption profile shown in Figure 5.4. The difference between the power consumption with and without energy efficient procedures is noticeable, and even for the considered peak traffic hours there is more than 300 W of gap between the two profiles. To be noticed, is the difference of power consumption values at low traffic hours, where the energy efficient power consumption profile consumes almost half the power consumed without energy savings.

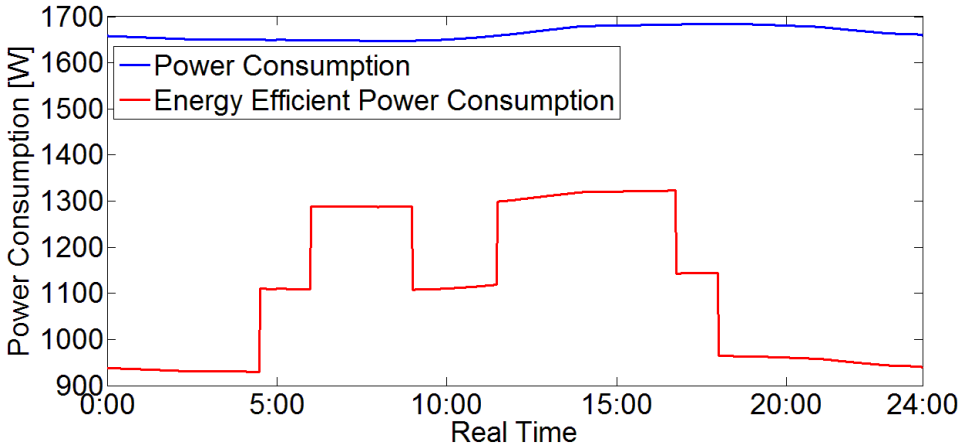

Figure 5.4 – Urban mixed traffic scenario daily power consumption profile.

To reinforce the relation between power consumptions observed in Figure 5.4, one has the results for the co-localised BSs reference scenario, with a considerable amount of energy saved along the day. The energy savings go up to 33%, saving over 13 kWh in one day.

5.3 Parameter variation results analysis

5.3.1 Traffic load amplitude variation

The traffic load amplitude is not equal for every day, meaning that along the week, different traffic load and data rate peak values must be analysed. By varying the daily traffic profiles' amplitude, with the sum of standard deviation to the average traffic load, one can perceive what is the effect of the variation of the traffic load amplitude on energy saving.

In Table 5.6, the results of the absolute and relative energy savings and total energy consumption with the traffic load amplitude variation are presented. As the traffic load standard deviation is added with the average amplitude, energy savings decrease as expected, but even for the least favourable situation the achieved energy saving is almost 30%, which is a considerable value for the energy efficiency of the whole site, allowing one to save more than 11.5 kWh in one day. With a variation of twice the standard deviation, one only sacrifices 3.5% or 1.5 kWh of energy savings, which guarantees a consistently high value of energy efficiency despite unexpected variations of the traffic load amplitude.

Table 5.6 – Traffic load amplitude variation energy efficiency results.

Traffic load amplitude	μ		$\mu + \sigma_{avg}$		$\mu + 2\sigma_{avg}$		**Total Energy Consumption [kWh]**
Energy Savings	**[%]**	**[kWh]**	**[%]**	**[kWh]**	**[%]**	**[kWh]**	
U Scenario	33.43	13.35	30.63	12.23	29.73	11.87	39.94

5.3.2 Carrier capacity variation

Concerning the variation of the carrier capacity, the procedure is similar to the traffic load variation analysis, as three considered carrier capacity scenarios are assumed, with just the average value of SNR, and then with the reduction of once and finally twice the value of the standard deviation for the chosen data traffic model, because the SNR variation only affects the 3G carriers. Once again one obtains the energy saving and consumption for all mixed traffic scenarios for both weekdays and weekends, Table 5.7.

Table 5.7 – Carrier capacity variation energy efficiency results.

Carrier Capacity	μ		$\mu - \sigma_{avg}$		$\mu - 2\sigma_{avg}$		**Total Energy Consumption [kWh]**
Energy Savings	**[%]**	**[kWh]**	**[%]**	**[kWh]**	**[%]**	**[kWh]**	
DU Scenario	33.02	14.61	32.11	14.21	26.58	11.76	44.26
U Scenario	33.43	13.35	33.43	13.35	32.07	12.81	39.94

For the Urban scenario, although there is degradation in SNR, and therefore a decrease of the carrier capacity, only for the case where twice the value of the standard deviation is subtracted to the average carrier capacity one obtains a reduction on the energy savings, coming from the need to switch on the secondary 3G carrier. Even though the period of time in which the second carrier is switched on is too short to result in a considerable reduction in energy savings, being kept above 32%.

For this scenario, one can conclude that the power consumption is insensitive to unexpected variations on the radio link quality. On another perspective, one can conclude that for the considered scenario, which is based on the collected data from the live network, the deployment of the second 3G carrier is negligible as there is an over dimensioning of the 3G network within the studied urban areas.

On the other hand, considering the Dense Urban scenario, as the carrier capacity decreases, the energy efficiency of the model is reduced, as the use period of the second carrier becomes longer. So, with the use of this scenario for the carrier capacity variation, one can perceive the sensitivity of the power consumption outcome with the degradation of the radio link signal quality. Although there is only a decrease of 6.5% in energy savings, it originate a reduction of almost 3 kWh in the total energy saved. Nevertheless, even for the worst case scenario, the co-localised energy efficient model produces energy savings of more than 26.5%, allowing savings over 11.5 kWh in one day.

5.3.3 Environment variation

A comparative analysis is made between the daily power consumption profiles with and without energy efficient algorithms for all four scenarios configurations, from Dense Urban to Rural areas. These power consumption profiles, based on the co-localised energy efficient model, can also be analysed in Annex I, where the outcome of the DU scenario is shown, with the 4 TRXs and its switch off procedure at low traffic hours. On the opposite view point, the Ru scenario also shows how in days that one has very low traffic load values, there is no need to use the second TRX dimensioned for this scenario, leading to high percentages of energy savings. From these energy efficient power consumption profiles, one obtain the daily savings on the electricity expenditure within the Co-localised BSs.

As seen in Table 5.8, there is a similarity among the energy saving absolute values, but their relative values grow from the DU to the Ru scenarios. This situation is explained by the assumptions made on the scenarios' definition, considering the growth of the traffic load amplitude, and the number of carriers chosen for each scenario. Finally, the S and Ru scenarios have the same total daily energy consumption, as their BS configuration is the same, taking into account the number of carriers. So, one can conclude that, assuming the BS configuration chosen for each scenario to be a good approximation of the network deployment done at the studied urban areas, the energy saving is guaranteed to be kept above 33% for all scenarios with the use of the developed energy efficiency procedures.

Table 5.8 – Environment variation energy efficiency results.

	Energy Savings		Total Energy Consumption [kWh]	Daily Saving [€]
Scenario	**[%]**	**[kWh]**		
DU	33.02	14.61	44.26	1.62
U (Ref.)	33.43	13.35	39.94	1.52
S	35.24	12.55	35.62	1.46
Ru	36.39	12.96		1.51

As for the economic savings, one can perceive that with the energy efficiency procedures, one can save more than 1.46 € each day, at each BS. Furthermore, one can conclude that although the relative energy saving is lower for the U and DU scenarios, the daily economic savings is the highest obtained, in particular considering the DU scenario. This situation is explained by the number of deployed TRXs assumed for these urban centre scenarios, leading simultaneously to higher energy consumption at peak hours and, on the other hand, to a bigger difference between the peak energy consumption and the low traffic hours energy efficient consumption.

5.3.4 Weekday/weekend comparison

From the analysis of the traffic load amplitude developed on Chapter 3, one concluded that there is a decrease in 50% for the volume of the voice traffic load at weekends. In this way, one assumed two situations for the analysis between weekdays and weekends energy consumption profiles, both with and without energy efficient procedures. Therefore, one obtained the outcome of absolute and relative energy savings. The first situation considered is equal to the one defined for the reference scenario, with the co-localised energy efficient model. Then, for the weekends, it is assumed half the voice traffic load amplitude as input of the energy efficient model.

The resulting energy savings' and total consumption values, Table 5.9, show considerable increase on the values of energy savings from weekdays to weekends. Similarly to Section 5.3.3, one obtained as well the economic daily savings for the weekend scenarios, in order to drawn some conclusions.

Table 5.9 – Weekday to weekend comparison energy efficiency results.

Scenario	Weekday			Weekend			Total Energy Consumption [kWh]
	Energy Savings		Daily Saving [€]	Energy Savings		Daily Saving [€]	
	[%]	[kWh]		[%]	[kWh]		
DU	33.02	14.61	1.62	43.92	19.44	2.25	44.26
U	33.43	13.35	1.52	40.54	16.19	1.89	39.94
S	35.24	12.55	1.46	36.39	12.96	1.51	35.62
Ru	36.39	12.96	1.51	36.39	12.96	1.51	

With the analysis of the weekdays to weekend energy consumption comparison, one can conclude that even higher values of energy efficiency can be achieved if one takes into consideration the decrease of the traffic load at weekends. At these days, the energy savings achieved can go up to 40%, with absolute values of more than 16 kWh saved within one day, considering the Urban co-localised scenario. Considering that the percentage of variable power consuming equipment is 60% of both 2G and 3G power consumption models, one can conclude that more than half of this equipment is always switched off.

If one takes into account the economic daily saving at the weekend scenarios, one can conclude that, once again, the BSs placed within urban areas revealed to be the most rewarding scenarios, as there is a larger power consumption gap between peak consumption and low traffic hours power

consumption. Therefore, considering the DU Scenario, one achieves 2.25€ of daily savings at weekends. Regarding the S and Ru Scenarios, one can perceive that the traffic load is so low that there is no major difference between weekdays and weekend daily energy consumption.

From these values, one can obtain the monthly and the annual savings in the BSs electrical expenditure. So, considering five weekdays and two days for the weekends, one can assume an average monthly bill with four weeks and two additional weekdays. These calculations are presented in Table 5.10, for each developed scenario.

Considering the developed scenarios, one can conclude that the reduction of the electricity bills is within the interval of 45€ to 55€ and, according to [OPTI11], this saving in the electrical expenditure leads to a monthly cost reduction of 25% to 35% on the current electricity bills.

Table 5.10 – Monthly economic savings at BS level.

Scenario	Monthly Saving [€]
DU	53.64
U	48.56
S	44.30
Ru	45.30

To conclude the economic analysis, it is also important to refer that, if one considers one year being composed of 52 weeks, and 200 co-localised BSs deployed within the studied urban areas, one obtains the global annual economic saving of 118 352€, which is a considerable value taking into account that it comes from optimisation on the power consumption process, and that it only embraces two small sized urban areas, considering the Portuguese demographic situation.

Chapter 6

Conclusions

In this chapter, the main conclusions of this thesis work are drawn, and then some future work perspectives are proposed.

This thesis intends to evaluate the existence and the feasibility of the development of traffic models from traffic load data collected in two areas. With this traffic profiling, one intends to reduce BSs energy consumption, with the use of Energy Efficient Algorithms. So, with the use of the developed traffic models, one followed two distinct paths.

In Chapter 2, one describes GSM and UMTS fundamental aspects, traffic, power consumption and energy efficient models, from the theoretical view point. In the first section, aspects such as network architecture, radio interface configurations, and capacity and coverage limitations are approached. Then, an extensive description of traffic models is made, regarding both voice and data traffic characteristics, and temporal traffic variations. Thereafter, the most consuming elements of a mobile communications site are described, where the dependencies of the carriers' consumption with the traffic load amplitude and the air conditioning consumption with air temperature are identified. Furthermore, several power consumption models are described, with different complexity levels. Finally, different energy efficiency approaches are described, considering BS cooperation schemes, FFR, and finally, adaptive network solutions. Within these solutions, the attention was focused in adaptive carrier switch off procedures, taking into account their implementation in the network, and the expected energy saving results from these implementations.

In Chapter 3, the process of data analysis is described, which leads to the development of the traffic models used to simulate the traffic load variation at the Energy Efficient Model. In the first section, a brief description of the areas, where the traffic load data was collected, is done. Then, the process of voice and data traffic load analysis is described, taking into consideration the use of the average profiles for the weekday and the weekend, and the gathering of the similar profiles to produce a single sector profile that represents one type of daily traffic variation. From this procedure, three voice and four data traffic models are obtained, and the approximation between the sector profiles and the traffic models are evaluated, revealing, as expected, the good approximation of the Double Gaussian Voice Model, with an RMSE of 4.28%, and the Pyramid Data Model, with an RMSE of 3.61%. The low values obtained lead to confirm that these models have the best similarity with the daily traffic load variation.

A parallel analysis is also developed, concerning the distribution of the traffic load amplitude between 2G and 3G sectors. These values are used as inputs to the Energy Efficient Model, to better adjust the traffic models with each scenario BS configuration. One can conclude that, concerning voice traffic load amplitude, there is a clear distinction between the 2G and 3G networks, as the voice service is typically forwarded for the 2G, leading to a difference of more than twice the voice traffic load observed in the 3G network. Taking into account the relation between weekdays and weekends traffic load amplitudes, the analysed data from the studied areas lead to conclude that there is a decrease at weekends for the voice traffic peak values of 50%, while for the data traffic there is no noticeable variation in the traffic load amplitude, and one can say that usually the data traffic load may be slightly higher at weekends, especially when the maximum traffic load value registered belongs to one day of the weekend.

Reproducing the same analysis, but considering a higher level of complexity, one presents as well the

achieved maximum traffic load for each the traffic profiles associated to the developed voice and data models. This study allows one to perceive the existence of distinct geographical areas within the cities, based on the daily traffic profiles that one obtained at each cell. One concluded that the Tree Stump Model is the most associated model within the 2G sites, with 59.5% of the 2G sectors, due to the suburban and rural cells' association. On the other hand, the Double Gaussian Traffic Model has 50.8% of the 3G voice sectors, leading to conclude that this model is better associated within urban areas. For the data traffic profiles, the Pyramid Traffic Model is definitely the most used model for the data services, with 68.8% of the sector profiles associations.

Finally, one inferred about the use of an alternative sector profiles distribution, with differences on voice and data Trapezoidal Model amplitudes. This analysis led to conclude that, for voice, the sectors are more evenly distributed, and for data, no conclusions were achieved. Similarly, one attempted to develop correlations between voice and data profiles, and weekdays and weekends ones, leading to no major conclusions, as there are many different aspects to consider in order to obtain an achievable relation among these profiles.

In Chapter 4, one presents a description of the Power Consumption Model, and its four configurations, for 2G macro-, and 3G macro-, micro- and pico-cells, as well as the 2G and 3G Energy Efficient Algorithms that were developed in this thesis. An extensive list of the elements responsible for the 2G and 3G site power consumption is developed, and then the variation of the air conditioning consumption with air temperature is modelled. 2G and 3G Energy Efficient Algorithms were developed to be used together with the Power Consumption Model, in order to obtain the Energy Efficient Models, and therefore both absolute and relative power savings results. These models were developed according to the concept of carrier switch off, which takes into account the traffic load observed at a certain instant. The assessment of the power consumption model produces the expected minimum power consumption of 560 W for 2G and 740 W for 3G, and the maximum BS consumption of 1200 W.

Finally, in Chapter 5, distinct scenarios were developed and their energy consumption is analysed, considering co-localised site configurations. An extensive description of the power consumption scenarios is done, considering the different inputs, their assumed values, and the respective variation analysis. From this point, four scenarios are defined, where one consider three of them to characterise the present users' traffic generation, and the fourth considering a medium to long term approach of the network traffic load evolution. Regarding the parameter variation, one decided to vary the traffic load amplitude, carrier capacity, BS environment, and finally one performed the weekday to weekend comparison.

The parameter variation analysis is performed with the reference to the obtained energy saving values from the Urban Scenario, as it considers collected data from the live network. Therefore, the reference scenario can achieve energy savings of 33% for the co-localised BS configuration, allowing to save up to 13.35 kWh at each day. From this point, for the traffic load amplitude and the 3G carrier capacity variation analysis, one observed that for the Urban scenario, where the traffic load is very low compared with the available resources, even with some degradation on the radio link there were no

changes in the energy efficiency of the BS. The traffic load amplitude caused a variation of around 3.5% on the energy savings, which is translated in 2.5 kWh of decrease on the energy saved in one day. For the carrier variation, there was almost no need to switch on the second carrier in the Urban Scenario. On the other hand, when the Dense Urban scenario is considered, there is a considerable decrease on the energy efficiency, consisting in a reduction of 6.5%, and therefore leads to an increase of almost 3kWh in the daily total power consumption.

For the environment variation, one can conclude that even assuming different BS configurations with the variation on the number of deployed carriers, the energy savings are kept over 33%, guaranteeing more than 12.5 kWh of absolute energy saving in one day. Then, the traffic load amplitude variation is developed to ensure that even with high traffic load maximum values, the energy efficiency of the network is not compromised. Therefore, with the sum of standard deviation values, the percentage of energy saved lowers to 29.7%, but even in this situation almost 12 kWh of energy can be saved within one day. Finally, the comparison between the energy consumption at weekdays and weekends produced an increase on the energy saved by 7%, comparing to the one obtained at the reference scenario. So, at weekends, the energy efficiency saves more than 16 kWh, which consists of 40.5% of energy saving. Finally, one assumed a carrier capacity variation analysis, with the decrease of the SNR level, and therefore, the data rate supported at one carrier.

Summarising, one can obtain on average 30% to 40% of energy savings in any considered scenario, which leads to a high amount of energy saved at the BSs. Anyway, considering that 40% of the total 2G and 3G sites' power consumption is fixed or independent with the traffic load variation, the resulting values of 30% to 40% daily energy savings are quite considerable, if one considers that those are the outcome of 60% of variable power consuming equipment. So, just regarding the 2G and the 3G BS power consumption, on average, one half of the energy consumed by these varying power consuming equipment's is saved with the use of the Energy Efficient Model.

Considering at last the economic evaluation of the energy efficient procedures, one can withdraw from 45€ to 55€ at each month within one co-localised BS electricity bill, which consists of improvements on the electrical expenditures of 25% to 35%. Considering the annual perspective for the entire studied urban area, savings up to 120 000€ need to be considered with the use of energy efficiency, and therefore, one can assume that, considering the BSs deployed in Portugal for this operator, one can achieve annual energy savings in the order of one million Euros.

For future work, at first, a more extensive process of data collecting using urban areas with larger number of inhabitants is important, because within large cities the urban regions are better defined within the urban mesh, enabling a better urban region classification. Considering the traffic models, the geographical localisation of both data and traffic models, at weekdays and weekends could provide a good overview of the user's traffic generation within urban areas, and this behaviour understanding can be advantegous for the operators. Then, the application of the energy efficient algorithm can also be studied with the introduction of LTE in the live network, the use of smaller cells and therefore, smaller equipment, and even on the dependence of the electronic equipment with the traffic load variations. Finally, the 2G Energy Efficient Model developed in this thesis can be improved

and produce better energy savings with a more global view of the network, instead of a self-centred Energy Efficient Model for either 2G or 3G where each sector only concerns with its own traffic load. Two approaches could be used: in the case of co-localised 2G and 3G BSs, a cooperative intra-site solution can be developed, especially for voice, where there could be the possibility to shut down all TRXs and guarantee voice service using the 3G BS, for low traffic hours; using the already suggested global overview of the traffic patterns within the live network, a cooperative inter-site approach can be developed, mainly to adapt 3G data traffic capacity to the user's needs. From this point of view, one site could be shut down and their coverage and capacity would be assured by its neighbours.

In conclusion, the subject of Energy Efficiency is of major importance in today's mobile networks operators, due to its results when it comes to creating more profits, using small investments to create a great reduction in expenses, while keeping revenues, instead of large investments in new technologies to increase the income and keeping the expenditures. For instance, one can take the work developed in this thesis, and use it with other traffic load variation patterns. If one considers the network capacity needed to embrace a summer festival, or some annual event, the operator simply deploys additional carriers in that area in order to ensure that there is enough capacity to receive the traffic generated. However, at the surroundings of stadiums, or at areas where there is a considerable increase of mobile phone users at night, with a weekly basis, the BSs already deployed must take into account this weekly traffic load peaks. So, on the remaining days, these energy efficient procedures can be very effective in reducing the expenditure of having too much 2G and 3G active carriers.

With this path for networks evolution, the way of thinking in mobile communications goes from always on, to always available.

Annex A

Daily Traffic Profiles

This annex contains two sets of daily traffic profiles, from one 2G voice sector and one 3G data sector. In these profiles, 8 days of collected data, 6 weekdays and 2 weekend days are represented.

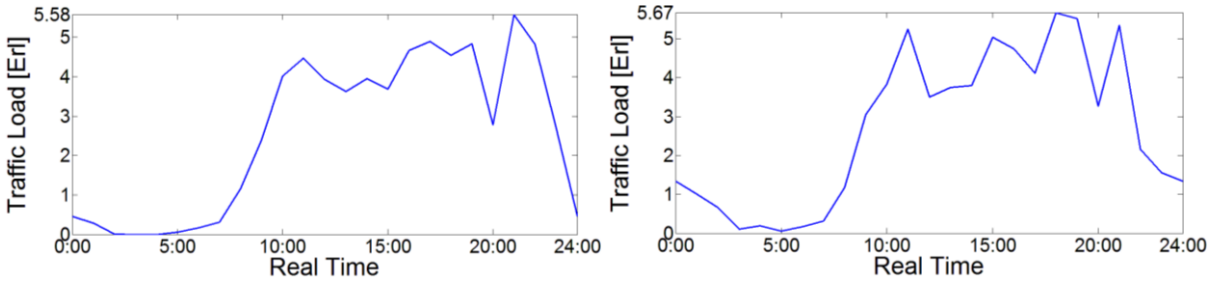

a) Weekday 1.

b) Weekday 2.

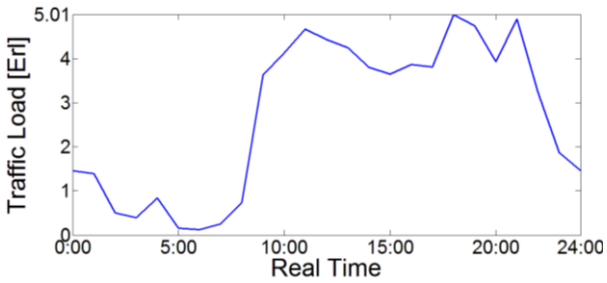

c) Weekday 3.

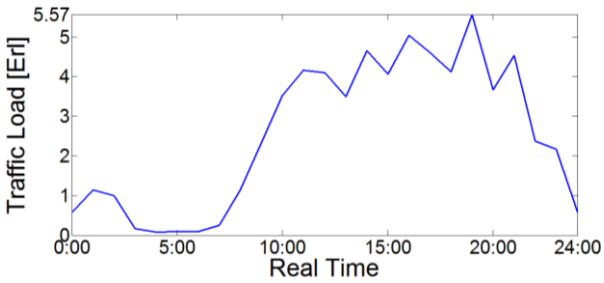

d) Weekday 4.

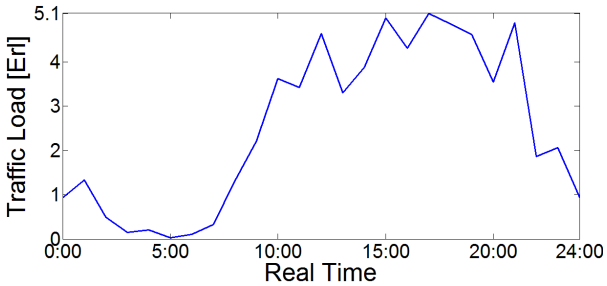

e) Weekday 5.

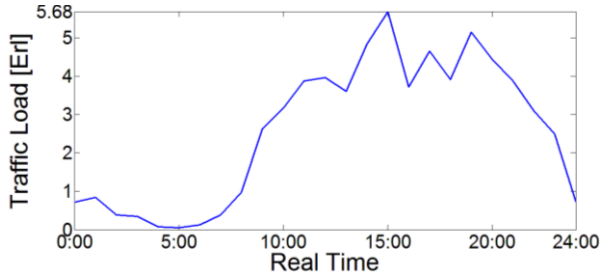

f) Weekday 6.

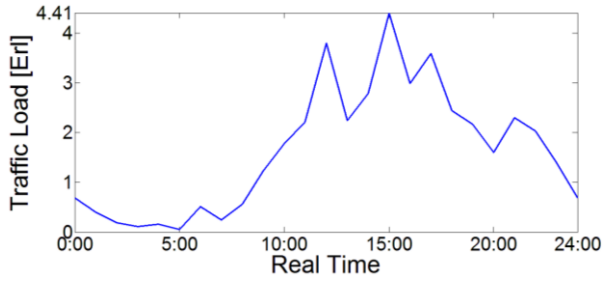

g) Weekend 1

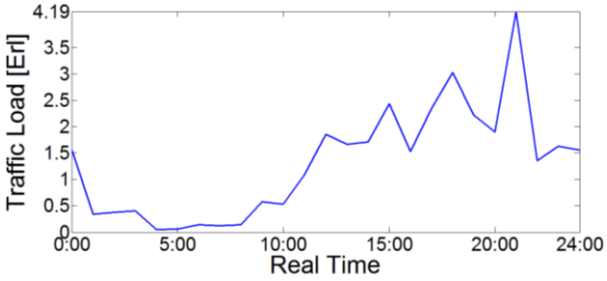

h) Weekend 2.

Figure A.1 – Daily voice traffic profiles from 2G sector.

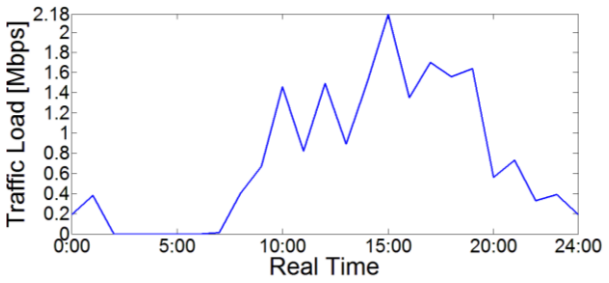

i) Weekday 1.

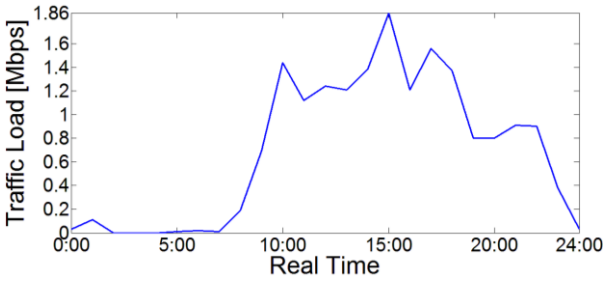

j) Weekday 2.

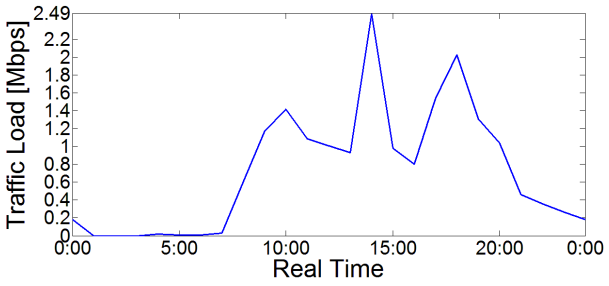

k) Weekday 3.

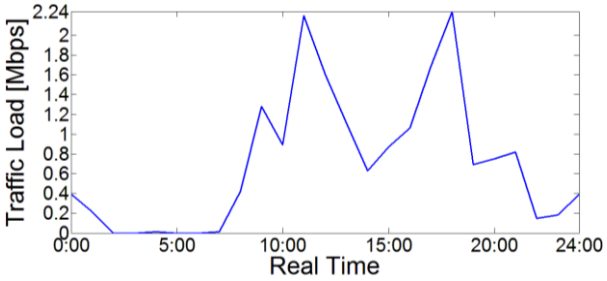

l) Weekday 4.

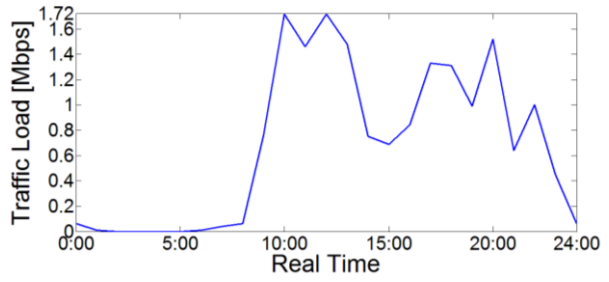

m) Weekday 5.

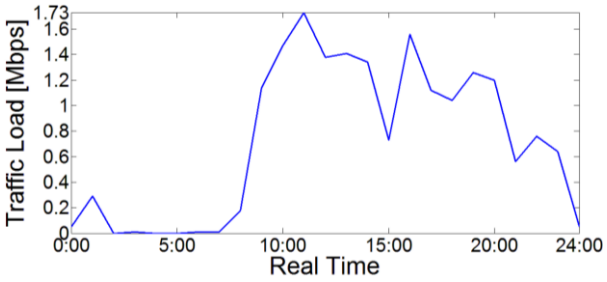

n) Weekday 6.

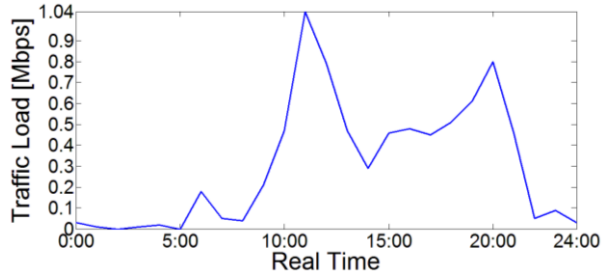

o) Weekend 1

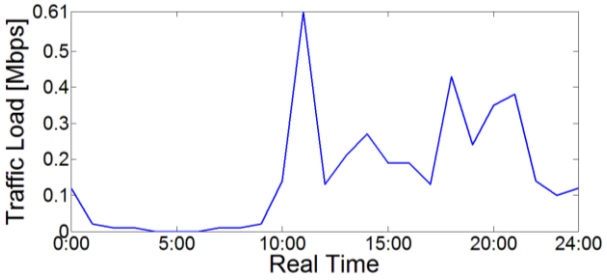

p) Weekend 2.

Figure A.2 – Daily data traffic profiles from 3G sector.

Annex B

Sector Classification

This annex contains a list of all collected BSs and their respective sectors, the maximum traffic load verified and the automatic classification obtained.

Table B.1 – Voice Traffic information collected from the live network.

City 1 – 2G			City 2 – 2G			City 1 – 3G			City 2 – 3G		
BS	Tr_{MAX}[Erl]	Reg.	BS	Tr_{MAX}[Erl]	Reg.	Node B	Tr_{MAX}[Erl]	Reg.	Node B	Tr_{MAX}[Erl]	Reg.
1_1	0.603	DGM	22_1	2.720	DGM	51_1	0.035	TS	70_1	0.677	DGM
1_2	3.365	TS	22_2	1.318	DGM	51_2	0.502	TS	70_2	0.635	DGM
1_3	1.827	DGM	23_1	3.832	DGM	51_3	0.198	DGM	71_1	0.780	DGM
2_1	4.837	DGM	23_2	2.043	DGM	52_1	1.337	DGM	71_2	0.292	DGM
2_2	6.490	DGM	23_3	1.975	TS	52_2	2.135	DGM	71_3	0.213	DGM
2_3	1.142	DGM	24_1	1.788	DGM	52_3	0.720	DGM	72_1	0.382	DGM
3_1	1.127	TS	24_2	1.720	TS	53_1	0.090	DGM	72_2	0.142	DGM
3_2	0.852	TS	24_3	0.595	TS	53_2	0.113	DGM	72_3	0.305	DGM
3_3	0.817	TS	25_1	3.927	DGM	53_3	0.062	DGM	73_1	0.515	DGM
4_1	1.938	DGM	25_2	2.680	DGM	54_1	0.512	TS	73_2	0.682	DGM
4_2	4.033	TS	25_3	4.240	TS	54_2	0.465	TS	73_3	0.600	DGM
4_3	2.698	TrM	26_1	4.522	TrM	54_3	0.647	TS	74_1	1.592	DGM
5_1	1.410	TS	26_2	3.272	TS	55_1	0.088	TS	74_2	1.012	DGM
5_2	0.810	TS	26_3	4.062	TS	55_2	0.352	DGM	74_3	0.873	DGM
5_3	1.703	TS	26_4	5.075	TS	55_3	0.225	DGM	74_4	0.403	TS
6_1	0.540	TS	26_5	3.500	TS	56_1	0.260	DGM	74_5	0.073	DGM
6_2	3.138	TS	26_6	4.187	TS	56_2	0.168	DGM	74_6	0.168	TS
6_3	1.938	DGM	27_1	4.968	DGM	56_3	0.273	DGM	75_1	0.453	DGM
7_1	2.523	TS	27_2	4.282	TS	56_4	0.052	TS	75_2	1.295	DGM
7_2	3.148	TS	27_3	1.875	TS	56_5	0.073	DGM	75_3	0.525	DGM
7_3	6.715	TS	27_4	0.000	DGM	56_6	0.050	TS	75_4	0.465	DGM
8_1	3.638	DGM	27_5	6.495	DGM	57_1	0.300	DGM	75_5	0.477	DGM
8_2	0.855	DGM	27_6	0.000	DGM	57_2	0.103	DGM	75_6	0.165	DGM
8_1	2.172	DGM	28_1	1.597	TS	57_3	0.182	TS	76_1	0.350	DGM
9_2	1.590	TS	28_2	9.468	TrM	58_1	0.675	DGM	76_2	1.105	DGM
9_3	1.647	TS	28_3	4.567	TS	58_2	0.105	DGM	76_3	0.408	DGM
10_1	3.253	TrM	29_1	0.718	TS	58_3	0.120	DGM	76_4	0.222	TS
10_2	3.545	TS	29_2	2.360	DGM	59_1	1.008	DGM	76_5	0.337	TS
10_3	6.560	TS	29_3	6.472	DGM	59_2	1.430	DGM	76_6	0.093	DGM
10_4	3.692	DGM	30_1	2.380	DGM	59_3	1.548	DGM	77_1	0.318	TS
10_5	6.502	TS	30_2	2.112	TS	59_4	0.138	DGM	77_2	0.393	DGM
10_6	4.265	TrM	31_1	3.133	TS	59_5	0.635	TS	77_3	0.490	TS
11_1	5.247	TS	31_2	4.293	DGM	59_6	0.657	TS	77_4	0.138	TS
11_2	2.972	TS	31_3	1.275	TS	60_1	0.553	DGM	77_5	0.235	DGM
11_3	5.177	TS	32_1	1.035	TS	60_2	0.297	TS	77_6	0.263	TS
12_1	3.142	TS	32_2	1.887	TS	60_3	0.617	TS	78_1	0.272	DGM
12_2	4.018	DGM	32_3	2.438	TS	60_4	0.265	TS	78_2	1.532	TrM
12_3	7.307	TS	33_1	3.203	TS	60_5	0.198	TS	78_3	0.987	TS
13_1	0.608	TS	33_2	3.188	TS	60_6	0.182	TS	79_1	0.097	TS

Table B.1 (cont.) – Voice Traffic information collected from the live network.

13_2	1.277	TS
13_3	2.920	TS
14_1	1.652	TS
14_2	0.150	DGM
14_3	1.263	TS
15_1	1.577	DGM
15_2	1.085	TS
15_3	0.707	DGM
16_1	1.162	TS
16_2	0.618	TS
16_3	0.295	TS
17_1	0.962	TS
17_2	0.175	DGM
17_3	0.177	DGM
18_1	1.545	TS
18_2	3.228	TS
18_3	1.185	TS
19_1	2.130	TS
19_2	1.380	DGM
19_3	1.483	TS
20_1	4.795	DGM
20_2	2.070	DGM
20_3	3.630	DGM
21_1	2.947	TS
21_2	3.780	TS
21_3	2.197	DGM

33_3	2.410	DGM
34_1	0.552	TS
34_2	1.445	TS
34_3	2.240	DGM
35_1	4.443	DGM
35_2	2.672	DGM
35_3	7.843	DGM
36_1	3.240	DGM
36_2	2.543	DGM
36_3	2.263	TS
37_1	1.628	TS
37_2	1.815	DGM
37_3	0.648	TS
38_1	2.075	TS
38_2	3.100	TS
38_3	7.860	TS
39_1	2.867	TS
39_2	5.558	DGM
39_3	3.847	TS
40_1	1.368	DGM
40_2	2.045	TS
40_3	1.102	TS
41_1	0.017	TS
41_2	0.005	TS
41_3	0.095	TS
41_4	0.072	TS
41_5	0.005	TS
42_1	4.172	TS
42_2	0.660	TS
42_3	0.982	TS
43_1	2.622	DGM
43_2	3.915	TS
43_3	2.440	DGM
44_1	8.383	TS
44_2	1.010	DGM
44_3	1.902	DGM
45_1	7.382	TrM
45_2	1.988	DGM
45_3	3.190	TS
46_1	0.535	TS
46_2	1.290	DGM
46_3	2.583	TS

61_1	0.590	TS
61_2	0.807	DGM
61_3	0.547	TrM
61_4	0.390	TS
61_5	0.278	DGM
61_6	0.345	TS
62_1	0.095	TS
62_2	0.110	TS
62_3	0.072	DGM
63_1	0.213	TS
63_2	0.105	TS
63_3	0.163	TS
64_1	0.177	TS
64_2	0.215	TS
64_3	0.182	TS
65_1	0.358	TS
65_2	0.188	DGM
65_3	0.162	TS
66_1	0.610	DGM
66_2	0.360	DGM
66_3	0.398	TS
66_4	0.433	DGM
66_5	0.147	TS
66_6	0.202	TS
67_1	0.203	TS
67_2	0.112	DGM
67_3	0.035	TS
68_1	0.047	DGM
68_2	0.137	TS
68_3	0.093	DGM
69_1	0.362	TS
69_2	0.572	TS
69_3	0.522	TS

79_2	0.670	DGM
79_3	1.142	DGM
80_1	0.542	TS
80_2	0.677	DGM
81_1	0.918	DGM
81_2	0.748	DGM
81_3	0.922	DGM
81_4	0.358	DGM
81_5	0.505	DGM
81_6	0.388	DGM
82_1	0.312	DGM
82_2	1.202	DGM
82_3	0.097	DGM
83_1	0.137	TS
83_2	0.222	TS
83_3	0.117	DGM
84_1	0.107	TS
84_2	0.300	DGM
84_3	0.622	DGM
85_1	0.048	TS
85_2	0.073	TS
85_3	0.140	TS
86_1	1.157	DGM
86_2	0.685	DGM
86_3	1.250	DGM
86_4	0.613	DGM
86_5	0.303	DGM
86_6	0.463	TS
87_1	0.522	DGM
87_2	0.265	DGM
87_3	0.050	DGM
88_1	0.220	TS
88_2	0.238	TS
88_3	0.107	DGM
89_1	0.238	TS
89_2	0.153	TS
89_3	0.710	DGM
89_4	0.092	TS
89_5	0.032	DGM
89_6	0.292	DGM
90_1	0.520	DGM
90_2	0.323	DGM

Table B.1 (cont.) – Voice Traffic information collected from the live network.

47_1	1.375	TS
47_2	0.683	TS
47_3	0.463	TS
48_1	0.687	TS
48_2	0.678	TS
48_3	0.667	TS
49_1	0.807	TS
49_2	1.213	TS
49_3	0.797	TS
50_1	2.313	TS
50_2	1.453	TS
50_3	2.745	TS

90_3	0.280	DGM
90_4	0.090	DGM
90_5	0.303	TS
90_6	0.067	TS
91_1	0.047	TS
91_2	0.088	DGM
91_3	0.015	TS
92_1	0.155	DGM
92_2	0.057	DGM
92_3	0.022	DGM
93_1	0.657	DGM
93_2	0.643	DGM
93_3	0.412	DGM
93_4	0.450	DGM
93_5	0.175	TS
93_6	0.070	DGM
94_1	1.435	DGM
94_2	0.323	DGM
94_3	0.613	DGM
95_1	1.112	DGM
95_2	0.552	DGM
95_3	0.528	DGM
96_1	0.210	DGM
96_2	0.898	DGM
96_3	0.453	DGM
96_4	0.333	TS
96_5	0.225	TS
96_6	0.132	DGM
97_1	0.095	DGM
97_2	0.285	DGM
97_3	0.215	DGM
98_1	0.123	DGM
98_2	0.058	TS
98_3	0.038	TS
99_1	0.023	TS
99_2	0.062	DGM
99_3	0.050	TS
100_1	0.045	TS
100_2	0.095	DGM
100_3	0.110	DGM
101_1	0.065	TS

Table B.1 (cont.) – Voice Traffic information collected from the live network.

101_2	0.197	DGM
101_3	0.043	TS
102_1	0.192	DGM
102_2	0.320	DGM
102_3	0.337	DGM

Table B.2– Data Traffic information collected from the live network.

City 1 – 3G		
Node B	R_{bMAX} **[Mbps]**	**Region**
103_1	1.065	PyM
103_2	0.625	PyM
103_3	1.193	PyM
104_1	0.987	DTrM
104_2	0.338	PyM
104_3	0.773	PyM
105_1	0.815	PyM
105_2	0.117	PyM
105_3	0.265	PyM
106_1	0.345	SwM
106_2	1.132	DTrM
106_3	0.622	DTrM
107_1	0.527	PyM
107_2	0.748	PyM
107_3	0.720	PyM
108_1	0.130	PyM
108_2	0.410	PyM
108_3	0.583	DTrM
108_4	1.578	SwM
108_5	0.818	PyM
108_6	0.788	DDGM
109_1	1.825	SwM
109_2	1.012	PyM
109_3	0.578	PyM
110_1	0.990	DTrM
110_2	0.620	PyM
110_3	0.642	PyM
111_1	1.017	PyM
111_2	1.073	DDGM
111_3	0.832	DDGM
111_4	0.633	PyM

City 2 – 3G		
Node B	R_{bMAX} **[Mbps]**	**Region**
122_1	1.155	PyM
122_2	0.522	PyM
123_1	0.613	PyM
123_2	0.578	PyM
123_3	2.273	PyM
124_1	0.267	PyM
124_2	0.217	PyM
124_3	0.428	PyM
125_1	0.242	PyM
125_2	0.578	PyM
125_3	1.223	PyM
126_1	1.577	PyM
126_2	0.080	PyM
126_3	0.438	DDGM
126_4	0.583	SwM
126_5	0.930	SwM
126_6	0.703	PyM
127_1	1.288	PyM
127_2	0.530	PyM
127_3	0.407	PyM
127_4	1.272	PyM
127_5	0.930	DTrM
127_6	0.578	PyM
128_1	0.160	PyM
128_2	1.000	PyM
128_3	0.235	PyM
128_4	0.302	PyM
128_5	1.183	PyM
128_6	1.838	PyM
129_1	2.057	PyM
129_2	0.583	PyM

Table B.2 (cont.) – Data Traffic information collected from the live network.

111_5	0.415	PyM
111_6	0.398	DTrM
112_1	0.312	PyM
112_2	0.178	PyM
112_3	0.785	PyM
112_4	2.162	PyM
112_5	0.682	PyM
112_6	0.658	PyM
113_1	1.555	PyM
113_2	2.502	PyM
113_3	1.090	PyM
113_4	0.750	PyM
113_5	0.703	PyM
113_6	1.313	PyM
114_1	0.480	PyM
114_2	0.677	PyM
114_3	1.088	PyM
115_1	0.907	SwM
115_2	0.600	PyM
115_3	0.632	PyM
116_1	0.267	PyM
116_2	0.587	PyM
116_3	0.707	PyM
117_1	0.587	PyM
117_2	1.085	PyM
117_3	1.497	DDGM
118_1	1.407	SwM
118_2	0.163	PyM
118_3	1.323	PyM
118_4	0.493	PyM
118_5	0.432	SwM
118_6	0.288	PyM
119_1	0.412	PyM
119_2	0.400	PyM
119_3	0.177	PyM
120_1	0.408	PyM
120_2	1.507	SwM
120_3	0.508	PyM
121_1	1.310	PyM
121_2	0.413	PyM
121_3	0.505	DTrM

129_3	2.260	PyM
129_4	1.863	PyM
129_5	1.013	PyM
129_6	0.812	PyM
130_1	1.090	PyM
130_2	0.917	PyM
130_3	0.793	PyM
131_1	0.658	PyM
131_2	1.418	SwM
131_3	1.183	PyM
132_1	1.708	PyM
132_2	1.120	DDGM
133_1	1.035	PyM
133_2	1.170	PyM
133_3	0.232	PyM
133_4	1.358	PyM
133_5	1.003	PyM
133_6	0.832	PyM
134_1	0.218	PyM
134_2	0.198	DDGM
134_3	0.638	PyM
135_1	0.562	PyM
135_2	0.360	PyM
135_3	0.668	PyM
136_1	0.637	DTrM
136_2	0.495	DDGM
136_3	0.260	PyM
137_1	1.027	PyM
137_2	1.032	PyM
137_3	0.187	PyM
138_1	0.725	DDGM
138_2	1.762	PyM
138_3	0.482	PyM
138_4	0.153	SwM
138_5	0.407	DDGM
138_6	0.313	PyM
139_1	0.492	PyM
139_2	0.197	PyM
139_3	0.797	PyM
140_1	1.703	PyM
140_2	0.813	DTrM
140_3	0.147	PyM

Table B.2 (cont.) – Data Traffic information collected from the live network.

141_1	1.667	PyM
141_2	0.285	PyM
141_3	1.162	DDGM
141_4	0.542	PyM
141_5	0.635	SwM
141_6	1.032	DDGM
142_1	0.670	PyM
142_2	0.757	PyM
142_3	0.517	PyM
142_4	0.270	PyM
142_5	0.500	PyM
142_6	0.435	SwM
143_1	0.712	PyM
143_2	0.415	PyM
143_3	0.720	PyM
144_1	0.775	DDGM
144_2	0.230	PyM
144_3	0.137	PyM
145_1	0.137	PyM
145_2	1.402	PyM
145_3	1.118	DDGM
145_4	0.255	PyM
145_5	1.320	PyM
145_6	1.178	SwM
146_1	1.880	PyM
146_2	0.157	PyM
146_3	0.505	PyM
147_1	2.110	SwM
147_2	0.595	SwM
147_3	0.265	PyM
148_1	0.577	PyM
148_2	0.648	PyM
148_3	0.480	PyM
148_4	0.220	PyM
148_5	0.358	PyM
148_6	0.353	PyM
149_1	0.137	PyM
149_2	0.485	SwM
149_3	1.088	PyM
150_1	0.372	PyM

Table B.2 (cont.) – Data Traffic information collected from the live network.

150_2	0.160	PyM
150_3	0.303	PyM
151_1	0.040	PyM
151_2	0.333	SwM
151_3	0.033	PyM
152_1	0.173	PyM
152_2	0.632	PyM
152_3	0.488	PyM
153_1	0.145	PyM
153_2	0.755	PyM
153_3	0.145	PyM
154_1	0.625	PyM
154_2	1.083	PyM
154_3	1.622	PyM

Annex C

Sectors’ Maximum Traffic Load

In this annex, one presents PDFs containing the maximum traffic load distribution for voice and data sectors, for each voice and data region, at weekdays and weekends.

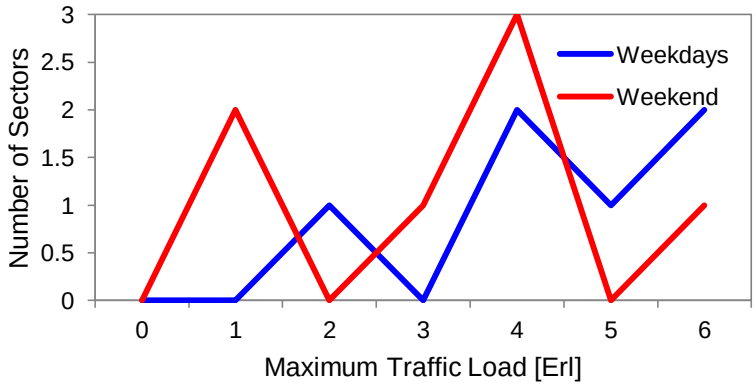

Figure C.1 – Trapezoidal region PDF, representing the maximum values of traffic load, for voice.

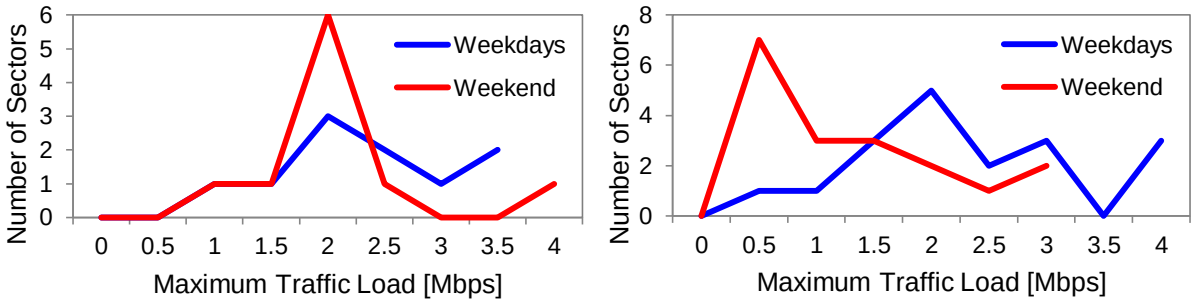

a) Trapezoidal.

b) Swing.

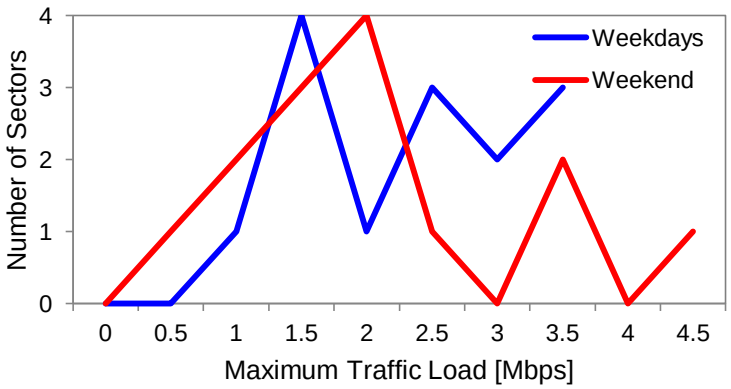

c) Double Gaussian.

Figure C.2 – Urban region PDF, representing the maximum values of traffic load, for data.

Annex D

Traffic Correlation Analysis

Voice and data, as well as weekdays and weekends correlation analysis results, are presented in this annex, with the traffic profiles that outcome from this procedure.

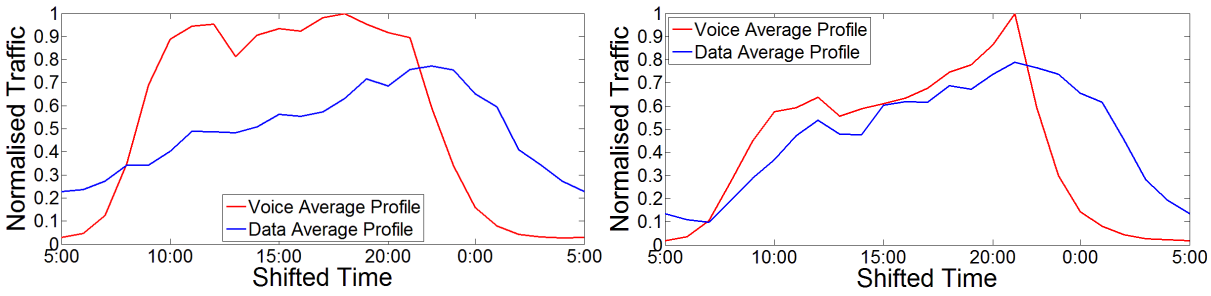

a) Trapezoidal. b) Tree Stump.

Figure D.1 – Voice to Data profiles correlation results.

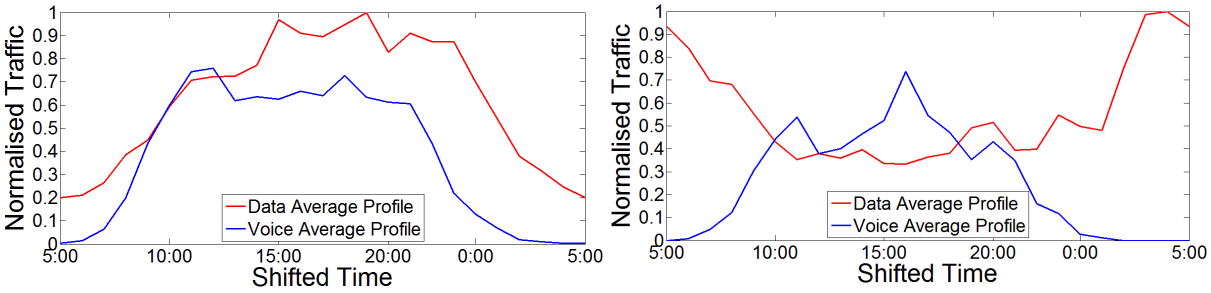

a) Data Trapezoidal. b) Swing.

Figure D.2 – Data to Voice profiles correlation results.

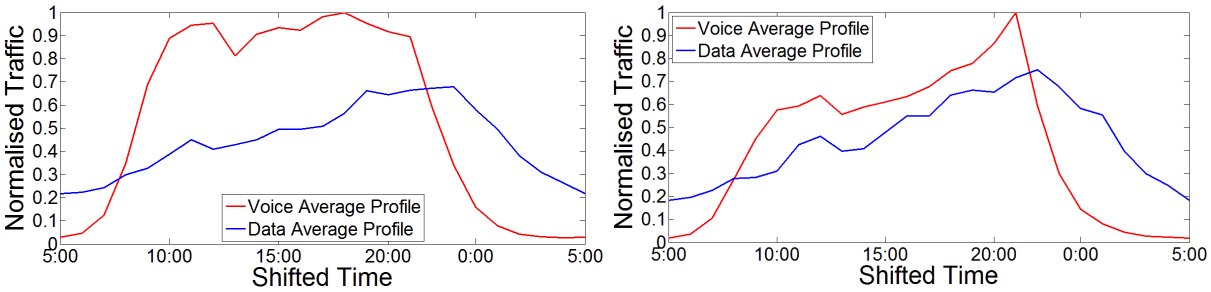

a) Trapezoidal. b) Tree Stump.

Figure D.3 – Voice to Data profiles' correlation results, with alternative distribution.

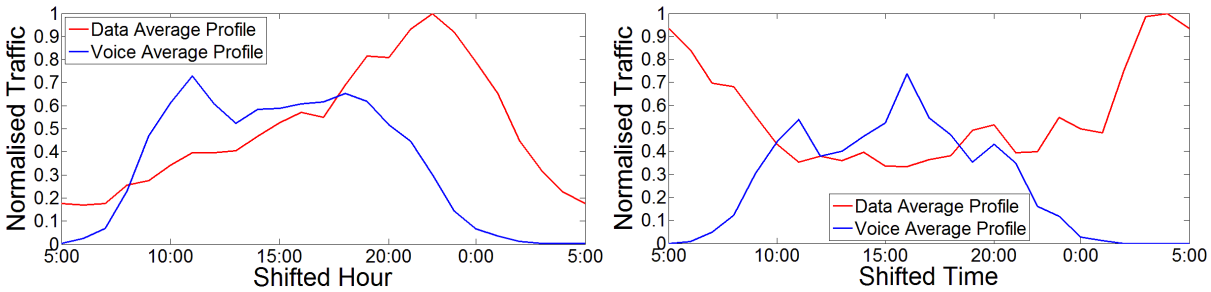

c) Pyramid. b) Swing.

Figure D.4 – Data to Voice profiles' correlation results, with alternative distribution.

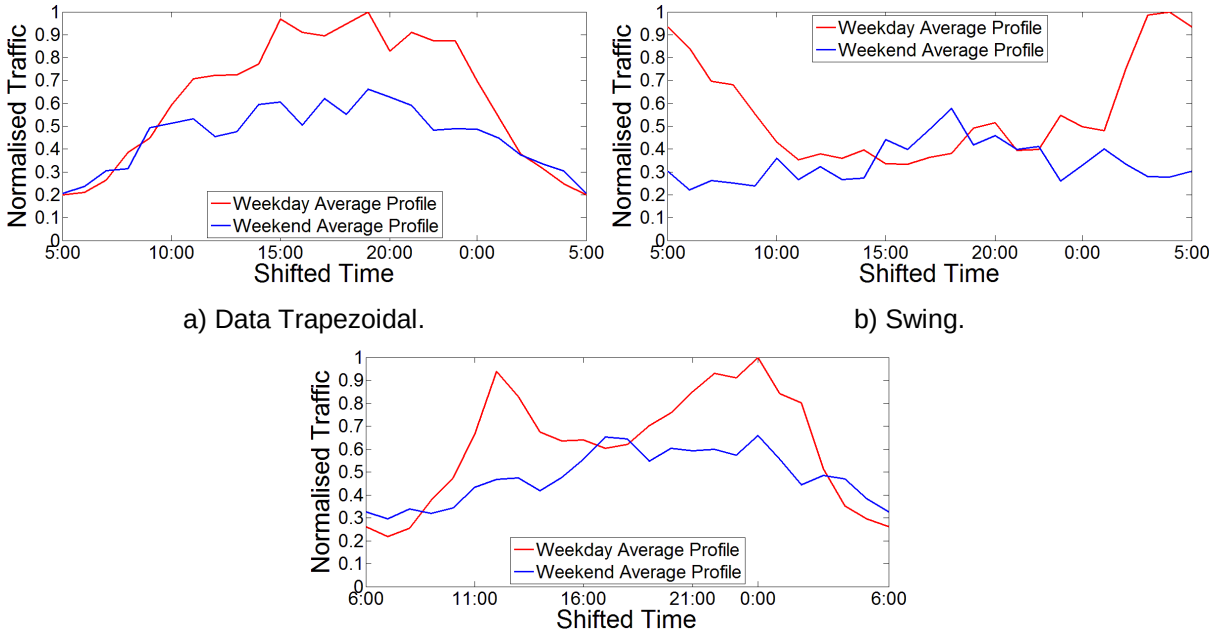

a) Data Trapezoidal.

b) Swing.

c) Data Double Gaussian.

Figure D.5 – Weekday to Weekend Data Average Profiles Correlation.

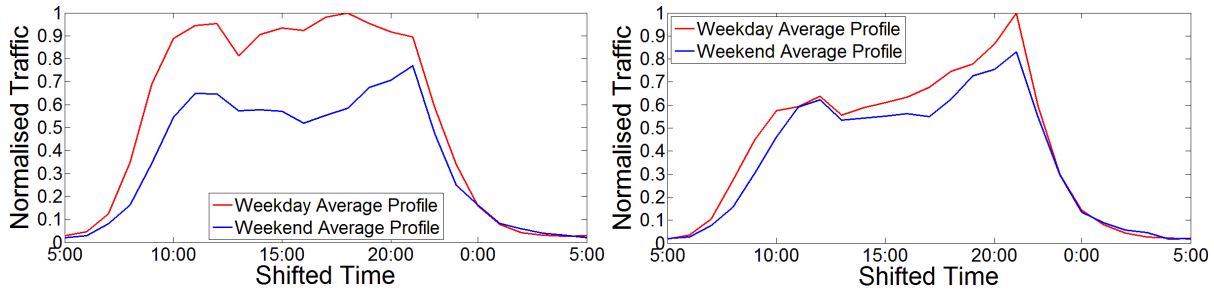

a) Trapezoidal.

b) Tree Stump.

Figure D.6 – Weekday to Weekend Voice Average Profiles Correlation, with alternative distribution.

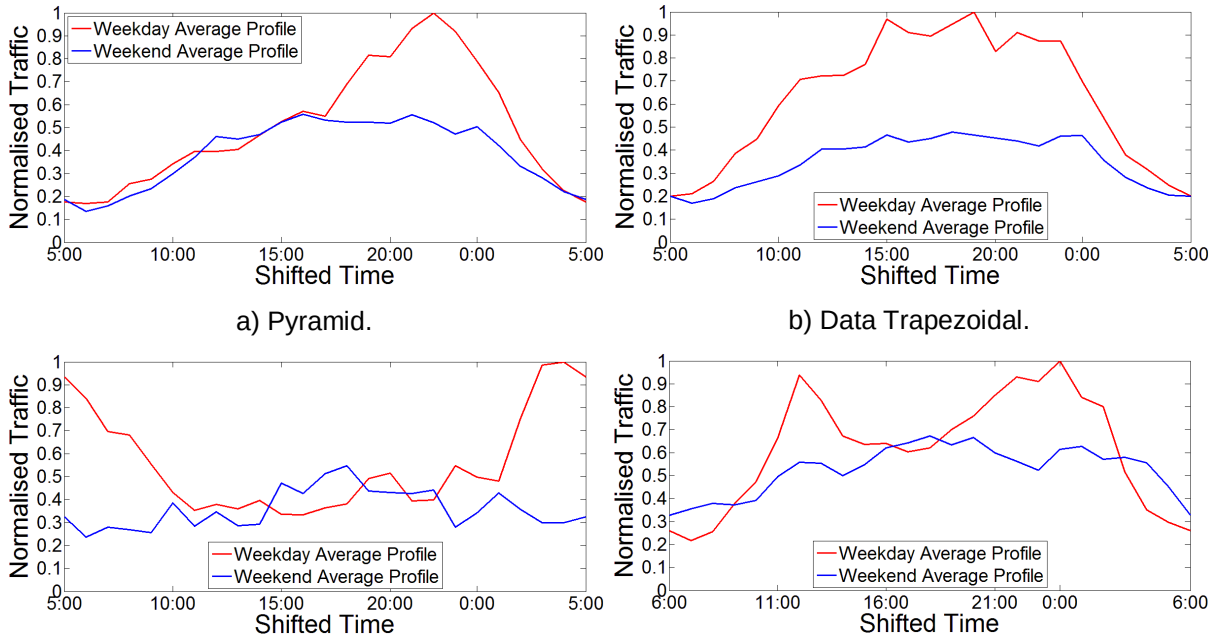

a) Pyramid.

b) Data Trapezoidal.

c) Swing.

d) Data Double Gaussian.

Figure D.7 – Weekday to Weekend Data Average Profiles Correlation, with alternative distribution.

Annex E

Daily Temperature Profile

In this annex, a temperature profile is presented, containing daily temperature variations for two areas.

The daily temperature variation profile is used as an input to the Power Consumption models, and for this effect, data was collected to create one average temperature profile to simulate the temperature outside every modelled 2G and 3G site.

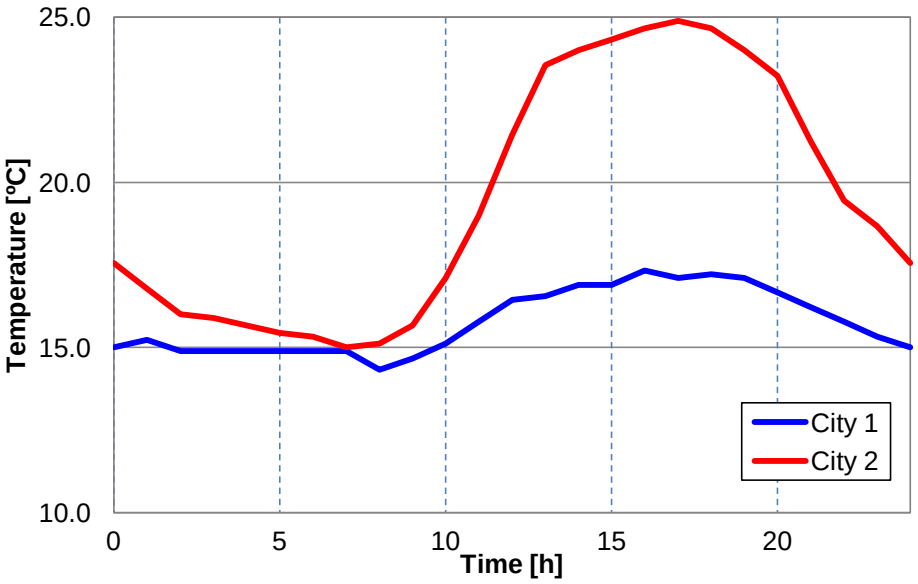

Figure E.1 – Daily Temperature variation profile of the studied areas.

Annex F

HSDPA Throughput Models

The current annex presents the HSDPA data rate models, in particular the variation of the offered data rates with the average SINR.

HSDPA data rate models accurate the SINR and throughput of each considered system for several configurations. These models are composed by experimental expressions to precise throughput, R_b, as a function of SINR, ρ_N, for several types of modulations.

Considering a SISO configuration with QPSK, for DL, one has:

$$R_{b\,[\text{Mbps}]} = \begin{cases} 0.0072 \times \rho_N{}^2 + 0.1743 \times \rho_N + 1.383, & -10 \le \rho_{N\,[\text{dB}]} < -6 \\ 0.025 \times \rho_N{}^2 + 0.425 \times \rho_N + 2.25, & -6 \le \rho_{N\,[\text{dB}]} < -1 \\ 0.00779 \times \rho_N{}^2 + 0.368 \times \rho_N + 2.193, & -1 \le \rho_{N\,[\text{dB}]} < 10 \\ -0.0148 \times \rho_N{}^2 + 0.499 \times \rho_N + 3.0, & 10 \le \rho_{N\,[\text{dB}]} < 16 \\ 7.2, & \rho_{N\,[\text{dB}]} \ge 16 \end{cases} \quad \text{(F.1)}$$

For a SISO configuration with 16QAM, one has:

$$R_{b\,[\text{Mbps}]} = \begin{cases} 0.0143 \times \rho_N{}^2 + 0.3486 \times \rho_N + 2.7657, & -10 \le \rho_{N\,[\text{dB}]} < -6 \\ 0.05 \times \rho_N{}^2 + 0.85 \times \rho_N + 4.5, & -6 \le \rho_{N\,[\text{dB}]} < -1 \\ 0.0223 \times \rho_N{}^2 + 0.631 \times \rho_N + 4.3203, & -1 \le \rho_{N\,[\text{dB}]} < 10 \\ -0.05 \times \rho_N{}^2 + 1.5757 \times \rho_N + 1.9286, & 10 \le \rho_{N\,[\text{dB}]} < 16 \\ 14.4, & \rho_{N\,[\text{dB}]} \ge 16 \end{cases} \quad \text{(F.2)}$$

For a SISO configuration with 64QAM, the throughput is given by:

$$R_{b\,[\text{Mbps}]} = \begin{cases} 0.0143 \times \rho_N{}^2 + 0.3586 \times \rho_N + 2.7657, & -10 \le \rho_{N\,[\text{dB}]} < -6 \\ 0.0005 \times \rho_N{}^3 + 0.0208 \times \rho_N{}^2 + 0.6167 \times \rho_N + 4.3131, & -6 \le \rho_{N\,[\text{dB}]} < 11 \\ -0.0652 \times \rho_N{}^2 + 2.87 \times \rho_N - 9.7048, & 11 \le \rho_{N\,[\text{dB}]} < 20 \\ 21.6, & \rho_{N\,[\text{dB}]} \ge 20 \end{cases} \quad \text{(F.3)}$$

Annex G

Traffic Profiles with Standard Deviation

In this annex, the traffic profiles with the added standard deviation hourly values are represented. These profiles are used as inputs of the Power Consumption and Energy Efficient Models.

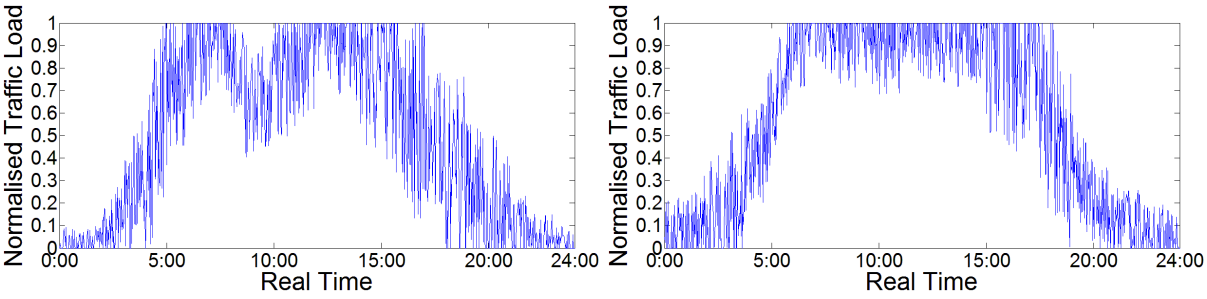

a) Double Gaussian.

b) Trapezoidal.

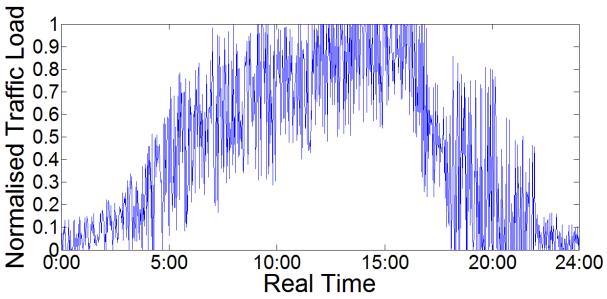

c) Tree Stump.

Figure G.1 – Voice daily traffic profiles, with standard deviation.

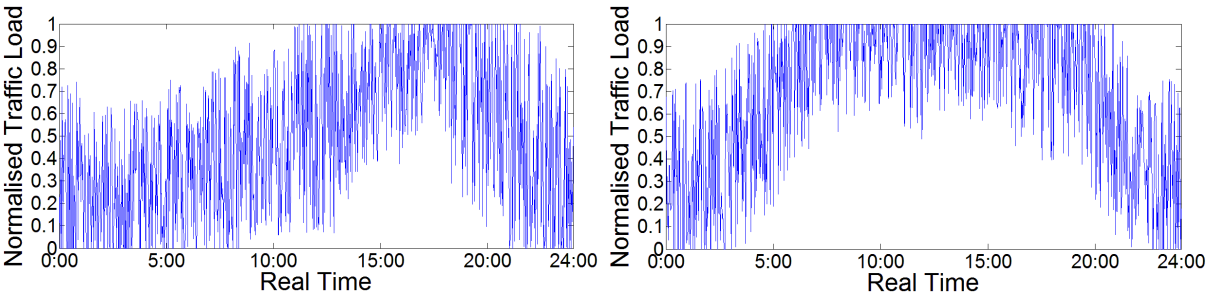

a) Pyramid.

b) Trapezoidal.

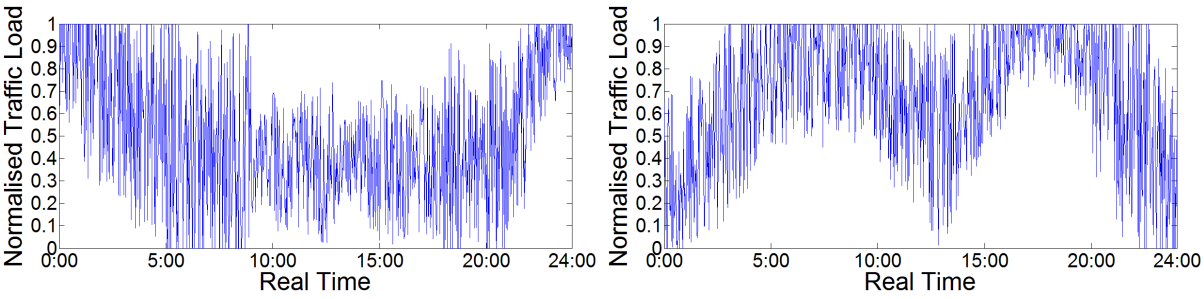

c) Swing.

d) Double Gaussian.

Figure G.2 - Data daily traffic profiles, with standard deviation.

Annex H

Standard Deviation Profiles

In this annex, one shows the obtained standard profiles, for each of the developed traffic models included in the distinct power consumption scenarios.

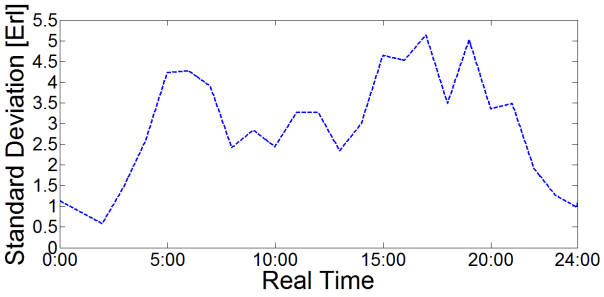

a) Double Gaussian.

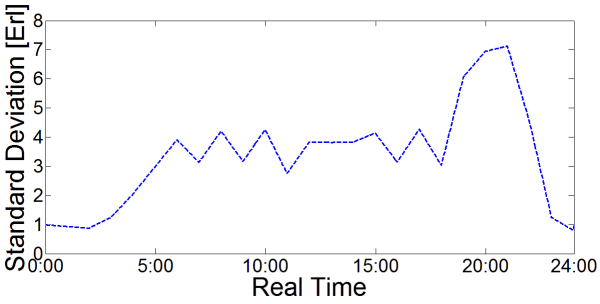

b) Tree Stump.

Figure H.1 – Voice Traffic Models standard deviation profiles.

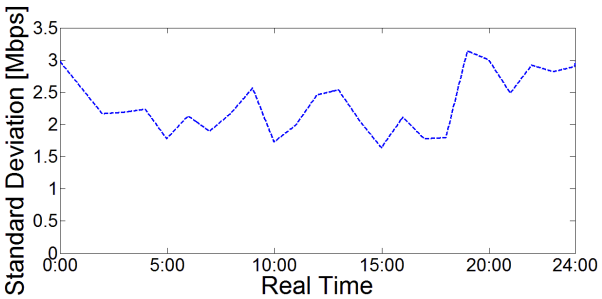

a) Pyramid.

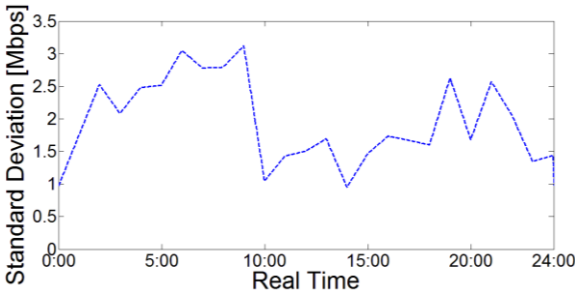

b) Swing.

Figure H.2 – Data Traffic Models standard deviation profiles.

Annex I

Scenarios' Power Consumption Profiles

In this annex, one shows the power consumption profiles, for each of the developed scenarios, regarding the 2G and 3G networks, and finally taking into account the co-localised BSs configuration.

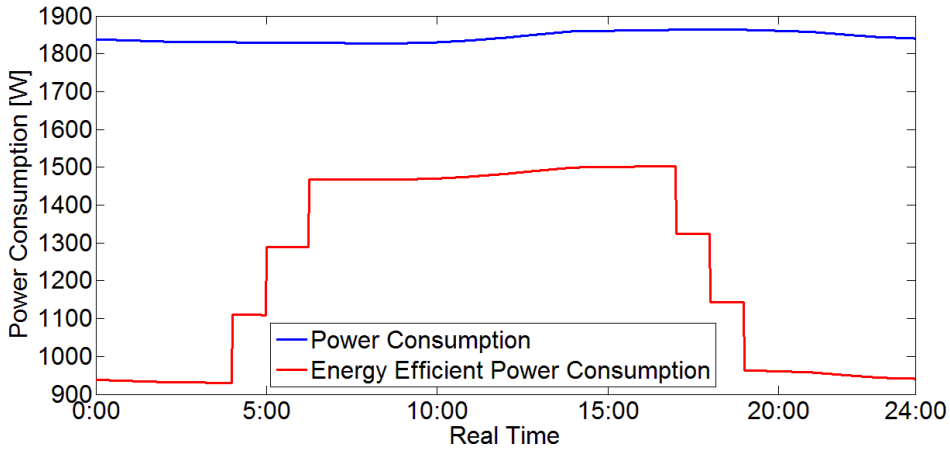

Figure I.1 – DU scenario daily power consumption profiles.

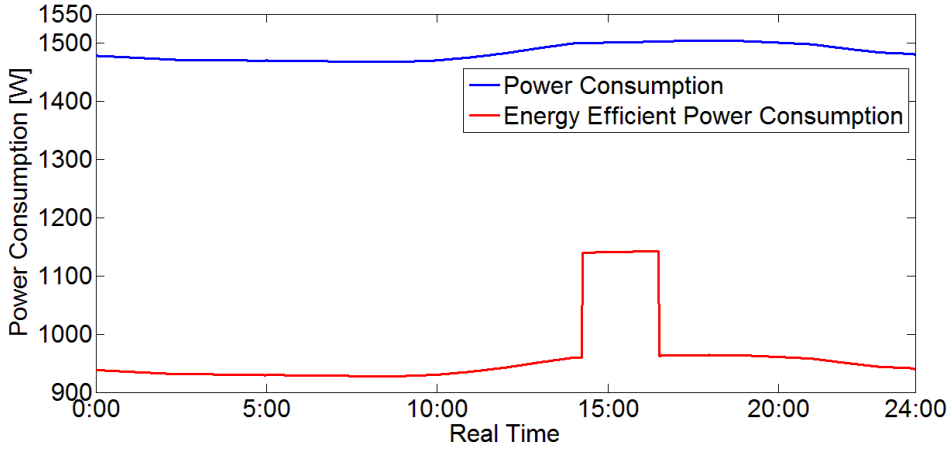

Figure I.2 – S scenario daily power consumption profiles.

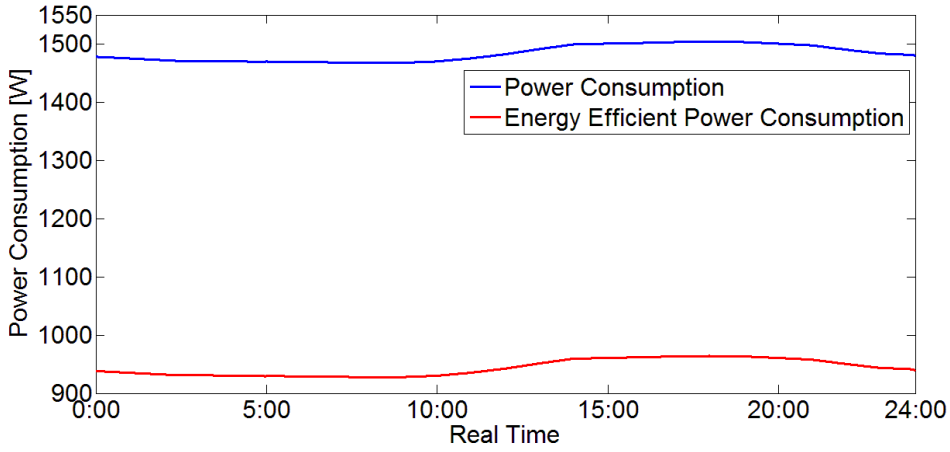

Figure I.3 – Ru scenario daily power consumption profiles.

References

[3GPP10] 3GPP, *Carrier aggregation deployment scenarios*, TSG-RAN WG2 #68bis, R2-100531,Valencia, Spain, Jan. 2010.

[AlQu98] Almeida,S. and Queijo,J., *Spatial and Temporal Traffic Distributions Models for GSM (*in Portuguese*)*, Diploma Thesis, Instituto Superior Técnico, Lisbon, Portugal, Sep. 1998.

[ARFB10] Arnold,O., Richter,F., Fettweis,G. and Blume,O., "Power Consumption Modelling of Different Base Station Types in Heterogeneous Cellular Networks", in *Proc. of Future Networks and Mobile Summit*, Florence, Italy, June 2010.

[Bati11] Batista,R., *Performance Evaluation of UMTS/HSPA+ Data Transmission for Indoor Coverage*, M.Sc. Thesis, Instituto Superior Técnico, Lisbon, Portugal, Oct. 2011.

[BoCo11] Bogucka,H. and Conti,A., "Degrees of Freedom for Energy Savings in Practical Adaptive Wireless Systems", *IEEE Communications Magazine,* Vol. 49, No. 6, June 2011, pp. 38-45.

[Carv09] Carvalho,G., *Data Rate Performance Gains in UMTS Evolution at the Cellular Level*, M.Sc. Thesis, Instituto Superior Técnico, Lisbon, Portugal, Oct. 2009.

[CCMM09] Chiaraviglio,L., Ciullo,D., Meo,M. and Marsan,M., "Energy-Efficient Management of UMTS Access Network", in *Proc. of 21st International Teletraffic Congress (ITC 21)*, Paris, France, Sep. 2009.

[Corr10] Correia,L.M., *Mobile Communications Systems* – Lecture Notes, Instituto Superior Técnico, Lisbon, Portugal, Feb. 2010.

[CTZK09] Chang,R., Tao,Z., Zhang,J. and Kuo,C., "A Graph approach to Dynamic Fractional Frequency Reuse (FFR) in Multi-Cell OFDMA Networks", in *Proc. of IEEE International Conference on Communications – ICC '09*, Dresden, Germany, June 2009.

[CZBF10] Correia,L. Zeller,D., Blume,O., and Ferling,D., "Challenges and enabling technologies for energy aware mobile radio networks", *IEEE Communications Magazine*, Vol. 48, No. 11, Nov. 2010, pp.66-72.

[DBMK10] Dufková,K., Bjelica,M., Moon,B. and Kencl,L., "Energy Savings for Cellular Network with Evaluation of Impact on Data Traffic Performance", in *Proc. of European Wireless 2010*, Lucca, Italy, Apr. 2010.

[DVTJ10] Deruyck,M., Vereecken,W., Tanghe,E., and Joseph,W., "Power consumption in wireless access network", in *Proc. of European Wireless 2010*, Lucca, Italy, Apr. 2010.

[EARTH10a] EARTH, *Energy efficiency analysis of the reference systems, areas of improvements and target breakdown*, Deliverable D2.3 Dec. 2010. (https://bscw.ict-earth.eu/pub/bscw.cgi/d31515/EARTH_WP2_D2.3.pdf)

[EARTH10b] EARTH, *Most Promising Tracks of Green Networks Technologies*, Deliverable D3.1, Dec. 2010. (https://bscw.ict-earth.eu/pub/bscw.cgi/d31509/EARTH_WP3_D3.1.pdf)

[Eric11] Ericson,M., "Total Network Base Station Energy Cost vs. Deployment", in *Proc. of IEEE 73rd Vehicular Technology Conference*, Yokohama, Japan, May 2011.

[FBZF10] Ferling,D., Bohn,T., Zeller,D., Frenger,P., Gódor,I., Jading,Y. and Tomaselli,W., "Energy Efficient Approaches for Radio Nodes", in *Proc. of Future Network & Mobile Summit 2010*, Florence, Italy, June 2010.

[GCJH10] Ge,X., Cao,C., Jo,M., Chen,M., Hu,J. and Humar,I., "Energy Efficiency Modelling and Analyzing Based on Multi-cell and Multi-antenna Cellular Networks", *KSII Transactions on Internet and Information Systems*, Vol. 4, No. 4, August 2010, pp. 560-574.

[HaRM03] Halonen,T., Romero,J. and Melero,J., *GSM, GPRS and EDGE Performance*, John Wiley, Chichester, UK, 2003.

[HHAK11] Han,C., Harrold,T., Armour,S., Krikidis,I., Videv,S., Grant,P.M., Haas,H., Thompson,J.S., Ku,I., Wang,C., Le,T.A., Nakhai,M.R., Zhang,J. and Hanzo,L., "Green Radio: Radio Techniques to Enable Energy-Efficient Wireless Networks", *IEEE Communications Magazine,* Vol. 49, No. 6, June 2011, pp. 46 - 54.

[HoTo04] Holma,H. and Toskala,A., *WCDMA for UMTS (*3rd Edition), John Wiley & Sons, Chichester, UK, 2004.

[HoTo07] Holma,H. and Toskala,A., *WCDMA for UMTS – HSPA Evolution and LTE (*4th Edition), John Wiley & Sons, Chichester, UK, 2007.

[Jaci09] Jacinto,N., *Performance Gains Evaluation from UMTS/HSPA+ to LTE at the Radio Network Level*, M.Sc. Thesis, Instituto Superior Técnico, Lisbon, Portugal, Nov. 2009.

[KhVT02] Khedher,H., Valois,F. and Tabbane,S., "Traffic Characterization for Mobile Networks", in *Proc. of VTC'02 – 56th IEEE Vehicular Technology Conference,* Vancouver, Canada, Dec. 2002.

[KoDe10] Koutitas,G. and Demestichas,P., "A Review of Energy Efficiency in Telecommunication Networks", *Telfor Journal*, Vol. 2, No. 1, 2010, pp. 1-4.

[KrFr97] Kronestedt,F. and Frodigh,M., "Frequency Planning Strategies for Frequency Hopping GSM", in *Proc. of* VTC'97 *–47th IEEE Vehicular Technology Conference*, Phoenix, USA, May 1997

[MaFe08] Marsch,P., Fettweis,G., "On Base Station Cooperation Schemes for Downlink Network MIMO under a Constrained Backhaul", in *Proc. of IEEE GLOBECOMM 2008*, New Orleans, USA, Dec. 2008.

[MCCM09] Marsan,M., Chiaraviglio,L., Ciullo,D., and Meo,M., “Optimal Energy Savings in Cellular Access Networks”, in *Proc. of GreenComm’09 – First International Workshop on Green Communications*, Dresden, Germany, June 2009.

[METE11] http://www.freemeteo.com, May 2011.

[Mica10] Micallef,G., “Methods for Reducing the Energy Consumption of Mobile Broadband Networks”, *Telektronikk*, No. 1, Jan. 2010, pp. 121-128.

[MiMS10a] Micallef,G., Mogensen,P., Scheck,H., “Cell Size Breathing and Possibilities to Introduce Cell Sleep Mode”, in *Proc. of European Wireless 2010*, Lucca, Italy, Apr. 2010.

[MiMS10b] Micallef,G., Mogensen,P., Scheck,H., “Dual-Cell HSDPA for Network Energy Saving”, in *Proc. of* VTC’10 *–71st IEEE Vehicular Technology Conference*, Taipei, China, May 2010.

[Moli05] Molisch,A.F., *Wireless Communications*, John Wiley, Chichester, UK, 2005.

[OPTI11] Optimus, Private Communications, 2011.

[RiFF09] Richter,F., Fehske,A.J., and Fettweis,G.P., “Energy Efficiency Aspects of Base Station Deployment Strategies for Cellular Networks”, in *Proc. of VTC’09 – IEEE Vehicular Technology Conference*, Anchorage, USA, Sep. 2009.

[SaEl10] Saker,L. and Elayoubi,S., “Sleep mode implementation issues in green base stations”, in *Proc. of IEEE 21st International Symposium on Personal Indoor and Mobile Radio Communications*, Istanbul, Turkey, Sep. 2010.

[SaMu10] Sánchez,L. and Muñoz,L., “Energy efficiency of simple ON/OFF scheme in mobile cellular networks”, *Electronics Letters,* Vol. 46, No. 20, Sep. 2010, pp. 1404-1405.

[ToDI98] Tomiyama,K., Daniel,J.P. and Ihara,S., “Modelling Air Conditioner Load for Power System Studies”, *IEEE Transactions on Power Systems*, Vol. 13, No. 2, May 1998, pp. 414 - 421.